People's Democratic Republic of Algeria

Ministry of Higher Education and Scientific Research

University 08 May 1945 – Guelma-

Faculty of Sciences and Technology

Department of Electrotechnique and Automatic Engineering

A THESIS

Submitted in Partial Fulfillment of

the Requirements for the Degree of

DOCTOR of SCIENCES

Title

Parametric Optimization of PI Speed Regulators and State Observer based Control Systems with Viscous Friction Coefficient Account using Mini-Max Approach

By

Yassine YAKHELEF

Before the jury:

Pr. H. TEBBIKH	Prof. at Univ. of 08 May 1945-Guelma	President
Dr. M. BOULOUH (MCA)	S. Lecturer at Univ. of 08 May 1945-Guelma	Supervisor
Pr. E. HADJADJ AOUL	Prof. at Univ. of Badji Mokhtar-Annaba	Examiner
Pr. S. SAAD	Prof. at Univ. of Badji Mokhtar-Annaba	Examiner

GUELMA 2015

République Algérienne Démocratique et Populaire

Ministère de l'Enseignement Supérieur et de la Recherche Scientifique

Université 08 Mai 1945- Guelma

Faculté des Sciences et de la Technologie

Département de Génie Electrotechnique et Automatique

THÈSE

Présentée pour l'Obtention du Grade de

DOCTEUR en SCIENCES

Titre:

Optimisation Paramétrique des Systèmes de Commande à Régulateurs PI et Observateur d'Etat sous l'Influence de la Friction Visqueuse par l'Approche MiniMax

Par:

Yassine YAKHELEF

Jury:

Dr., Prof. H. TEBBIKH	Université 08 Mai 1945 Guelma	Président
Dr., M.C.A M. BOULOUH	Université 08 Mai 1945 Guelma	Rapporteur
Dr., Pr. E. HADJADJ AOUL	Université Badji Mokhtar Annaba	Examinateur
Dr., Pr. S. SAAD	Université Badji Mokhtar Annaba	Examinateur

GUELMA 2015

Parametric Optimization of PI Speed Regulators and State Observer based Control Systems with Viscous Friction Coefficient Account using Mini-Max Approach

A thesis submitted for the degree of

Doctor of Sciences

By

Yassine Yakhelef

Department of Electrotechnics and Automatic Engineering

Faculty of Sciences and Technology

University of 08 May 1945 of Guelma

2015

Acknowledgements

This thesis was written during my Doctoral studies at the department of Electrotechnique and Automatic Engineering at University of 8 May 1945- Guelma, Faculty of Engineering Sciences and Technology. For this:

First of all, I would like to express my deepest gratitude to my supervisor **Dr. Boulouh Messaoud** for his guidance, support and motivation during the achievement of this work.

My sincere and deep gratitude is due to **Pr. Tebbikh Hicham**, **Pr. Hadjadj Aoul Elias** and **Pr. Saad Salah** for their acceptance to evaluate this work.

I have to express my grateful thanks to the president of Laboratory of Automatics and Informatics of Guelma (L.A.I.G) and all the members of the Lab., for giving me the opportunity to discuss the most parts of this work during the organized days of JSS, grateful thanks go to them for their many comments and valuable discussions.

I cannot forget to thank the staff of Electrotechnique and Automatic Engineering Department for their kindness.

Yakhele Yassine

2015.

Abstract

The need to improve the quality and performance of electromechanical drive control systems is crucial, where the objective is to increase the production quality of industrial processes and to use rationally our resources. In order to attain this aim, it is necessary to improve and perfecting all quality performance indices of these systems and maintaining them at the required level.

Separately excited DC drive speed control systems, especially those used in rolling mill industries, are characterized by joint elasticity and some aspects of non linearity. This is mainly due to the long shaft coupling the driving motor and the load, which causes substantial torsional vibration in case of load side parameters variation of speed and /or torque changes. These inherent properties can greatly affect the quality of the rolling material and even influence the stability of the used closed loop control system.

In case of minor changes of these parameters, their influence on drive dynamic behavior may be satisfactorily compensated using conventional speed control algorithms, such as PI controller, and ensuring the required quality and accuracy performance of the system response. However, the effects of substantial parameter changes and variations, which is generally the case for this type of application, can no longer be effectively compensated by these algorithms and it is not possible to obtain satisfactory performance by applying only standard and conventional PI controllers. Therefore, looking for control methods and techniques capable of solving the problem of these applications' drives and achieving improvement of their performances is crucial. In this vein, our work consists of applying the proposed Mini-Max optimization approach in conjunction with other compensation techniques on chosen system models to improve and perfecting the performances of an already existing PI speed controller based separately excited DC drive system and increasing thereafter its

order of astatism under variable operational conditions of set point speed change and load torque disturbance.

On the other hand, these drives are also equipped with current limiter to protect against any damage of the drive components when abrupt set point change or load torque disturbance occur. Unfortunately, the presence of these devices may lead, under those conditions, to saturation of PI speed controller output and consequent serious degradation in system performance is evident. Therefore, the effect of inherent actuator saturation (non-linearity) on degrading the drive's transient and steady-state performances is also studied, where the effectiveness and efficiency of the proposed novel conditional integration anti-windup compensation technique is verified for this purpose.

Key words: Mini-max Optimisation Approach, Double PI Speed Controller, State Observer, Order of Astatism, Anti Wind up, Saturation, Control Performance Quality.

Résumé

“Optimisation Paramétrique des Systèmes de Commande Electrique à Régulateurs PI et Observateurs d’Etat sous l’Influence de la Friction Visqueuse, par l’Approche Minimax**”**

Le problème du perfectionnement des équipements et des technologies dans le but d’améliorer la qualité de production et d’augmenter la productivité et l’utilisation rationnelle des ressources est l’une des priorités primordiales en industrie. Sa résolution est impossible sans l’amélioration progressive de tous les indices de performance de la qualité de commande des systèmes électromécaniques et des processus industriels et leur maintien au niveau requis.

Les systèmes électromécaniques d’entrainement à base des moteurs à courant continu sont largement utilisés dans, particulièrement, les laminoirs industriels pour les métaux, les laminoirs à papier, à verre …etc. Dans ces industries, ce système de commande en vitesse est caractérisé par son élasticité avec quelques aspects non linéaires dûs principalement à la longueur de l’arbre liant le moteur d’entrainement avec la charge mécanique. A cet effet, des vibrations prennent naissance pendant le fonctionnement sous la présence d’une variation ou changement des paramètres extérieurs de vitesse de consigne et/ou du couple de la charge. Ces conditions de fonctionnement ont certainement une influence sur la qualité du produit ainsi que les performances du système de commande utilisé.

Dans le cas où ces variations paramétriques sont légères, leur influence sur le comportement dynamique du système peut, d’une manière satisfaisante, être compensée par les algorithmes de commande conventionnels tels que le correcteur PI. Mais cette compensation devient insuffisante, lorsque ces variations de vitesse ou du couple de la charge sont importantes, ce qui peut nuire aux performances du système.

Par conséquence, les chercheurs dans ce domaine, ont pu développer des méthodes et des techniques capables de résoudre ce problème de commande et améliorer ainsi les performances de ces systèmes, ce qui représente une issue primordiale pour le développement technologique.

Ce travail s'insère dans le cadre de l'exploitation rationnelle des ressources matérielles des industries, des différents types de systèmes de régulation de vitesse en cascade à courant continu, utilisant des régulateurs PI ou PID, où on a proposé d'optimiser les paramètres de ses régulateurs par l'approche MiniMax, en la comparant avec d'autres techniques de perfectionnement, sur des modèles choisis, en vue de réaliser une amélioration et un perfectionnement des performances et augmenter l'ordre d'astatisme de ces systèmes durant leur fonctionnement selon les conditions de variation ou changement de la vitesse de consigne et le couple de la charge.

Par ailleurs, une étude approfondie lié au problème de la stabilité en présence de la limitation en courant par la non linéarité "saturation" a été exposée. Cette limitation, précédemment introduite, conduit à un comportement non linéaire, lorsque la boucle de courant se sature, en fort signal pour le cas d'un système à un seul correcteur PI et en faible signal pour le cas d'un correcteur PI double, ce qui provoque l'apparition de fortes oscillations, voire des cycles limites instables. Pour pallier à ce problème d'instabilité, une solution a été proposée sous forme de schémas de structure et de principe, qui peut être utilisée en cas de limitation en courant pour la classe des systèmes de régulation de vitesse en cascade avec un nombre d'intégrateurs variable, assurant ainsi une stabilité et une qualité de commande optimale.

Mots clés: Approche Minimax, Régulateur de Vitesse PI, Observateur d'État, Ordre d'Astatism, Saturation, performance et qualité de commande.

ملخص

إن مشكلة تطوير المعدات والتكنولوجيا لتحسين جودة الإنتاج وزيادة الإنتاجية والكفاءة في استخدام الموارد الصناعية هي واحدة من أولويات الصناعة الأساسية. لتحقيق هذا الهدف لابد من التحسين التدريجي لجميع مؤشرات جودة الأداء مراقبة الأنظمة الكهروميكانيكية والعمليات الصناعية والحفاظ على المستوى المطلوب.

وتستخدم على نطاق واسع نظم حملة الكهروميكانيكية على أساس المحركات ذات التيار المستمر في، بشكل خاص، المطاحن الصناعية للمعادن، مصانع الورق والزجاج ... الخ في هذه الصناعات، ويتميز نظام التحكم في سرعة ذلك من خلال مرونته مع بعض جوانب المستحقة غير الخطية أساسا إلى طول رمح ربط محرك أقراص مع الحمل الميكانيكي. لهذا الغرض، تنشأ الاهتزازات أثناء التشغيل في وجود اختلاف أو تغيير المعالم الخارجية ضبط سرعة و / أو عزم الدوران من هذا العبء. هذه الظروف لديها بالتأكيد تأثير على جودة المنتوج، فضلا عن أداء نظام التحكم المستخدمة.

في حالة هذه الاختلافات صغيرة، وتأثيرها على السلوك الديناميكي للنظام يمكن أن يعوضها خوارزميات التحكم التقليدية مثل المدقق تناسبي- تكاملي لكن, هذا التعويض يصبح غير كاف عند هذه الاختلافات في سرعة أو عزم الدوران من الحمل أمر مهم، والتي يمكن أن تخل بأداء النظام. ونتيجة لذلك، فان البحث في هذا المجال، وتطوير أساليب وتقنيات قادرة على حل مشاكل مكافحة هذه ولتحسين أداء هذه الأنظمة، يعد مسألة أساسية في التطور التكنولوجي.

هذا العمل هو جزءا من الاستخدام الرشيد للصناعات الموارد المادية، وأنواع مختلفة من أنظمة التحكم في سرعة تتالي المحرك، وذلك باستخدام منظم سرعة تناسبي- تكاملي أو تناسبي- تكاملي- مشتق ، حيث نقترح لتحسين إعدادات المنظمين من خلال طريقة 'مينيماكس'، ومقارنة ذلك مع التقنيات و نماذج الأخرى مختارة، لتحقيق تحسين وتطوير الأداء وزيادة درجة الاستقرار لهذه النظم في ظل ظروف الاختلاف أو التغير في السرعة المحددة وعزم دوران الحمل.

وعلاوة على ذلك، فقد تم التعرض في هذا البحث لدراسة شاملة تتعلق بمشكلة الاستقرار في وجود قيود الحالي من قبل اللاخطية "التشبع." هذا القيد، قدم سابقا، مما يؤدي إلى سلوك غير الخطية عندما يتشبع حلقة الحالية في إشارة قوية في حالة نظام مع تصحيح تناسبي- تكاملي واحد وإشارة ضعيفة في حالة وجود مصحح تناسبي- تكاملي المزدوج، والذي يسبب ظهور اهتزازات قوية أو دورات حد غير مستقرة .للتغلب على هذه المشكلة ، فقد اقترح حلا كهيكل والرسوم البيانية من حيث المبدأ، والتي يمكن استخدامها في حالة القيد الحالي لفئة السرعة أنظمة التحكم في أجهزة الطرد مع عدد من تكامل متغير، وبالتالي ضمان الاستقرار ومراقبة الجودة المثلى.

كلمات المفتاح : طريقة مينيماكس, درجة الاستقرار, منظم سرعة تناسبي- تكاملي , مراقب الحالة, التشبع , الأداء و ضبط الجودة.

Contents

List of Figures

List of Tables

Nomenclature

The following lists contain the most important symbols, notations and abbreviations used in the manuscript of this thesis.

Symbols

b	Dead zone gain
$d(t)$	Input Disturbance Signal
$e(t)$	Tracking Error Signal
e_b	The Instantaneous Back Electromotive Force Voltage
$e_{sat}(t)$	Saturation Error Signal
$e_{ss}(t)$	Steady State Error Signal
i_a	The Instantaneous Component of the Armature Current
i_f	The Instantaneous Currents of the Field Circuit
J	The Moment Of Inertia
K_b	The Back e.m.f. Voltage Constant
k_d	Derivative Gain Constant
K_f	Field Constant
k_i	Integral Gain Constant
k_p	Proportional Gain Constant
K_t	Motor Torque Constant
K_u	Ultimate Gain
$q(t)$	Integrator Output Signal
$r(t)$	Input Reference Signal
s	The Complex Variable
t	Continuous Time

t_f	Final Time Instant
t_0	Initial Time Instant
t_p	Peak Time
t_r	Rise Time
t_s	Settling Time
u	Actuator Saturation Output Signal
u_c	Controller Output Signal
v_a	The Instantaneous Armature Input Terminal Voltage
v_f	The Instantaneous Applied Field Voltage
$x(t)$	State Variable Vector
$\hat{x}(t)$	Estimated State Variable Vector
$y(t)$	Output Vector
$y_{es}(t)$	Estimated Output Signal
$\hat{y}(t)$	Estimated Output Vector
$\tilde{y}(t)$	Output Estimated Error Vector
A	State Matrix
B	Control Matrix
C	Output Matrix
D	Denominator Polynomial
E_b	The Back Electromotive Force Voltage
G	Transfer Function
G_c	Controller Transfer Function
G_{cl}	Closed Loop Transfer Function
G_M	Gain Margin
G_{OL}	Open Loop Transfer Function
G_p	Plant Transfer Function
H	Feedback Transfer Function
I_a	The Steady State Component of the Armature Current
$I_{aref.}$	Reference Value of Armature Current
I_f	Steady State Current of the Field Circuit

L	State Observer Gain Matrix
L_a	The Inductance of the Armature Circuit
L_f	The Winding Inductance of the Field Circuit
M_p	Peak Percent Overshoot
N	Numerator Polynomial
R_a	The Resistance of the Armature Circuit
R_f	The Winding Resistance of the Field Circuit
T_e	The Developed Electromagnetic Torque
T_d	Derivative Time Constant
T_i	Integral Time Constant
T_L	The Load Torque
T_u	Ultimate Period
$T_{viscous}$	Viscous Friction Torque
V_a	Steady State Armature Input Terminal Voltage
V_f	Steady State Applied Field Voltage
Y_{ss}	Steady State Value Of The Response
α	Order Of Astatism
β	Viscous Friction Coefficient
$\varphi(t)$	The Field Produced Air Gap Flux
ϕ_M	Phase Margin
ω_m	The Motor Speed
$\omega_{mref.}$	Reference Value of Output Speed
ω_0	Natural Frequency of Second Order System
π	Pi
ρ	Parameter Vector
τ_a	Armature Time Constant
τ_m	Mechanical Time Constant
ζ	Damping Ratio

Notations

$\frac{d}{dt}$	Derivative With Respect To Time
L^{-1}	Inverse Laplace Transform
$\frac{\partial}{\partial x}$	Partial Derivative With Respect To x
$\dot{q}(t)$	Derivative of Integrator Output
$\dot{x}(t)$	Derivative of State Variable Vector
$\dot{\hat{x}}(t)$	Derivative of Estimated State Variable Vector

Abbreviations

DC	Direct Current
e.m.f	Electro-Motive Force
FC	Fuzzy Controller
FCL	Fuzzy Control Logic
FOPDT	First Order Plus Dead Time
GA	Genetic Algorithm
IAE	Integral of Absolute Error
IE	Integral of Error
IFT	Iterative Feedback Tuning
IMC	Internal Model Control
ISE	Integral of Square Error
ITAE	Integral of Time Multiplied by Absolute of Error
ITSE	Integral of Time Multiplied by Square Of Error
IT^2SE	Integral of Time Squared Multiplied by Square Of Error
LQR	Linear Quadratic Regulator
MPC	Model Predictive Control
NN	Neural Network
P	Proportional
PI	Proportional plus Integral
PID	Proportional plus Integral plus Derivative
PSO	Particle Swarm Optimization

QAD	Quadratic Amplitude Damping
SEDC	Separately Excited Direct Current
SI	International System of Units
SIMC	Skogestad Internal Model Control
SMC	Sliding Mode Control

Chapter 1

Introduction

1.1 Motivation and Background

The development of high performance motor drives is very important in industrial as well as other purpose applications. Generally, a high performance motor drive system requires good dynamic speed control, accurate tracking and load disturbance responses. In spite of the development of power electronics resources that has reinforced the position of AC motor drives in the industrial market, the direct current (DC) motor drives are also becoming more and more useful insofar because of their simplicity, ease of application, high reliability, flexibility and favorable cost, and they have long been a backbone of an extensively large field of industrial applications [16]. particularly, the superiority of torque-speed characteristics offered by the separately excited DC motor, which provide excellent speed controllability regarding the precise, wide, simple, and continuous control characteristics; have made this type of motor drives still employed in a multitude of industrial and manufacturing processes such as pulp, paper and steel rolling mills, conveyors, mining, robotics, electrical traction and other applications where speed and position control of the motor are required [2]. This motor is used, however, to drive a coupled load characterized, generally, by an inertia J, viscous friction coefficient, β and load torque T_L.

Regarding the extensive employment of these electromechanical drive systems, the need to improve their control quality and performance for these industrial applications is crucial. The objective is to increase the production quality of industrial processes and to use rationally the material resources of these industries.

Designing a speed controller of desired performance characteristics represents, therefore, an essential issue in achieving these objectives. Traditionally, rheostatic armature control method was widely used for speed control of low power dc motors. However the controllability, cheapness, higher efficiency, and higher current carrying capabilities of semiconductor static power converters brought a major change in the performance of speed controlled electrical DC drives. Thanks to this advanced technology, and exploiting the speed controllability potential features, the desired torque-speed characteristics of DC motor could now be achieved and its speed can be adjusted to a great extent so as to provide easy control and high performance. Several control techniques and algorithms are currently available and can be utilized to control the speed of DC drive system, including conventional Proportional plus Integral (PI), Model Predictive Control (MPC) [1], Adaptive [2, 3], State Space Optimal Control schemes [4] as well as novel Neural Network (NN) and Fuzzy Logic (FL) [5, 6, 7, 8, 9]. A hybrid combined speed controllers are also available such as PID-Neural Network, PID-Fuzzy Logic and Neuro-Fuzzy controllers [10, 11, 12].

Among this multitude of techniques that can be used to control the speed of DC electromechanical system, the Proportional – Integral – Derivative (PID) or its option (PI) controller is still operating the majority of industrial control systems in the world. It has been reported that more than 95% of the controllers in the industrial process control applications are of PID type [13] as no other controller matches the simplicity, clear functionality, applicability and ease of use offered by this type of controller. Consequently, The PI (D) controller now is used for most of industrial control problems, not only implemented in motor drive systems, but also extends to include process control, automotive systems, flight control, instrumentation, etc., and it comes in many different forms; as standard single loop controller, or as a software component in programmable logic controllers and in distributed control systems [14].

DC drive systems, especially those used in rolling mill industries, are characterized by joint elasticity and some aspects of non linearity. This is mainly due to the long shaft coupling the driving motor and the load, which causes substantial torsional vibration in case of load side parameters variation of speed and /or torque.

These inherent properties can greatly affect the quality of the rolling material and even influence the stability of the used closed loop control system.

In case of minor changes of these parameters, their influence on drive dynamic behavior may be satisfactorily compensated using conventional control algorithms, such as PI controller, and ensuring the required quality and accuracy performance of the system response. However, the effects of substantial parameter changes and variations, which is generally the case for this type of application, can no longer be effectively compensated by these algorithms and it is not possible to obtain satisfactory performance by applying only standard and conventional PI controllers.

In order to treat this control problem, two perspectives are found. The first perspective consists of changing completely and replacing the classical cascade structure of the control system under the conventional PI speed controller; whereas the second perspective proposes to find control techniques that alter modification to classical control structure so it matches the control problem requirements.

Regarding to the first perspective and in addition to the above stated numerous control alternatives other than PI based cascade control structure, which are proposed to handle these inherent system's characteristics, the artificial intelligent control schemes have been widely employed to handle the AC drive inherent characteristics and achieving an important improvements of its control performance. These control methods represented by the design of Fuzzy logic controller, neural network controller or the combination of the two, are strongly proposed as an attempt to solve the problem of controlling the speed and/or position of DC drive systems which present difficulties of their modeling or those characterized by load changes, parameters variation and high nonlinearity such as friction and saturation [117, 119]. These methods, although they allowed achieving performance improvement of nonlinear systems and they are justified to be robust against model parameters variation, uncertainties and input disturbance changes characterizing these systems, they are either theoretically more complex or involve difficulties when they are being implemented. For this reason, some researchers have extensively worked; instead, to alter modification on the PI based conventional feedback control system structure in

order to design a robust controller capable of compensating for torsional vibrations effects of the underlying drive system and ensuring its high operational performances.

In addition to the employment of digital filters to avoid modal excitation of abrupt change of external disturbance of load torque or speed reference, the insertion of additional feedbacks from selected state variables that characterize the torsional torque, load speed and /or disturbance torque represents the more advanced method used in view of this perspective [38, 39]. The main drawback of this technique, however, resides in the fact that the direct feedbacks from these mechanical variables are very often difficult, cost effective and, as a result, reduces the system reliability. To solve this latter problem, many methods have been presented in the literature, which are based on the estimation of the mechanical state variables rather than feeding them back in the control structure. This is basically consisted of designing a state observer (state estimator) where the Kalman filter is the most known in this field [40].

Regarding the DC motor drive system, the design and implementation of state observer technique represents the best choice for one reason that it preserves simplicity and cost effectiveness of the whole control system. This method has, in fact, brought a great enhancement and amelioration to DC drive performances and has solved to a great extent the problem of load side non measurable parameters variation and changes. But when it is used with a conventional PI controller to control the speed of DC motor drive system, it is argued that the speed response transient and steady state performance properties (peak overshoot, rise time, settling time and steady state error) are not as good as it is desired. This problem can be attributed to the fact that when the PI controller operates with its fixed parameters, it fails to respond to desired process specifications and performances as the operating level or the external conditions move away from the original design, thus the controller parameters have to be tuned allowing the process to be kept at its desired operating performances. Special attention has been given to this topic since long time, where researchers have worked to find simple and practical tuning methods for this widely employed controller. Broadly speaking, PI and PID tuning methods can be classified into the following categories: trial-and-error feature-based methods, analytical methods and optimization methods. Under these categories, plenty of techniques and methods are reported in the literature.

In 1942s, Ziegler and Nichols [54] have proposed the first and most utilized method for selecting the parameters of PID controller based on a few features of the process dynamics that are easy to obtain experimentally. In 1953, Cohen-Coon [45], [55] has proposed his method based on the same experiments used by Zeigler and Nichols, but with an additional parameter used for PID settings. The poor results obtained using Zeigler–Nichols method was the reason for an intensive research done in the subject, resulting in new techniques. The Relay feedback method, proposed by Astrom and Hugglund [58, 59, 60] for automating the Zeigler and Nichols procedure is one of these techniques. Besides, the internal model control (IMC) is considered to be the most popular among the analytical methods [64, 65, 66].

Recently, tuning methods based on optimization approaches, with the aim of ensuring good stability and robustness, have received attention in the literature. Some of these are the Extremum Seeking (ES) algorithm [80] based on optimizing an error-based cost function generating the optimal PI (D) parameters. The same approach is used in the Iterative Feedback Tuning (IFT) method [72, 73, 74], with the only difference being the number of step response experiments required per iteration for determining the optimal controller parameters.

Many papers have also shown the utilization of the so called minimum criteria methods [75, 76, 77, 78, 79]. These are based on minimizing the mathematical criteria such as integral of error (IE), integral of absolute error (IAE), integral of time multiplied by absolute error (ITAE), integral of square error (ISE) and integral of time multiplied by square error (ITSE) to find the optimum controller parameters. In [94, 95, 96, 97], Genetic Algorithm, Particle Swarm Optimization, Fuzzy Logic and Neural Networks are also presented as a soft computing and artificial intelligent methods and algorithms of optimally tuning the parameters of PID controller and enhancing system performance properties.

Besides the problem of finding the optimal PI controller parameters, which highly improve the performance of PI based control systems, the substantial change and variation of set point and load torque characterizing, particularly, the operation of PI based speed controlled DC drive employed in paper and steel rolling mill industries render this conventional controller unable alone to track accurately these variations

and preventing, therefore, the deviation from the desired performance. In order to cope with this problem, a lot of work has been done by many researchers to find control methods and techniques that are capable, in conjunction with PI controller, of achieving accuracy performance improvement of the so called systems under variable input reference conditions. Consequently, many methods are proposed in the literature.

The proportional gain method [41] is traditionally used to improve the accuracy performance of a closed loop control system by increasing its loop gain. This method, although efficient of lowering the speed response steady state error, it degrades the system's transient performance by increasing the percent overshoot. The integral control method is also applied in [110] to improve both systems' order of astatism and accuracy by modifying the control structure and adding integral terms in the forward path of the control loop. The main drawback of this method is that these added integrators may lead to instability of the system. In an attempt of ensuring stability and desired tracking performance, the Sliding Mode Control (SMC) is used alone in [113] and with PI controller in [111, 112]. This robust and simple control technique is adaptively applied in [114, 115] to compensate model uncertainties of flexible-joint manipulator nonlinear dynamic systems and obtaining an accurate steady state response with zero error. These SMC based methods, although efficient and robust, they suffer from chattering problem which has to be eliminated.

Recently, the intelligent control methods of NN and hybrid Fuzzy-NN are, respectively, applied in [116] and [118] to adaptively improve both robustness and accuracy performance of induction motor speed control system under variable reference input signal. Regarding the achieved satisfactory results, these control methods are also applied for the same purpose on the speed and position controlled DC motor drive system [117], [119]. The feed-forward compensation is an alternative approach, also employed in different engineering branches to enhance the quality and performance of control system subjected variable external operating conditions. Using this approach, many techniques exist in literature among which, we find the Neural Network (NN) based feed-forward method, used in [120] to ameliorate the accuracy performance of PID based nonlinear control systems characterized by an input disturbance. The Fuzzy logic control combined with PI controller has also been used in

[121] as a feed-forward compensator to improve the already implemented sliding mode based positioning control system. Other feed-forward based compensation techniques are studied in [122].

As far as the PI based speed controlled DC drive system is concerned, the inherent nonlinear characteristics such as saturation and friction could degrade the whole performance of that system [123], [124]. In order to deal with this problem, which is caused by the integrator wind-up phenomenon, many anti-windup schemes are proposed to be used with PI controller for compensating saturation nonlinearity and overcoming performance deterioration of the drive system. Thanks to these compensators, PI controller is, now, able to sustain with these practical issues and is still the bread and butter of any automatic control system. In [134], [135] and [136], the Limiting Integrator anti-windup technique is used to reduce the effect of integrator wind up due to saturation of PI speed controller. The scheme basically consists of feeding back the integrator output through a dead zone with a high gain in order to reduce the integrator input and guarantees an operation in the linear range. This has one drawback mainly due to the mismatch between the saturation element and integrator dead zone limits which may lead to their independent operation and hence provoking overshoot or undershoot in system's response. The tracking back calculation, firstly proposed by Fertik and Ross [137], is another anti-windup compensation technique which is based on the calculation of the difference between the saturated and the unsaturated control input signals and generating the error feedback signal. The value of this latter is being used to control and reduce progressively, in case of saturation, the value PI integrator term through a properly chosen feedback gain constant [22], [127], [138, 139, 140, 141]. In general, this method can, conveniently, be applied for processes where the instantaneous reset of the integral term is not crucial. To overcome this disadvantage, the conditional integration anti-windup technique is slightly different scheme, which is applied to inhibit integrator action of the controller whenever saturation state is occurred [141], [144, 145]. This scheme, although it allows an immediate disabling of integration process when saturation occurs, it is criticized of having the disadvantage that the controller may get stuck at a non-zero control error if the integral term has a large

value at the time of switch off [22], [148]. However, for some applications with large change of set point, this anti-windup compensator may be more appropriate, where, the reader can advisably refer to [149], [150] for more details.

This extensive and huge effort has, in fact, represented the background of our work and motivated us to propose novel optimization approaches and methods either for tuning the PI controller parameters or dealing with some aspects of DC drive inherent properties affecting its required performances. In view of this idea, our work is basically about perfecting the performances of an already existing PI speed controller based separately excited DC drive system as it can be stated in the following scope and objectives.

1.2 Scope and Objectives of the Thesis

Mainly this study is about proposing some optimization methods and techniques to achieve more improvements and perfection in operating transient and steady state performances of state observer based PI speed controlled DC drive system, which extensively used in rolling mill industry. Therefore, typical observer based models are being investigated and studied for this purpose.

The proposed novel Mini-Max optimization approach is first applied to optimally select (tune) the parameters of the PI speed controller. The objective is to achieve improvement, particularly, in dynamic performance properties such as: percent overshoot, rise time and settling time. In order to justify the superiority of this method, these improvements are compared to those obtained using the integral based minimisation criteria.

In order to fulfill the high accuracy and fast response requirements of PI speed controlled DC drive system when operating under large disturbance changes of speed reference and load torque, a transfer function based feed-forward compensator is proposed as an efficient control technique to force the drive speed to accurately respond with higher order of astatism to the changed input reference and load torque disturbance.

Regarding the presence of actuator saturation as an inherent nonlinear property of DC drive system and in order to cope with the serious degradation of its both

transient and steady state performances due to PI integrator windup phenomenon, a novel conditional integration anti-windup compensation scheme is proposed and applied.

At the end, we verify the robustness and effectiveness of utilized optimization approach and control techniques. This is, hopefully, done by analyzing the response sensitivity of the system against some system parameters variation.

We have to point out that throughout the whole of this study, special attention is given to exploring and makes clear the effect of viscous friction coefficient on performance improvement of DC drive system. It is a continuous effort to that done in [15], in which the viscous friction coefficient was neglected.

1.3 Contribution

The contribution of this work consists in the fact that the obtained simulation results have shown that the proposed Mini-Max optimization approach in conjunction with the incorporation of the feed-forward control technique and conditional integration anti wind up compensator are effective in achieving both dynamic and steady state performance improvement of a widely used PI speed controlled DC drive system in paper and steel rolling mill industries. These improvements of control system performance have, indeed, an explicit impact on product quality improvement of these industries, where control solutions are usually required to attain this aim.

In attaining this end, a part of the work was a topic of research project within the Laboratory of Automatic and Informatics –Guelma (LAIG) at university of Guelma and which is entitled as « **Contribution in Improving the State Observer-Based Electric Control Systems under the Influence of Positive Damping Friction**».
Around these achieved results, our contribution had, also, illustrated through the participation in the symposium days of « Journées sur les Signaux et Systèmes » (JSS) by the following themes:

- « Comparative Analysis of Different Analytical and Parametric Methods of Optimization of Cascade Systems », 3-rd day of JSS'08, L.A.I.G. Laboratory, University of 08 May 1945 of Guelma, July 2008.
- « Parametric Optimization of PI/PID Based Control System using Mini-Max

Approach: Literature Overview », 2nd. day of Electrical Engineering Ph-D. Students, University of 08 May 1945 of Guelma, Oct. 2008.

- « Dynamic Performance Improvement of DC Servo Systems with Reduced Order State Observer using MiniMax Approach», 1st day of JSS'10, L.A.I.G. Laboratory, University of 08 May 45 of Guelma, Algeria, April 2010.
- « Performance Improvement of double PI Controller based Non Linear Regulatory Systems », 2nd. JSS'11, L.A.I.G. Laboratory, University of 08 May 45 of Guelma, Nov. 12, 2011.

Finally, the main results are resumed in the paper under the title of «PERFORMANCE IMPROVEMENT OF MINIMAX OPTIMIZED PI CONTROLLER-BASED DC DRIVE SYSTEM WITH ACTUATOR SATURATION » and published by ACTA Press in the Journal of Control and Intelligent Systems, Vol. 42, No. 4, 2014.

1.4 Thesis Structure

Based on the above mentioned issues, the thesis is organized, in addition to this introductory chapter, with four chapters as it is detailed in the following:

Chapter 2. Description of Separately Excited DC Drive Control System

In this chapter, we will discuss in details the whole structure of the DC drive system model that is being studied and analyzed for performance improvement and perfection.

Chapter 3. DC Drive Dynamic Performance Optimization using Mini-Max Approach

We devote the content of this chapter to study and analyze the dynamic performance properties and its relation to the stability of our state observer PI speed controlled DC drive system, where, we propose Mini-Max optimization approach to improve these performance characteristics.

Chapter 4. Improving Accuracy Performance and Order of Astatism of DC Drive using Feed-Forward Compensation

The intention in this chapter is to study and investigate the steady state performance of the different system models in response to input reference and load torque changes, where an appropriate feed-forward compensating transfer function is applied to enhance their order of astatism without inserting additional integrators in the forward path of the closed loop system and therefore achieving improvement of the corresponding tracking error accuracy performance.

Chapter 5. Effects of Nonlinearity and Parameters Variation on System Performance

We discover in this chapter the behavior the different system models when they are subjected to actuator saturation nonlinearity. The phenomenon is known as integrator windup, which is highly pronounced when the PI controller is used to control the speed of the DC drive system. To overcome the consequent degradation in system performances, we propose the conditional integration anti-windup compensation technique. Furthermore, the sensitivity of the achieved dynamic and steady state performance of the system against parameters variation is also studied and analyzed.

Chapter 2

Description of Separately Excited DC Drive Control System

2-1 Introduction

Separately excited DC motor is the type of electromagnet brushed DC motor for which the armature and field windings are electrically separated from each other, where the field windings are excited by a DC source separate of that of armature source. Although it exhibits some drawbacks when used in various power range industrial applications such as high maintenance requirement as well as its unsuitability to operate in explosive environment due to commutators and brushes, it presents, on the other hand, some precious advantages such as: simplicity, ease of application, high reliability, flexibility and favorable cost. Moreover, the excellent speed controllability feature regarding the precise, wide, simple, and continuous control characteristics; have made this type of DC motor drives still employed in a multitude of industrial and manufacturing processes such as pulp, paper and steel rolling mills, conveyors, mining, robotics, electrical traction and other applications where speed and position control of the motor are required. In this chapter, we will discuss in details the whole structure of this DC drive control system that is being studied and analyzed for performance improvement and perfection.

2-2 Dynamic Model of Separately Excited DC Motor

The control of SEDC motor and analyzing its performance within a drive control system require, in most cases, the knowledge of its mathematical model. In order to

build this model, an equivalent electrical circuit for the SEDC electromechanical system is assumed in Fig. 2.1 [16].

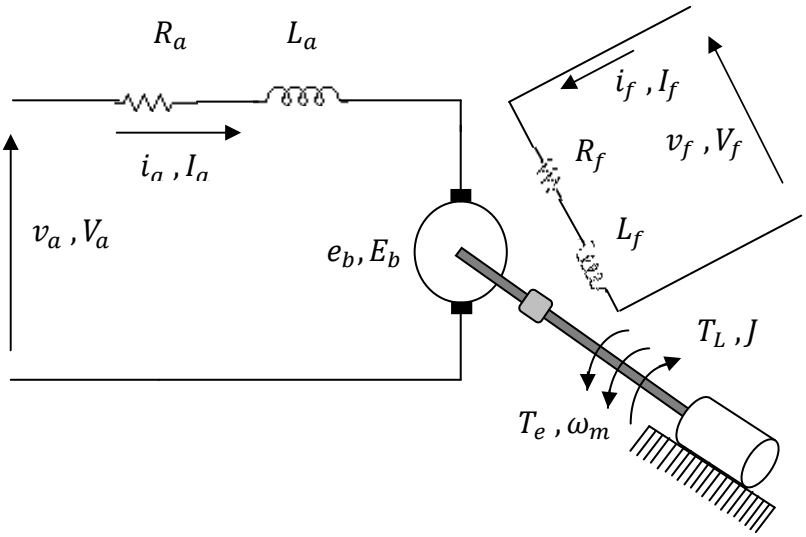

Figure.2.1 Equivalent Circuit of Separately Excited DC Motor based Electromechanical System

The physical parameters appearing in the circuit scheme are defined as follows:
R_f: The winding resistance of the field circuit (Ω). L_f: The winding inductance of the field circuit (H). i_f, I_f: are respectively, the instantaneous and steady state currents of the field circuit (A). v_f, V_f: are, respectively, the instantaneous and steady state applied field voltages (Volt). R_a: The resistance of the armature circuit (Ω). L_a: represents the inductance of the armature circuit (H). i_a, I_a: are respectively, the instantaneous and steady state components of the armature current (A). v_a, V_a: are respectively, the instantaneous and steady state armature input terminal voltages (Volt). e_b, E_b: are respectively the instantaneous and steady state back Electromotive force (e.m.f) voltages (Volt). T_e: is the developed electromagnetic torque (N.m). ω_m: is the motor speed (rad/sec).

The DC motor is used to drive a mechanical load, which is characterized by the following parameters:
J : which represents the load and motor moment of inertia (Kg.m^2). T_L: is the load torque (N.m).

In Table 1, we present the physical parameters values which characterize the utilized separately excited DC motor with the corresponding coupled load.

Table 2.1 Parameters values of DC Motor base Electromechanical System.

ω_m	Rated Motor Speed	157 rad / s
v_a	Rated Terminal Voltage	440 V
R_a	Armature Resistance	0.087 Ω
L_a	Armature Inductance	6.873 e -3 H
J	The Rotational Load Inertia	20 kg.m^2
K_b	Back E.M.F Voltage Constant	2.68 V.s / rad
K_t	Electromagnetic Torque Constant	2.68 N.m / A
T_L	Nominal Load Torque	1070 N.m

The above simplified representation of the SEDC motor based electromechanical system mention that it consists of two independent circuits, armature circuit and field circuit with the load is connected to the armature circuit. As shown, two voltages are separately applied to each of field and armature terminals, which results in two flowing currents known as field current, $i_f(t)$ and armature current, $i_a(t)$.

Basically, when the SEDC motor is excited by a field current i_f, an armature current i_a flows in the circuit. As a result, a motor back e.m.f e_b is induced and an electromagnetic torque T_e is developed to balance the load torque T_L at a particular speed ω_m. The exciting field current i_f is independent of the armature current i_a, because the two windings are supplied separately, which means that any change in the armature current has no effect on the field current [17].

By referring to the schematic model of the electromechanical system mentioned in Fig.2.1 and using the Newton's law combined with the Kirchhoff's law around the two circuit loops, the mathematical model of the system describing both electrical and

mechanical characteristics can now be derived and stated in the form of differential equations.

2-2-1 Electrical Characteristics of SEDC Motor

By applying Kirchhoff's voltage principle around the armature and field circuits of the dc motor; we obtain the following two differential equations, which describe its dynamic electrical behaviour:

$$v_a = R_a i_a + L_a \frac{di_a}{dt} + e_b(t) \tag{2.1}$$

$$v_f = R_f i_f + L_f \frac{di_f}{dt} \tag{2.2}$$

The back electromotive force, EMF voltage, $e_b(t)$ is induced by the rotation of the armature windings in the magnetic field due to the field excitation $i_f(t)$ and it acts in opposition to the current that produces the motion. This back EMF is related to the motor shaft angular speed, $\omega_m(t)$ by a linear relation given by the expression:

$$e_b(t) = K\varphi(t)\omega_m(t) \tag{2.3}$$

where K is a constant and $\varphi(t)$ is the field produced air gap flux proportional to the field current as it is expressed by the relation:

$$\varphi(t) = K_f i_f(t) \tag{2.4}$$

From equations (2.3) and (2.4), the back e.m.f voltage is expressed as a function of field current and motor angular velocity as:

$$e_b(t) = KK_f i_f(t)\omega_m(t) = K_b i_f(t)\omega_m(t) \tag{2.5}$$

With $K_b = KK_f$ is the motor back e.m.f voltage constant (in V/A-rad/s) [17].
Therefore, equation (2.1) becomes:

$$v_a = R_a i_a + L_a \frac{di_a}{dt} + K_b i_f(t)\omega_m(t) \tag{2.6}$$

2-2-2 Mechanical Characteristics of SEDC Motor

By performing the energy balance on the electromechanical system and using Newton's second law, the mathematical model describing the mechanical characteristics can be derived in the form of differential equation as follows:

$$\sum \vec{T} = J \frac{d\vec{\omega}_m}{dt} \tag{2.7}$$

If the load torque is denoted by T_L, equation (2.7) becomes:

$$\frac{d\omega_m}{dt} = \frac{1}{J}(T_e - T_{viscous} - T_L) \tag{2.8}$$

With: T_e being the electromagnetic torque developed by the DC motor and is represented by the torque equation (2.9), which couples the mechanical torque to the electrical armature current as:

$$T_e = K_t i_f(t) i_a(t) \tag{2.9}$$

Where K_t is the motor torque constant in (Nm/A). In SI unit system, we have [18]:

$$K_t = K_b \tag{2.10}$$

$T_{viscous}$ in equation (2.8) represents the viscous friction torque, which models the frictions due to motor brushes, bearings, gears, etc [17, 19]. To maintain the linear aspect of system model, this is the only friction torque type of the motor considered in this study and is modeled to be linearly proportional to the motor angular speed as:

$$T_{viscous} = \beta \omega_m(t) \tag{2.11}$$

Special attention is given, in fact, to this type of friction torque throughout this work, where its influence on the performance of the whole system is investigated by considering positive and negative values of viscous friction coefficient β (in N.m.s/rad) rather than neglecting its effect via assuming this coefficient equals zero.

Taking this important mechanical parameter into account, when substituting equations (2.9), (2.11) in (2.8), we obtain the following differential equation that models the mechanical characteristics of the separately excited DC motor [20].

$$K_t i_f(t) i_a(t) = J \frac{d\omega_r(t)}{dt} + \beta \omega_r(t) + T_L \tag{2.12}$$

The equations (2.2), (2.6) and (2.12) model completely the electrical and mechanical dynamics of SEDC motor based electromechanical system.

2-3 Block Diagram Representation of SEDC Motor Based Electromechanical System

The block diagram representation of SEDC motor based electromechanical system is built from the interaction of the equations (2.2), (2.6) and (2.12) in the time domain as they are rewritten in s-domain. Using Laplace transform, the following corresponding set of equations is obtained:

$$V_a(s) = (R_a + sL_a) I_a(s) + K_b I_f(s) \omega_m(s) \tag{2.13}$$

$$V_f(s) = R_f I_f(s) + sL_f I_f(s) \tag{2.14}$$

$$K_t I_f(s) I_a(s) = (\beta + sJ) \omega_m(s) + T_L \tag{2.15}$$

From equation (2.15), the rotational motor speed is expressed as:

$$\omega_m(s) = \left[\frac{1}{\beta + sJ}\right] [K_t I_f(s) I_a(s) - T_L] \tag{2.16}$$

From equation (1.13), the armature current is expressed as:

$$I_a(s) = \left[\frac{1}{R_a + sL_a}\right] [V_a(s) - K_b I_f(s) \omega_m(s)] \tag{2.17}$$

And from equation (2.14), the field current is given as:

$$I_f(s) = \frac{V_f(s)}{(R_f + L_f s)} \tag{2.18}$$

By implementing equations (2.16), (2.17) and (2.18), we obtain the following block diagram representing the SEDC motor based electromechanical system model in s-domain.

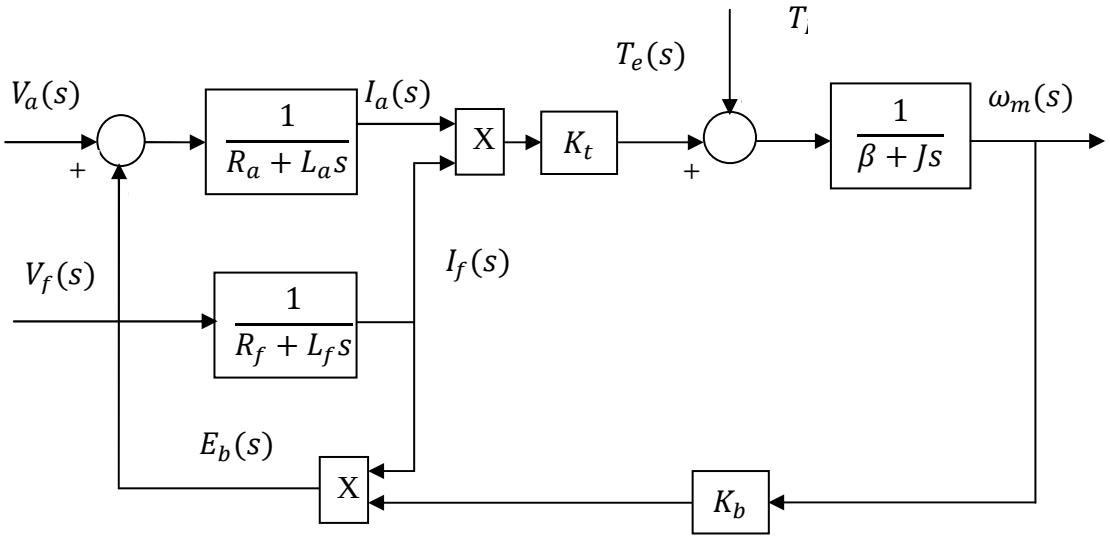

Figure 2.2 Block Diagram of SEDC Motor based Electromechanical System under Variation of both Field and Armature Currents

2.3.1 Suitable Block Diagram Representation

As far as the speed control of the electromechanical system is concerned, this block diagram shows clearly that the speed of the motor can be varied either by:

a) Controlling the field current (flux), also known as field flux control method, or;

b) Controlling the armature voltage $V_a(s)$, also known as armature voltage control method.

The first method is due to the fact that the rotational speed of the motor is inversely proportional to both field current and flux, as it is expressed by:

$$\omega_m \propto \frac{1}{\varphi_f} \propto \frac{1}{i_f} \tag{2.19}$$

In this method, the armature input voltage is maintained constant at its rated value and the rotor speed is changed by varying the field quantities φ_f and i_f. By weakening the field quantity, the motor speed can be increased beyond the nominal value, however, it can be decreased by progressively strengthening the field flux providing to not exceeding the maximum rated flux value for the reason of saturation. Due to this

restriction, this method of controlling the motor speed becomes not suitable for desired speeds below the rated (nominal) value [6].

The second method of controlling the rotational speed of separately excited DC motor is the result of the fact that its speed is directly proportional to the armature input voltage according the expression:

$$\omega_m \propto (v_a - R_a\, i_a) \tag{2.20}$$

When applying this method, the field quantity is maintained constant and the motor speed is changed via armature voltage variation. Armature control is limited in speed by the limited magnitude of the available dc supply voltage and armature winding insulation. Therefore, if the supply dc voltage is varied from zero to nominal value, then the motor speed can be controlled from zero to nominal value, which makes this method ideal for required operational speed from zero to rated value. These two ways of varying the speed of DC motor are explained by the graph illustrated in Fig.2.3.

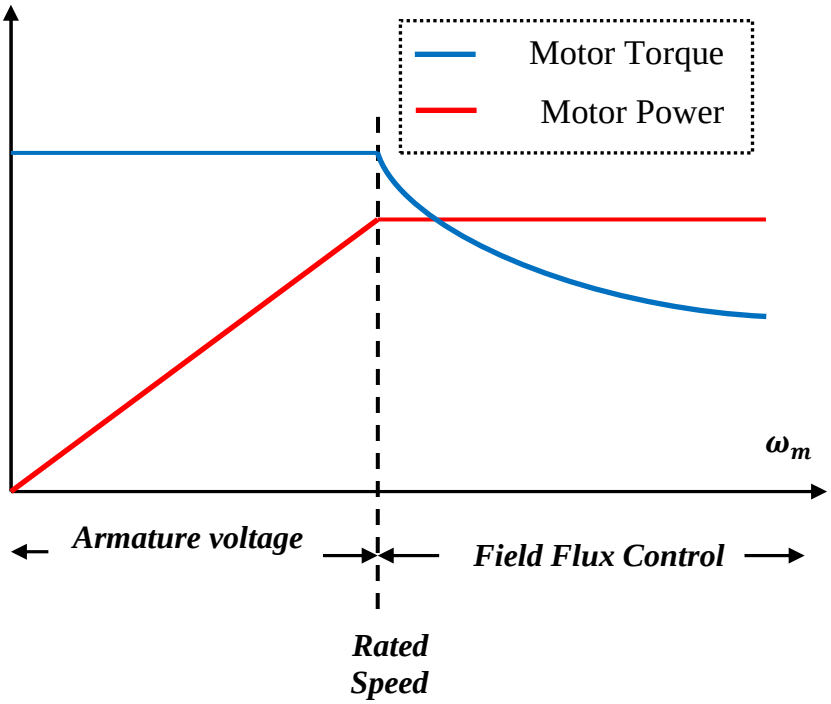

Figure 2.3 Combined Armature Voltage and Field Flux Speed Control of Separately Excited DC Motor

Based on this theory, the appropriate way of varying the motor speed can be chosen depending on the application requirements. Due to this fact, throughout the rest of our development, the focus will be on the armature voltage control that matches the rolling mill industries speed control requirement. Consequently, the block diagram representation of the separately excited DC motor based electromechanical system considered in this study will be that depicted by Fig. 2.4.

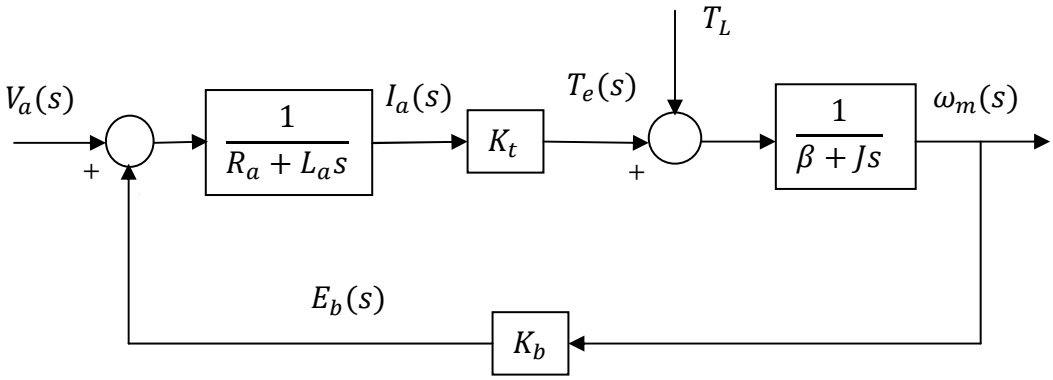

Figure 2.4 Block Diagram of SEDC Motor Electromechanical System under Armature Voltage Control only.

Many forms of transfer function can be derived using this block diagram. However, as far as the motor speed is controlled via the variation of armature voltage, the system can be represented by the following second order transfer function relating the input armature voltage, $V_a(s)$, and the output rotational speed, $\omega_m(s)$:

$$\frac{\omega_m(s)}{V_a(s)} = \frac{\frac{K_t}{L_a J}}{s^2 + \left(\frac{R_a}{L_a} + \frac{\beta}{J}\right) s + \left(\frac{R_a \beta}{L_a J} + \frac{K_b K_t}{L_a J}\right)} \tag{2.21}$$

Alternatively, we can write the above transfer function as follows:

$$\frac{\omega_m(s)}{V_a(s)} = \frac{K_b}{R_a \beta (1 + \tau_a s)(1 + \tau_m s) + K_t K_b} \tag{2.22}$$

With: $\tau_a = \frac{L_a}{R_a}$: is the armature time constant in [s] and;

$\tau_m = \frac{J}{\beta}$: is the mechanical time constant in [s].

2.4 State Space Representation of SEDC Motor

The electromechanical system used in our study is characterized by several inherent properties such as: set point and load disturbance changes, parameters variation, nonlinearities, etc. in order to meet the desired operational performance specifications of accuracy and stability robustness, we need to take into account these characteristics when designing the appropriate feedback controller. Therefore, for the purpose of designing an advanced control system that is able of satisfying the desired performance specifications, the state space representation of the DC motor based electromechanical system can be given by the following state equation:

$$\begin{bmatrix} \dot{i_a}(t) \\ \dot{\omega_m}(t) \end{bmatrix} = \begin{bmatrix} -\frac{R_a}{L_a} & -\frac{K_b}{L_a} \\ \frac{K_t}{J} & -\frac{\beta}{J} \end{bmatrix} \begin{bmatrix} i_a(t) \\ \omega_m(t) \end{bmatrix} + \begin{bmatrix} \frac{1}{L_a} & 0 \\ 0 & -\frac{1}{J} \end{bmatrix} \begin{bmatrix} v_a(t) \\ T_L(t) \end{bmatrix} \quad (2.23)$$

And the output equation:

$$\omega_m(t) = \begin{bmatrix} 0 \\ 1 \end{bmatrix} \begin{bmatrix} i_a(t) \\ \omega_m(t) \end{bmatrix} \quad (2.24)$$

With:

$[i_a(t) \quad \omega_m(t) \quad]$ is the state variables vector;

$[\omega_m(t)]$ is the output vector of single element, and;

$[v_a(t) \quad T_L(t)]$ is the input vector of the system.

This state space representation is the basis for the design of state observer based feedback control system of the electromechanical system used in this work.

2.5 Speed Control Structures of SEDC Motor

Due to its precise, simple, and continuous control characteristics [21], the separately excited DC motor is extensively employed in industrial drives. Particularly, the control of the position or/and speed of this motor with high accuracy and good dynamic response is an important issue and highly requested. On the other hand, the advances achieved in the field of power electronics have brought significant improvements in its operational performances, where the motor is necessarily being

used with the power electronic converter when operation under variable speed is required. Using this mechanism, two structures are, historically, presented to control the speed of DC motor.

2.5.1 Open Loop Speed Control of DC Motor

Generally speaking, the speed control of DC motor drive consists of taking the signal representing the set point speed and driving the motor to run at that speed. Historically, this is performed using either field resistance control or armature voltage control method, which are open loop methods. The field control method consists of maintaining constant the armature voltage and varying the field excitation current via an insertion of variable resistance in series with the stator windings, whereas in the armature voltage method, the field flux is held constant and the variation of motor speed is accomplished proportionally by increasing or decreasing the armature voltage. Due to the advances achieved in power electronics, both of the above methods can now implemented via open loop control structure using a rheostatic technique with the static converter. The main scope of application of this structure is in drives where an exact speed control is not essential [22]. However, in industrial applications such as rolling mills, where the drive response requires an accurate tracking of the set point speed and high operational performance of stability and robustness against reference and load disturbances, the system operation under open loop control structure becomes unsatisfactory and the closed loop control scheme is mandatory.

2.5.2 Closed Loop Control of DC Motor Speed

Modern industrial drives are required to present relatively high dynamical performance. Particularly, they have to achieve the reference signal tracking accurately and with fast dynamics. At the same time they have to ensure the system stability and robustness in all circumstances. In order to satisfactorily meet these requirements, the closed loop (feedback) structure of speed control system is designed.

The basic feedback loop structure which is used and implemented for the purpose of controlling the speed of DC motor is depicted in Fig. 2.5.

As it is illustrated in the figure, the used feedback control scheme is of cascade structure; which consists of an outer loop for rotational speed control and an inner loop

for the armature current control. The speed controller, in the outer loop, uses its output as a reference for the current controller, whereas the current controller, in the inner loop, uses its output as an input to the pulse width modulated (PWM) generator that controls the motor input voltage.

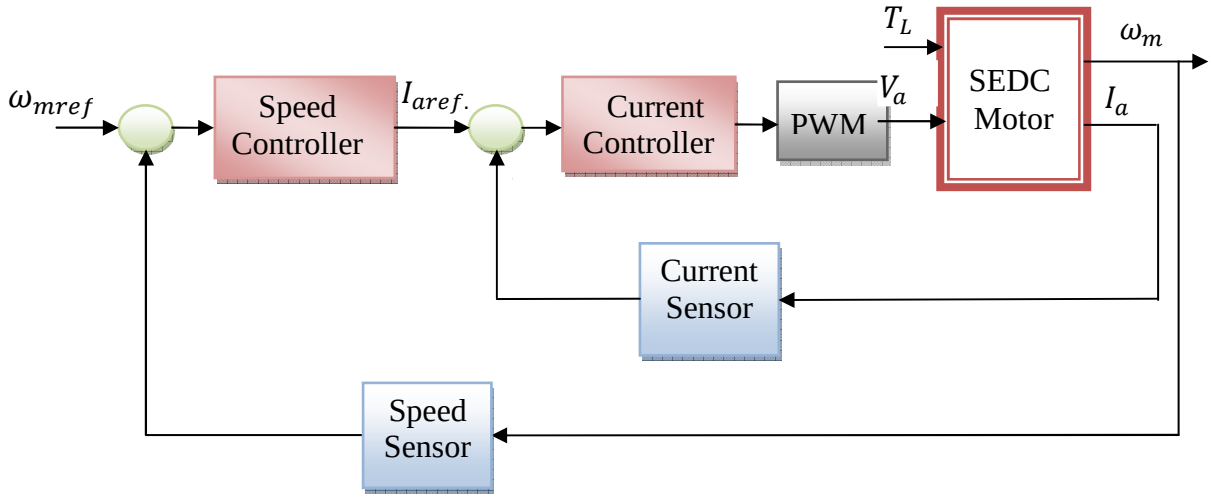

Figure 2.5 Cascade Structure of SEDC Motor Feedback Speed Control Loop.

2.5.2.1 Current Controller in DC Drive System

In DC drive control system, as for any electric drive, the need to control the current in motor armature is crucial because the mechanical time constant is very large compared with electric time constant. Consequently, at starting, the system with only speed controller present will produce a maximum error because of zero initial motor speed. As a result, a maximum voltage is given and resulting in very large current flow, which may exceed the motor maximum current limit and can damage the motor windings.

By applying current controller, the applied voltage V_a will become dependent not only on the speed error, but also on the current error that limits the produced current [23, 24]. On the other hand, the insertion of this controller in the whole control structure of the drive will speed up the output response [25].

2.5.3 Speed Controller Selection for SEDC Drive System

Now we see what type of controller is being selected to best fit the desired requirements. In fact, since researchers began to study automatic control in the 1930s [21], a wide spectrum of choices for control schemes and strategies have been introduced including the proportional-plus-integral-plus derivative (PID), adaptive, robust, and intelligent control algorithms. Studies and statistics have shown, however, that more than 95% of the industrial controllers are still implemented based around PI or PID algorithms [26],[22],[27], as no other controllers match the simplicity, clear functionality, applicability, and ease of use offered by this control algorithm [28],[29].

The PI (D) controller being used for most of industrial control problems, including process control, motor drives, automotive systems, flight control, instrumentation, comes in many different forms: as standard single loop controller, as a software component in programmable logic controllers or in distributed control systems [14]. Therefore, it is of prime importance to give more details on this particular control algorithm which represents the core element around which our study is about.

2.5.4 Implementation Forms of PID Controller

Basically, a PID controller generates control command signal $u(t)$ according to the controlled error signal $e(t)$. It consists of three parts: The proportional part generates a control action which is proportional to the error signal, the integral part which is the integral of the error signal, and the derivative part representing the changing rate of the error signal.

The study of the PID market, however, shows the existence of many forms or structures which are designed and manufactured, where, their knowledge, understanding as well as how their differences affect the determination of the tuning parameters is fundamental for the proper use and tuning of the controller and thus, ensuring good operating performance of the control system. Although the standard ideal structure is the mostly studied for design and implementation [30], there are different PID algorithm forms that are used by different manufacturers and which are mainly consisted in the following:

2.5.4.1 Standard Non Interacting Form

This structure is also known as the ideal form of PID controller. It is described, in time domain, by the following expression:

$$u(t) = K_p \left(e(t) + \frac{1}{T_i} \int_0^t e(\tau) d\tau + T_d \frac{d(t)}{dt} \right) \quad (2.25)$$

Where $u(t)$ is the control variable and $e(t)$ is the tracking error, defined as the difference between the set point or reference signal and the actual output one. The parameters of the controller are, respectively, the proportional gain K_p, the integral time constant T_i and the derivative time constant T_d.

The corresponding frequency domain of equation (2.25) is represented by the following controller transfer function:

$$G_c(s) = \frac{U(s)}{E(s)} = K_p \left(1 + \frac{1}{T_i s} + T_d s \right) = K_p \left(\frac{1 + T_i s + T_i T_d s^2}{T_i s} \right) \quad (2.26)$$

The block diagram representing this controller structure is illustrated in Fig.2.6 (a).

2.5.4.2 Parallel Non Interacting Form

An alternative non interacting structure version for PID controller (also known as parallel form) is represented, in time domain, by the following equation:

$$u(t) = K_p e(t) + K_i \int_0^t e(\tau) d\tau + K_d \frac{de(t)}{dt} \quad (2.27)$$

Its corresponding transfer function is given as:

$$G_c(s) = K_p + K_i \frac{1}{s} + K_d s = \frac{K_d s^2 + K_p s + K_i}{s} \quad (2.28)$$

Where, in this case, the controller's parameters are, respectively, the proportional gain K_p, the integral gain K_i and the derivative gain K_d.

This nomenclature of non interacting forms for the controller is because the integral time constant T_i (or integral gain K_i) does not influence the derivative part, and the derivative time constant T_d (or derivative gain K_d) does not influence the integral part;

thus, the parts are non interacting [30]. This is clearly depicted in the block diagram of Fig.2.6 (b).

2.5.4.3 Series Interacting Form

This form of PID structure is slightly different than the above two others in such a way the derivative part does influence the integral part. This interaction can be described, in the frequency domain, by the following transfer function:

$$G_c'(s) = K_p' \left(1 + \frac{1}{sT_i'}\right)(1 + sT_d') \tag{2.29}$$

Where K_p', T_i' and T_d' are the corresponding proportional, integral and derivative controller parameters respectively.

It is important to know that this interacting form can always be represented as a non interacting controller (eq. 2.26) whose coefficients are given by [30]:

$$K_p = K_p' \frac{K_i' + K_d'}{K_i'} \tag{2.30}$$

$$T_i = T_i' + T_d' \tag{2.31}$$

$$T_d = \frac{T_i' T_d'}{T_i' + T_d'} \tag{2.32}$$

Conversely, when $T_i \geq 4T_d$, the non interacting controller (2.26) can also be represented as an interacting form (2.29) whose coefficients are given by:

$$K_p' = \frac{K_p}{2}\left(1 + \sqrt{1 - \frac{4T_d}{T_i}}\right) \tag{2.33}$$

$$T_i' = \frac{T_i}{2}\left(1 + \sqrt{1 - \frac{4T_d}{T_i}}\right) \tag{2.34}$$

$$T_d' = \frac{T_i}{2}\left(1 - \sqrt{1 - \frac{4T_d}{T_i}}\right) \tag{2.35}$$

The interacting architecture of PID controller described earlier is, however, most common among single-loop controllers and, for historical reasons, it is still produced

by many manufacturers [21]; because early PID pneumatic controllers were easier to build using interacting form and when they changed the technology from pneumatic to analog electric and then to digital, they kept the interacting form.

The block diagrams of the above structures are grouped respectively in Fig.2.6.

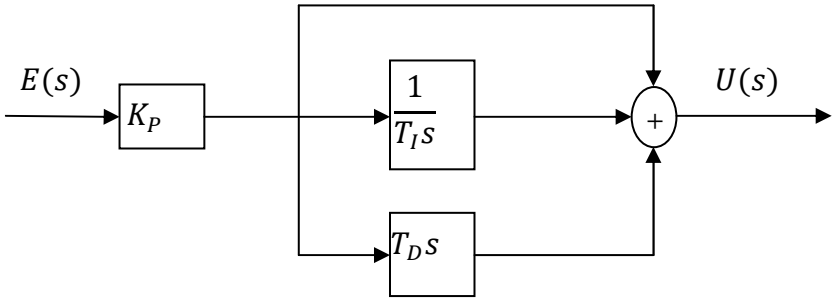

(a) Standard Non Interactive Structure.

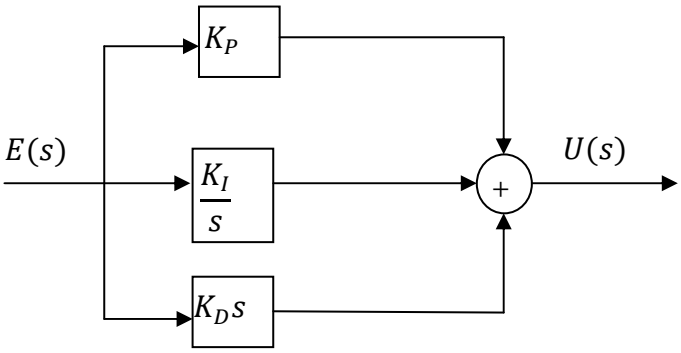

(b) Parallel Non Interacting PID Structure.

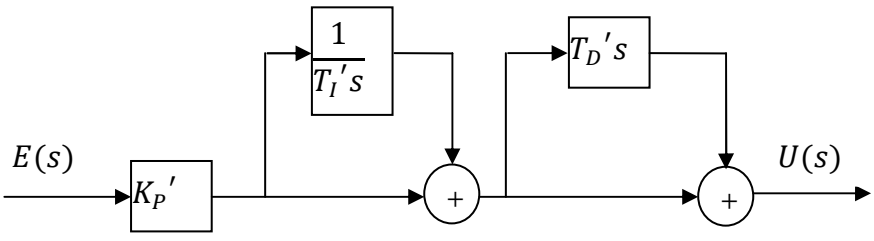

(c) Series Interacting PID Structure.

Figure 2.6 Interacting and Non- Interacting Forms of PID Controller.

From practical point of view, this typology of PID controller and its classification to the above structures are of paramount importance and significance due to the fact that these structures are of different parameter settings. Accordingly, if a controller of a certain form in a certain control loop is replaced by another controller form, the controller parameters are never the same and have to be changed. It is, however, interesting to note that the interacting and non-interacting forms are different only when the integral and derivative parts of the controller are used together. In other words, if we only use the controller as a P, PD, or PI controller, the two forms are equivalent [31], which can be deduced from the above presentation.

2.5.5 PI versus PID Utilization in DC Drive Control Systems

In the field of electric drive systems, the PI-type controller is rather used for speed/position and current control (or regulation) purposes [32, 28] because derivative action is not used very often due to its kicks effects on the drive performance. Consequently, this type of controller is being our choice as the basic speed and current controllers in the aforementioned cascade structure of speed controlled DC drive system.

2.6 State Observer Based Feedback Speed Control of DC Drive

It is common knowledge that electrical drives, especially DC drives, are essential parts of many manufacturing processes. As a fact of matter, they should be adequately controlled not only to decrease power consumption and making the exploitable life of the drive longer, but also to ensure drive safety and improved product quality.

Typically, when the industrial drive is designed, the different friction types, the elasticity of the shaft and its corresponding torsional vibration as well as noise effect, are neglected. In the case of the standard drive such an assumption is reasonable; however, there is a large group of drives, like: rolling-mill drives, conveyer belt, modern servo-drives, robot-arm, these characteristic features of the mechanical part cannot be neglected and have to be included in the analysis [33]-[35]. Therefore, satisfactory speed control of these drives cannot be attained using classical cascade

control system through direct feedback sensors and with a simple PI speed and current controllers [36].

To overcome this serious control problem, approaches have been developed or proposed in order to suppress the torsional vibrations effect and achieving high dynamical performance of the drive systems with elastic couplings. In this vein, one approach is based on proposing controller alternatives to replace completely the conventional PI controller within the feedback loop with those nonconventional controllers such as Fuzzy Controller (FC), NN controller and others which are stated previously in chapter one. The second approach consists of altering structural modifications on the original PI based speed control system of the drive with additional feedbacks or other compensators. One method of these is presented in [37] and is based on the modification of the speed controller parameters setting. More advanced control techniques are based on applying additional feedbacks from a selected state variable. This is reported in [38], where nine different control structures with one additional feedback are presented and compared. But the most advanced control structures, which allowed free setting of the system dynamics, are based on the application of the additional feedbacks from all state variables and known under the name State Feedback Control structure [39].

The design of state feedback controller is able to ensure and guarantee good and improved performance characteristics of both transient and steady state responses. Unfortunately, due to parameters variation, this control strategy does not maintain the desired performance of drives with elastic coupling. Moreover, the synthesis of state-feedback control assumes that all the process states are measurable or that they can be generated from the output. In many practical control systems it is physically or economically impractical to install all the transducers which would be necessary to measure all of the states. Under these conditions, it becomes necessary, if full state feedback is required, to observe or estimate the state variables [40] from the availability of only a reduced set of information. This estimation (reconstruction) of the plant states requires, however, that all the original control system states be observable [41]. If this is the case, the control solution consists of designing a dynamical control system based on building a state observer, which is used to estimate

the state variable vector $x(t)$ from the knowledge of the control inputs $u(t)$ and the output information $y(t)$. Using the state space model of the DC motor presented earlier, the idea of state observer based control system is illustrated by the block diagram of Fig.2.7.

By referring the equation (2.23), which describes the state space model of SEDC motor coupled to the mechanical load, we can define and identify the variables and matrices appearing in this block diagram as follows:

$x(t) = [x_1(t) \quad x_2(t)] = [\omega_m(t) \quad i_a(t)]$: Represents the state variables vector;

$y(t) = [y_1(t)] = [\omega_m(t)]$: Represents the output vector of single element;

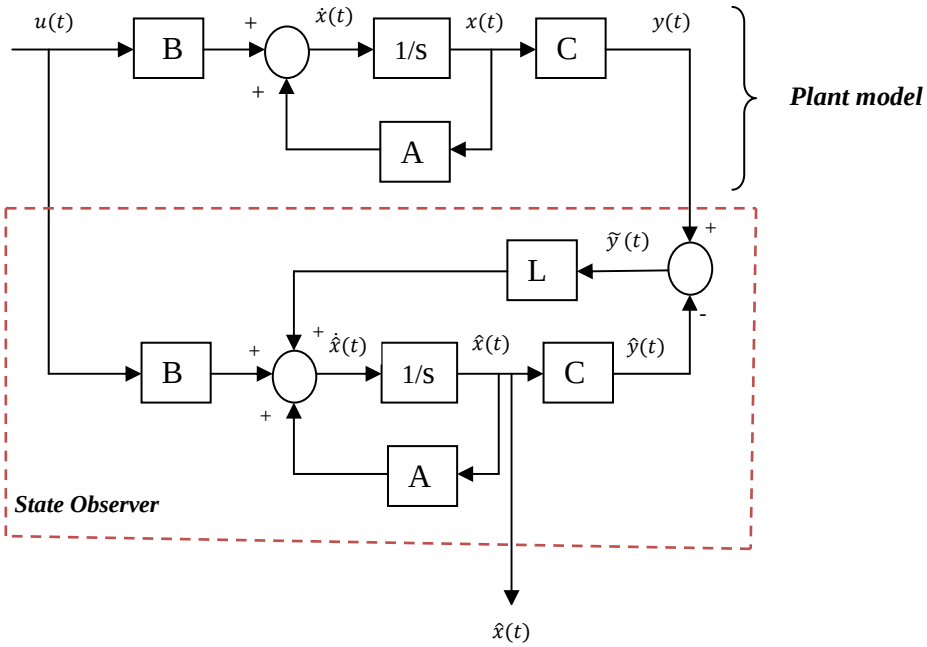

Figure 2.7 General Structure of State Observer based Control System of DC Motor

$u(t) = [u_1(t) \quad u_2(t)] = [v_a(t) \quad T_L(t)]$: is the input vector of the system;

$A = \begin{bmatrix} -\frac{R_a}{L_a} & -\frac{K_b}{L_a} \\ \frac{K_t}{J} & -\frac{\beta}{J} \end{bmatrix}$ is the (2×2) state matrix.

$B = \begin{bmatrix} \frac{1}{L_a} & 0 \\ 0 & -\frac{1}{J} \end{bmatrix}$ is the (2×2) control matrix.

$C = \begin{bmatrix} 0 \\ 1 \end{bmatrix}$ is the (2×1)output matrix.

$\hat{x}(t), \hat{y}(t)$: are respectively the estimated vectors of state variable and plant output.

When these are defined, the designed state observer is built based on the knowledge of the exact model of DC motor (A, B, C) and the error correcting part defined by:

$$L(y(t) - \hat{y}(t)) \tag{2.36}$$

With L represents the observer gain matrix.

As it is shown in Fig.2.7, the state observer uses the input signals $(u(t), y(t))$ and outputs the estimate state variable $\hat{x}(t)$, where its design is based on the selection of the gain matrix L.

With this design of state observer, the description of the whole structure of separately excited DC motor based speed control drive system is done. The design details, however, is beyond the scope of our study. Instead, basically we worked out four PI speed controlled and state observer based models, which are elaborated in [42] for improving and perfecting dynamic and steady state performance of PI based speed controlled DC drive system already implemented in steel rolling mill industries.

2.7 Elaborated PI based Speed Controlled DC Drive Models for Performance Improvement

Based on the details that we have presented throughout this chapter, we end up in this section to give the models resulted from the combined utilization of PI controller and state observer in controlling the speed of SEDC motor based electromechanical system. Furthermore, these models will be investigated and subjected to performance improvement study in the subsequent chapters.

2.7.1 System Model with 1PI Speed Controller and State Observer of Order 2

In this model, we will study the transient and steady state performance of the system when a single PI controller is used to control the speed of the DC motor together with state observer of order two to estimate the mechanical non measureable parameters. This model is represented by MATLAB/Simulink block diagram in Fig.2.8.

The state observer appearing in this model block diagram is of order two, where its structure is mentioned in Fig.2.9.

The same thing is done for the other models, where their block diagrams including the state observer ones are given in the subsequent figures.

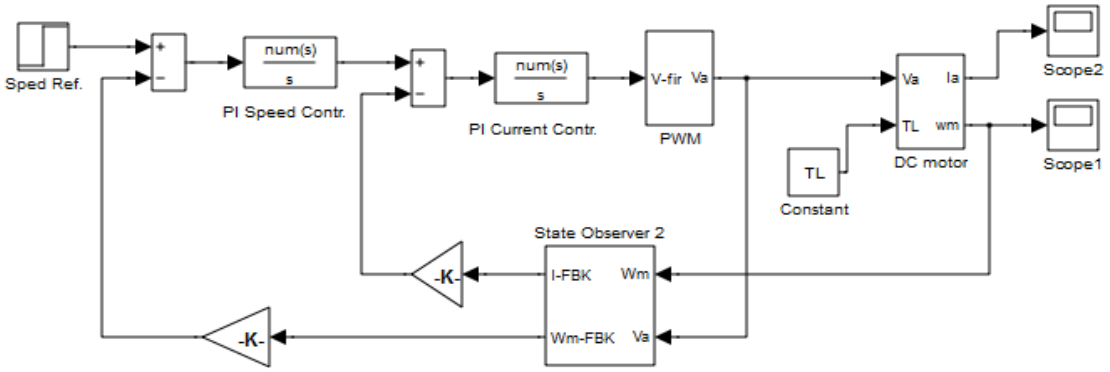

Figure 2.8 Simulink Block Diagram of Model with 1PI Speed Controller and 2nd order State Observer based DC Drive System.

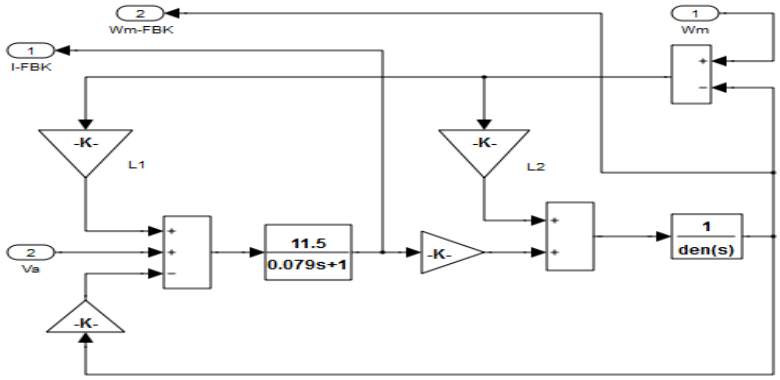

Figure 2.9 Simulink Block Diagram of 2nd order State Observer Structure.

2.7.2 System Model with 2PI Speed Controller and State Observer of Order 2

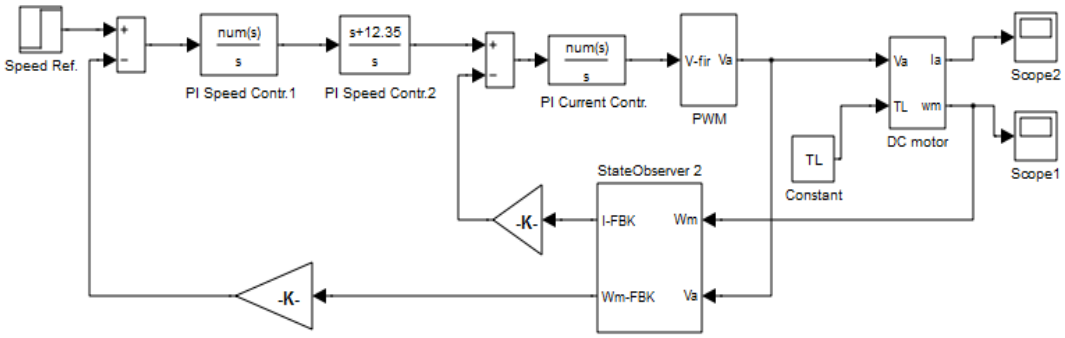

Figure 2.10 Simulink Block Diagram of Model with 2PI Speed Controller and 2nd order State Observer based DC Drive System.

The state observer block diagram of this model is the same as that of Fig.2.9.

2.7.3 System Model with 1PI Speed Controller and State Observer of Order 5

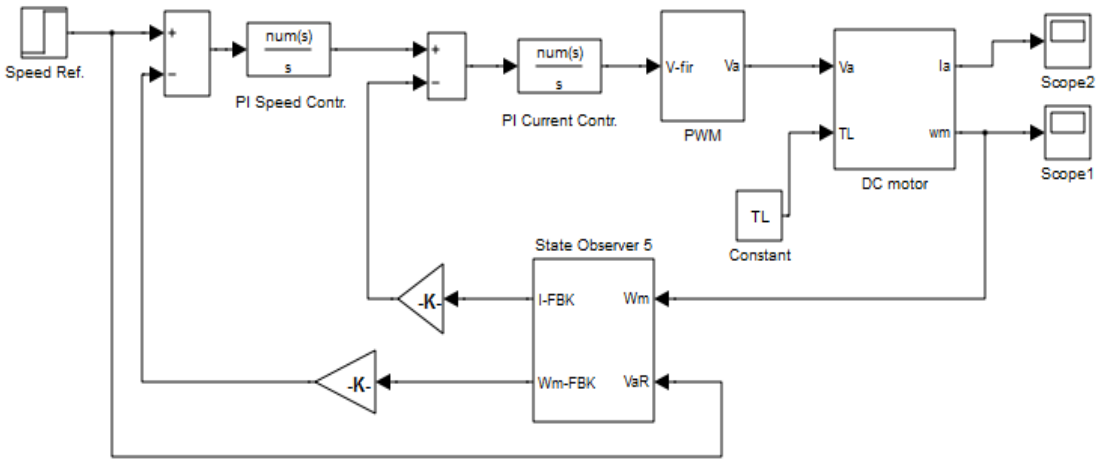

Figure 2.11 Simulink Block Diagram Model of one PI Speed Controller and 5th order State Observer based DC Drive System.

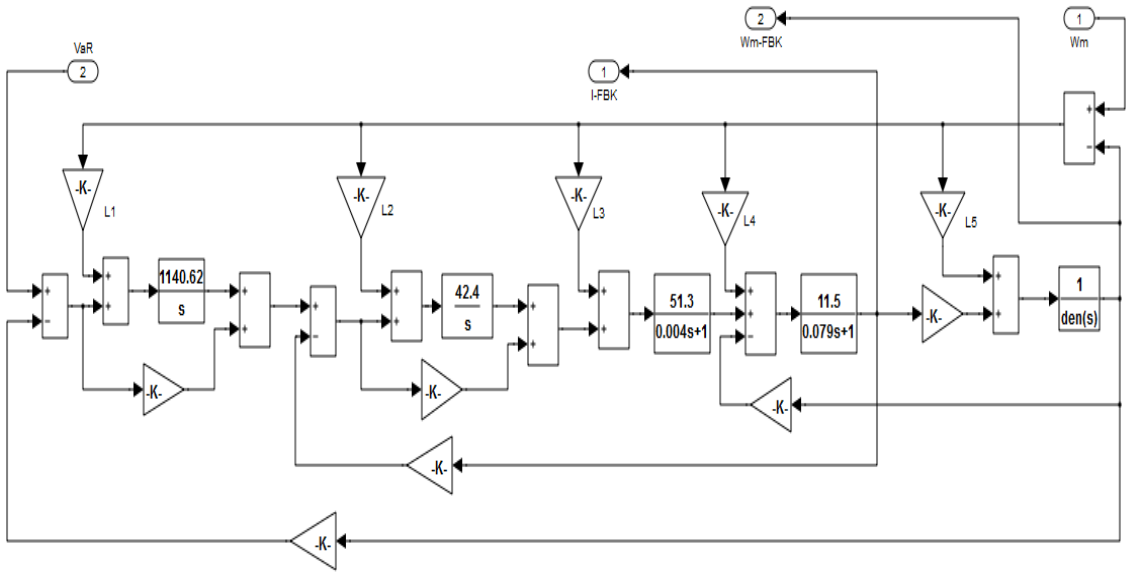

Figure 2.12 Simulink Block Diagram of 5th order State Observer Structure.

The used values for the gain matrix parameters of the above state observers are given in Appendix B (Table B.1).

2.7.4 System Model with 2PI Speed Controller and State Observer of Order 6

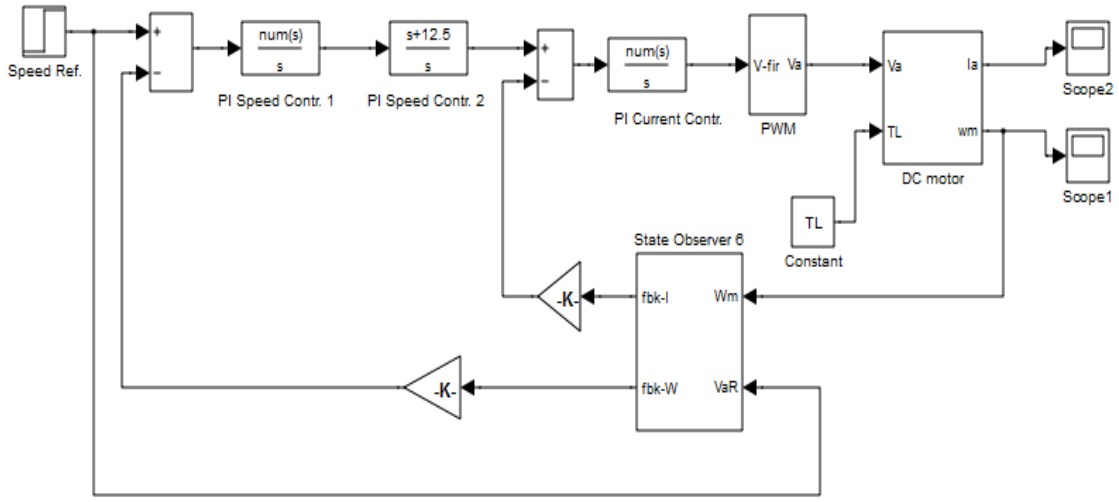

Figure 2.13 Simulink Block Diagram Model of 2PI Speed Controller and 6th order State Observer based DC Drive System.

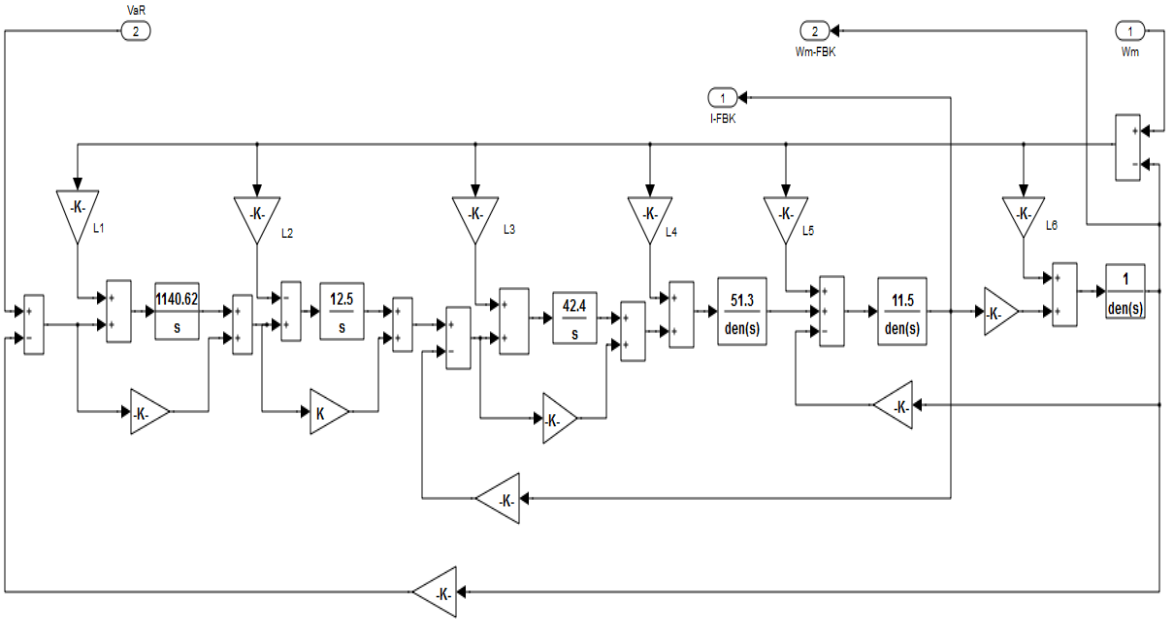

Figure 2.14 Simulink Block Diagram of 6th order State Observer Structure.

The used values for the gain matrix parameters of this state observer are given in Appendix B (Table B.1).

2.8 Conclusion

In this chapter, the objective was mainly to provide details on the control structure of the separately excited DC motor based electromechanical system widely used in paper and steel rolling mill industries and which is the subject of the whole study throughout the realization of this work.

First, the electrical and mechanical characteristics of the DC motor are modeled where the viscous friction is particularly considered via the appearance of its model in the whole model of the motor. The model is being used to implement the speed controller for the drive system.

After a thorough description of the fundamental components of the control structure that is being the basis of speed controller of SEDC drive system, an elaborated system models are selected to carry out the study of improvement and perfecting the systems' operating performances.

Chapter 3

DC Drive Dynamic Performance Optimization using Mini-Max Approach

3.1 Introduction

Feedback control systems are, generally, built to modify the behavior of a process so it behaves in a specific desirable way over time. For the rolling mill DC drive system at hand, we often require the speed response to have good dynamic and steady state performance characteristics although the variation and changes of external input and load disturbances.

When designing feedback control systems, however, we require that system to have clear criteria for what makes one controller preferable to another. Mainly, these criteria that allow us to qualify and quantify both dynamic (transient) and steady state performances are stability, overshoot, settling time, rise time and accuracy. All these performance metrics of control systems can be classified as stability, transient performance and steady state performance. By postponing the study of steady state performance for the next chapter, we devote the content of this chapter to study and analyze the dynamic performance properties and its relation to the stability of our state observer PI speed controlled DC drive system, where, we propose Mini-Max optimization approach to improve these performance characteristics.

3.2 Dynamic Performance Properties of PI Speed Controlled DC Drive

A practical control system cannot respond instantaneously to input excitation and disturbance; it exhibits, however, a transient response with damped oscillations

before reaching its steady state. This response is characterized by some index properties representing at the same time the parametric metrics used to describe the dynamic performance characteristics of the response. Frequently, such performance characteristics are specified in terms of transient response to step input, because such an input is easy to generate and is sufficiently drastic, in such a way, if the response of a linear system to a step input is known, it is mathematically possible to compute the system's response to any other input.

Most importantly, these characteristic terms are named as the following [40, 43]:

- **Rise Time (t_r):** this is defined as the time required for the response to rise from 10 % to 90 % of its final value. It is possible to define other limits as well, but in our work we shall use these percentages.

- **Peak Time (t_p):** it is defined as the time required for the response to reach the first peak of the overshoot.

- **Maximum Overshoot (M_p):** it is defined as the maximum peak value of the step response curve, measured from the final steady state value. If $Y(t_p)$ is maximum response at the peak time and Y_{ss} is the steady state value of the response, then it is common practice to use the following definition of the maximum percent overshoot as follows:

$$Maximum\ Percent\ Overshoot = \%\ M_p = \frac{Y(t_p) - Y_{ss}}{Y_{ss}} \times 100\ \% \qquad (3.1)$$

- **Settling Time (t_s):** is defined as the time required for the response curve to reach and stay within 5 % of the final steady state value. In some cases, 2% instead of 5 % is used as the percentage of the final value [44]. The settling time is the largest time constant of the system.

For the sake of illustration, these performance properties and specifications are mentioned in Fig.3.1 illustrating a typical control system step response of PI speed controlled DC drive system.

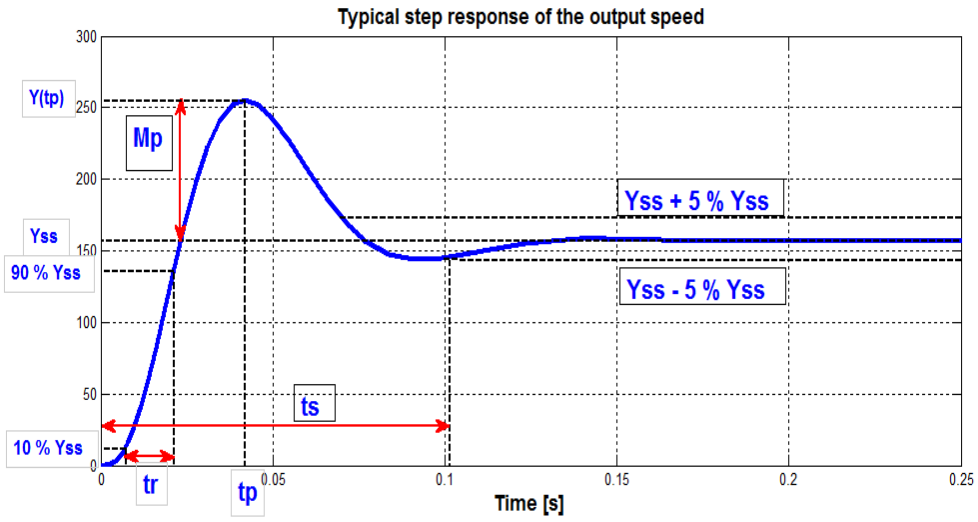

Figure 3.1 Typical Step Response of DC Drive Control System.

It is noticeable from this typical step response of control system that during the transient regime, the output response is quite different of the desired response due to the appearance of the above defined transient properties characterizing this portion of the response, which reveals its importance in any control system design.

In other words, in addition of requiring a dynamic system to be stable, i.e., its response does not increase unbounded with time; we also require its response:

• To be fast (**small rise time**);

• does not excessively overshoot the desired value (**small percent overshoot**); and

• To reach and remain close to the desired reference value in the minimum time possible (**small settling time**).

3.3 Stability vs. Overshoot Performance Properties

One may ask about the relationship between the stability criterion and the overshoot transient performance metric of the control system behavior. By definition, a stable system is the system for which a bounded input always produces a bounded output [45]. However, in practice we do not see unbounded outputs due to saturation effects and therefore, for systems with bounded (saturated) control inputs and/or outputs, instability can manifest itself as a *limit cycles* that cause the controlled system to behave with an oscillatory manner, which is an undesirable property. Consequently,

the stability of the whole control system represents the basic and important conceptual and practical performance property that should be guaranteed by the designed controller. Two commonly used quantities that measure the stability margin when designing a control system and which are directly related to the stability criterion stated by Nyquist [46, 47]. These are the gain margin (G_M) and phase margin (ϕ_M) defined, respectively, as the factor by which the open loop gain of the system can be raised before reaching the instability point and the amount by which the system's phase exceeds – 180° at unity gain. Thus, the transient response overshoot of a control system is, in fact, related to its stability via these two defined gain quantities.

3.3.1 Relationship between Stability Margins and Percent Overshoot

This relationship can be explained and mentioned by referring to the closed loop transfer function of any 2nd order control system, which can, in general, be expressed as [48]:

$$G_{cl}(s) = \frac{K{\omega_0}^2}{s^2+2\zeta\omega_0 s+{\omega_0}^2} \tag{3.2}$$

With $K, \omega_0 \; and \; \zeta$ are, respectively the system's loop gain, response natural frequency and the response damping ration.

In this case, the phase margin ϕ_M is more commonly used to specify both stability and transient performances of control system due to its relationship with the damping ratio of the system. For the case where the system is described by the transfer function (3.2), this relationship is expressed as [41, 49, 50]:

$$\phi_M = \; tan^{-1}\left[\frac{2\zeta}{\sqrt{\sqrt{1+4\zeta^4}-2\zeta^2}}\right] \tag{3.3}$$

When this expression is plotted in a (ζ, ϕ_M) plane, we can obtain that ϕ_M varies with respect to the damping ratio approximately as a straight line up to about: $\phi_M \cong 70^\circ$. For this reason, when the system is of order two, it is accurate enough to approximate the relationship between the phase margin (ϕ_M) below 70° and the damping ratio by the expression [41]:

$$\zeta \cong \frac{\phi_M}{100} \tag{3.4}$$

Additionally, for the sake of finding an aid to evaluate the second order control system performance based on its phase margin, it is derived an expression that relates the system damping ration (ζ) and the response maximum overshoot (M_P) as [41]:

$$M_P = e^{-(\frac{\pi\zeta}{\sqrt{1-\zeta^2}})} \tag{3.5}$$

The expressions (3.3) and (3.5) can be converted into graphical plots which mention clearly the relationship between the triple (M_P, ϕ_M, ζ) as it is depicted in Fig.3.2 [51].

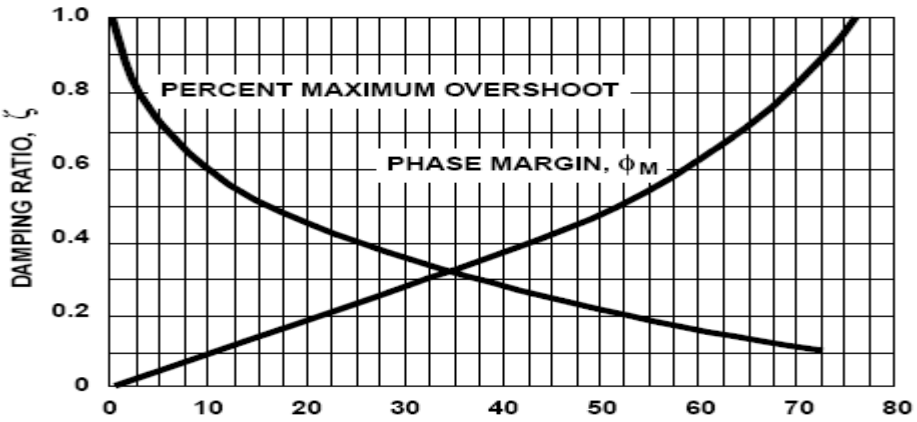

Figure 3.2 Percent Overshoot and Phase Margin as a function of Damping Ratio ζ.

Therefore, we see that, given the (ϕ_M), one can infer information about what the overshoot of the closed-loop step response would be and vice versa. Also, it is obvious that the reduction of percent overshoot leads to increasing the phase margin and hence more stability is achieved.

We will refer to this explanation when discussing the results that show the improvement achieved in dynamic performance of the drive system at hand.

3.4 Dynamic Performance Improvement by Tuning PI Parameters

In spite of the availability of advanced and intelligent control algorithms that have been developed, the PID controller remains the most popular and widely used in

industry. This is mainly due to the simplicity and few tuning parameters of this control law.

But the PID controller with fixed parameters fails, generally, to respond to the desired process specifications and performances as the operating level moves away from the original design [52], thus the controller parameters have to be tuned to the controlled variable allowing the process to be kept at its desired operating condition. Hundreds of tools, methods and theories are available for this purpose. However, finding appropriate parameters for the PID controller is still a difficult task, so in practice control engineers still often use trial and error for tuning the parameters of this controller based processes according to the following highlighted functionalities of three parameters:

• The proportional term (P): is used to provide an overall control action proportional to the error signal.

• The integral term (I): is used to reduce steady-state errors through low-frequency compensation by an integrator.

• The derivative term (D): used generally to improve transient response through high-frequency compensation by a differentiator.

The individual effects of these three terms on the closed-loop performance are summarized in Table 3.1.

Table 3.1 Effect of Changing Independently PID Parameters on System Response

Closed Loop Response	***Rise Time***	***Overshoot***	***Settling Time***	***Steady State Error***	***Stability***
Increasing K_P	decrease	Increase	Small Increase	Decrease	Degrade
Increasing K_I	Small Decrease	Increase	Increase	Large Decrease	Degrade
Increasing K_D	Small Decrease	decrease	Decrease	Minor Change	Improve

This table serves, however, as a first guide for stable open loop plants only [29]. But for optimum performance, the three controller parameters are mutually dependent in tuning.

In this sight, we present in this work the Mini-Max as a simple and model free optimization approach to optimally tuning the parameters of PI speed controller and hence achieving improvement of DC drive system performance. Before giving the results showing the efficiency of this approach, it is worthwhile to present a state of the art and literature overview of a number of the available methods for PID control design and tuning with discussion of advantages, disadvantages and applicability of these methods. We should notice here that these tuning methods and techniques are generally used for PID controller; however, they are also used for the particular case of PI controller.

3.5 Tuning Methods for PID Controller

Broadly speaking, PI and PID tuning methods can be classified into the following categories: trial and error feature based methods, analytical methods and optimization methods. Under these categories, a plenty of techniques and methods are reported in literature [53].

3.5.1 Plant Features Based Tuning Methods

3.5.1.1 Zeigler and Nichols Tuning Methods

In 1942, J. G. Ziegler and N. B. Nichols, both of the Taylor Instrument Companies (Rochester, NY) published a paper [54] that described two methods for PID controller tuning based on simple characterization of process dynamics in the time and frequency domains. The idea was to perform a simple experiment, extract some features of process dynamics from the experiment and determine thereafter the performance settings or tuning parameters of the controller according to the empirical formulas developed for this purpose, where the objective of the design was to find a P, PI or PID controller which give the Quarter Amplitude Damping (QAD) ratio of the control systems in response to load disturbance [55]. Both methods assume that the

process can be represented by two parameters model, comprising a pure integrator and dead time described under the form of:

$$G(s) = \frac{a}{sL}\, e^{-sL} \tag{3.6}$$

Ziegler and Nichols have recognized that a large variety of industrial processes can be approximated by the model (3.6) and if the system model cannot be physically derived, experiments are performed to extract the parameters for the approximate model (3.6). Effectively they performed two experiments which have led to their two famous tuning methods, respectively, named as step response and frequency response methods, which we will briefly describe in the following.

a- Ziegler-Nichols Step Response Method

The first method is the open loop method, also known as the step response and process "reaction curve" method. It consists of measuring the open loop unit step response of the process, which is characterized by the parameters *a* and *L* describing, respectively, the intercept of the steepest tangent of the step response with the coordinate axis and the approximating system time delay. With these two measured parameters, Ziegler and Nichols have put the formulas shown in Table 3.2 that can be used to determine the controller settings.

Table 3.2 Ziegler-Nichols Formulas for Step Response Tuning Method.

Controller type	K_p	T_i	T_d
P	$1/a$	-	-
PI	$0.9/a$	$3L$	-
PID	$1.2/a$	$2L$	$L/2$

b- Ziegler-Nichols frequency Response Method

This is the second experiment done by Ziegler and Nichols to formulate their frequency response method of PID controller tuning. This method, also known as closed loop tuning method [31], consists of performing the following steps:

1. Place controller into P mode with low gain, no reset or derivative.

2. Gradually increase the gain, and making small changes in the set point (or load), until oscillations start.
3. Adjust the gain to make stable oscillations on the stability limit with constant amplitude.
4. Note this gain (ultimate gain, K_u) and period of oscillations (ultimate period, T_u)

Having these two experimentally measured parameters, Ziegler and Nichols have deduced the formulas mentioned in Table 3.3 for obtaining P, PI and PID controller settings.

Table 3.3 Ziegler-Nichols Formulas for Frequency Response Tuning Method.

Controller type	K_p	T_i	T_d
P	$0.5K_u$	-	-
PI	$0.4K_u$	$0.8T_u$	-
PID	$0.6K_u$	$0.5T_u$	$1.2T_u$

Due to their simplicity to use and the very little information required about the process, these methods of Ziegler and Nichols had a huge impact when they were introduced in the 1940s, and they gave initial conditions for manual tuning. Consequently, they are still widely used and adopted by manufacturers of controllers for routine use.

Unfortunately, the application of Ziegler–Nichols tuning rules has found several severe drawbacks. Mainly, the system needs to be brought to its limit of stability, which may affect, under some disturbance, the system operation. This is apparent especially in the case when the process is an electromechanical system. In addition to the applicability restriction for the industrial processes, the obtained control system using these methods suffers the lack of robustness [45], [56].

3.5.1.2 Cohen-Coon Tuning Method

In 1953, G.H. Cohen and G.A. Coon proposed an experimental tuning method for PID controller. The method is based on the First Order Plus Dead Time (FOPDT) process model comprising the parameters process static gain *k*, process time constant *T*

and the dead time *L*, the whole are represented in the following transfer function modelling the engineering process [57]:

$$G(s) = \frac{k}{1+sT}\, e^{-sL} \tag{3.7}$$

The Cohen-Coon method is similar to the Ziegler-Nichols reaction curve method to determine the three parameters of FOPDT model and achieving the design specification for quarter decay amplitude (QAD) ratio in response to set point (or load disturbance) change.

The experiment has led to the controller parameters settings shown in the Table 3.4.

Table 3.4 Cohen-Coon Controller Tuning Parameters

Controller type	K_p	T_i	T_d
P	$\frac{1}{k}\frac{T}{L}\left[1+\frac{L}{3T}\right]$	-	-
PI	$\frac{1}{k}\frac{T}{L}\left[0.9+\frac{L}{12T}\right]$	$\frac{L[30T+3L]}{9T+20L}$	-
PD	$\frac{1}{k}\frac{T}{L}\left[1.25+\frac{L}{6T}\right]$	-	$\frac{L[6T-2L]}{22T+3L}$
PID	$\frac{1}{k}\frac{T}{L}\left[\frac{4}{3}+\frac{L}{4T}\right]$	$\frac{L[32T+6L]}{13T+8L}$	$\frac{4TL}{11T+2L}$

This method, besides its restriction to only FOPDT process model, the obtained tuning parameters are more complex, involving more arithmetic operations.

3.5.1.3 Relay Feedback Tuning Method

In an attempt of improving Ziegler-Nichols frequency response tuning method and overcoming some of its drawbacks, Karl Johan Astrom and Tore Hagglund proposed, in 1984, their novel relay feedback technique of PID controller tuning [58]. The method is described by the block diagram of Fig.3.3.

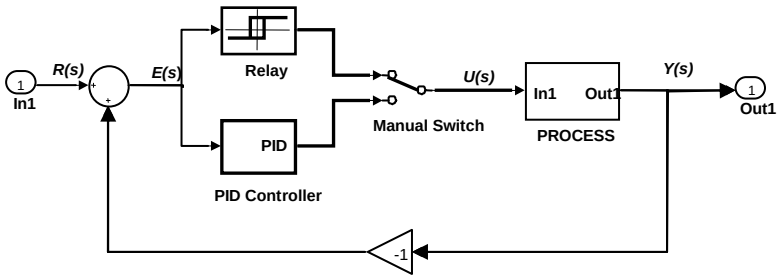

Figure 3.3 Block Diagram of Relay Feedback Tuning Method, in Tuning Mode the Process is connected to Relay Feedback [22].

For many years, Ziegler-Nichols tuning techniques were strictly manual operations executed whenever a new control loop was commissioned. An engineer would run a Ziegler- Nichols test, record the control effort and resulting process variable on a strip chart, divine the behaviour of the process from trend line shapes, tune the loop to match the process, and then start production with the new loop in automatic mode.

It was tedious and repetitive work to commission every loop this way, and results weren't always satisfactory. Several iterations were often necessary to generate tuning parameters that produce acceptable closed-loop performance.

With relay feedback tuning method, the whole of this manual procedure is automated. This is done by connecting the process in a feedback loop with a nonlinear element having a relay function as shown in Fig.3.3 [45]. When it is desired to tune the system, the PID function is disconnected and the system is connected to relay control. The system then starts to oscillate. The period and the amplitude of the oscillation are determined when steady-state oscillation is obtained. This gives the ultimate period and the ultimate gain. The parameters of a PID controller can then be determined from these values. The PID controller is then automatically switched in again, and the control is executed with the new PID parameters.

In spite of the enhancements achieved to render the method more performing auto-tuner, critics have claimed its lack of robustness against load disturbance, measurement noise and model uncertainties [58]-[60].

We can notice that many of the methods presented in this section are based on the work done by Ziegler and Nichols, and use very simple process models to derive

tuning rules. The advantage is that the methods are very easy to use, and do, in general, not require extensive knowledge of the process. However, this leads also to unknown stability robustness and no good control over the resulting performance, where the applicability of these methods is generally limited only to the worked out process industry.

3.5.2 Analytical Tuning Methods

There are several analytical tuning methods where the controller parameters and thus its transfer function are obtained from the specifications by a direct calculation. If $G_p(s)$ and $G_c(s)$ are, respectively, the transfer functions of the process and controller, the corresponding closed loop transfer function for a unity feedback control system is given as follows:

$$G_{cl}(s) = \frac{G_c(s)G_p(s)}{1+G_c(s)G_p(s)} \tag{3.8}$$

Solving this equation for the controller transfer function, we obtain:

$$G_c(s) = \frac{1}{G_p(s)} \frac{G_{cl}(s)}{1-G_{cl}(s)} \tag{3.9}$$

Based on the knowledge of process and closed loop transfer functions, the PID controller parameters can be determined. In the following we will discuss the different methods proposed for this purpose.

3.5.2.1 Pole Placement Tuning Method

The pole placement tuning method simply attempts to find a controller that gives desired closed-loop Poles [61], [62]. It is based on the knowledge of process transfer function.

By choosing arbitrarily the closed loop poles of the system, the parameters of the PID controller can be determined by solving the closed loop characteristic equation of unknown controller parameters, defined generally as:

$$1 + G_c(s)G_p(s) = 0 \tag{3.10}$$

The pole placement tuning method, as it is obvious from the equation, requires the equality of the controller parameters to be obtained to the number of closed loop

desired poles. Which means that a second-order closed loop system of two poles can be specified to determine the two parameters of PI controller. The calculations involved, however, in finding the controller parameters are more complicated, especially for the case of high order and complex process models, which implies an increased order of the controllers. Therefore, to obtain PID controllers it is necessary to restrict the models to first- or second-order systems, otherwise, model approximation techniques should be applied for those complex processes of order higher than three and which are controlled using PID controller [63].

3.5.2.2 Dominant Pole Placement Tuning Method

The difficulty with the direct pole placement tuning method presented previously is that further to the more computation involved in controller parameters settings calculation, it leads to complex controller design for complex and high order process model. An improvement version of this method is the dominant pole placement tuning method proposed by Astrom and Hagglund [62] and which is based on placing just a few poles of the closed loop, which are considered dominant for the closed loop response. Astrom and Hagglund noted that the behavior of many closed loop systems is determined by two dominant poles and they configured this in the s-plane as it is illustrated in Fig.3.4.

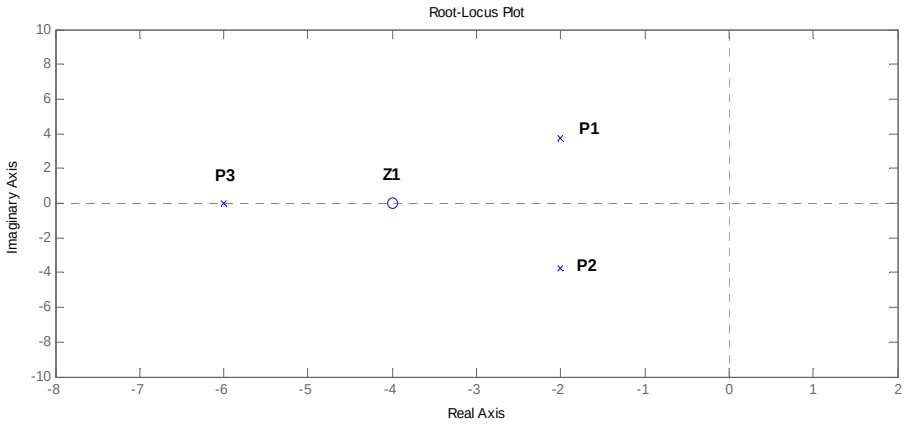

Figure 3.4 Pole-Zero Configuration of a Simple Feedback System used by Dominant Pole Tuning Method

Where ‘P1’ and ‘P2’ are considered as dominant poles.

If this configuration applies to the controlled system, it is possible to place the dominant poles at desired locations and the parameters of the controller are calculated, such that the dominant poles are located at desired pole locations, specified by their frequency ω_0 and relative damping ζ as:

$$P1 = -\zeta + j\omega_0\sqrt{1-\zeta^2} = -\sigma + j\omega \tag{3.11}$$

$$P2 = -\zeta - j\omega_0\sqrt{1-\zeta^2} = -\sigma - j\omega \tag{3.12}$$

For PID controller, three closed loop poles can be positioned, so a third pole is chosen at ($-\alpha_0\omega_0$), according to [62].

This method is applicable to higher-order processes, with ω_0 and ζ as the design parameters and provided that the process pole-zero configuration resembles to that of Fig.3.4, which is a disadvantage aspect of the method, because if the process has a pole far away in the left half plane can be moved towards the right and become a dominating pole, this will lead to an unexpected response. Although, this can be prevented by choosing the desired frequency ω_0 not too high, the application of the method remains restricted for processes that fall in the class of test processes representing time delay, high order and non-minimum phase behavior [41].

3.5.2.3 Internal Model Control (IMC) Tuning Method

The internal model principle, first proposed by Danlel E. Revera *et al.* in 1986 [64], is a general method for designing control systems that can be applied to PID control. To briefly explain its use in controller parameters tuning, we consider the block diagram of Fig.3.5.

In the block diagram, it is assumed that all disturbances acting on the process are reduced to an equivalent disturbance *D(s)* at the process output and the dynamics of the process are described by first order plus dead time (FOPDT) model [22], defined previously by the equation (3.7) and restated here for convenience as:

$$G_p(s) = \frac{k}{1+sT}\, e^{-sL} \tag{3.13}$$

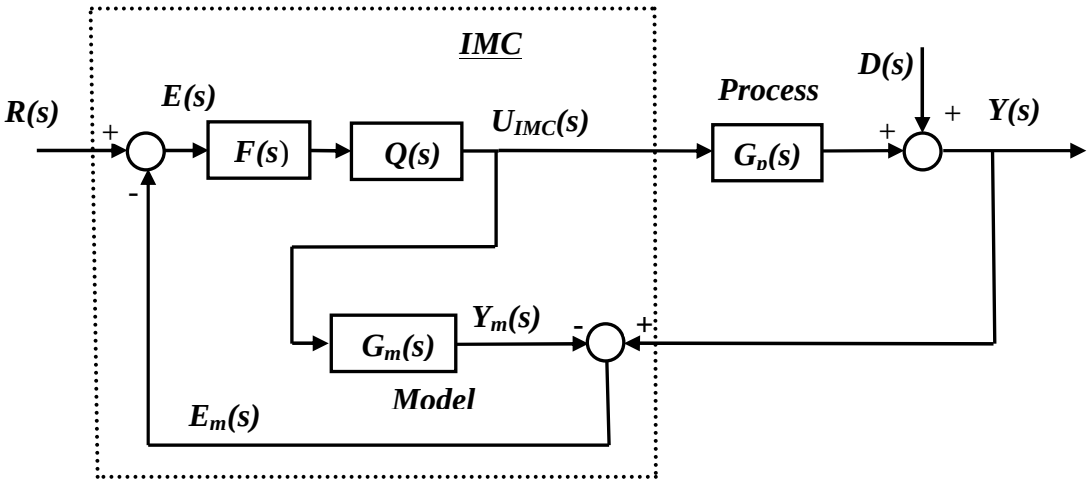

Figure3.5 Internal Model Control Structure Block Diagram for PID Tuning

As it is noticeable, internal model control is model based controller design and tuning method. It makes use of process model to infer analytically the tuning parameters of the controller, whose transfer function contains explicitly the suggested process model $G_m(s)$ and is expressed as [64]-[66]:

$$G_c(s) = \frac{F(s)Q(s)}{1-F(s)Q(s)G_m(s)} \tag{3.14}$$

The IMC principle requires, after identifying the FOPDT process, the determination the transfer function $Q(s)$ to optimize the system's response to the reference signal of interest, with the sole constraint that this function be asymptotically stable [67]. It is found that the best policy to choose $Q(s)$ is the approximate inverse of the minimum phase part of process model transfer function $G_m(s)$, which is given as:

$$Q(s) = \frac{1+sT}{k} \tag{3.15}$$

In order to ensure the robustness, the IMC filter $F(s)$ is introduced, where the structure and the parameters of the filter are chosen to achieve a balance between robust stability and performance. For simplicity, it is chosen to be of first order with unity gain as it is described by the following equation:

$$F(s) = \frac{1}{1+\lambda s} \tag{3.16}$$

Where λ is the sole unknown design parameter.

The IMC approach can be applied in a very straightforward manner to PI/PID tuning. It has been firstly employed by Skogestad in [68] to derive rules for model reduction and PI/PID controller tuning called Skogestad's IMC (SIMC in short) tuning rules. These are analytically derived and proved their simplicity and effectiveness for wide range of processes. The relevant feature is that, because SIMC rules are intended for PI/PID controllers, a first- or second order process model of the process must be obtained. Hence, the method is based on a simple procedure to obtain an approximate first or second order model of the process. Once these reduced-order models are obtained, the PI/PID controller gains are computed to adjust the closed-loop response to a first- or second-order model reference response [22, 69].

Overall, the use of more sophisticated model-based analytical tuning methods allows a better definition of desired closed-loop behavior and robustness with a main disadvantage consists of the fact that an accurate model of the process has to be obtained and defined, which is time-demanding and often difficult.

3.5.3 Optimization Based Tuning Methods

3.5.3.1 Iterative Feedback Tuning (IFT) Method

The Iterative Feedback Tuning (IFT) method is a model-free technique for the optimization of the controller parameters of fixed structure using only signal information on the closed-loop system.

The method was initially derived by Hjalmarsson, Gunnarsson, and Gevers [70] and has quickly proved its efficiency in both laboratory and industrial applications [71].

To explain the principle of the method, we first consider the feedback control system represented by the block diagram of Fig.3.6.

Using this method, the unknown system to be controlled is described by input-output relationship as:

$$y_t = G_p\, u_t + d_t \tag{3.17}$$

With G_p being the transfer function of the linear time invariant system to be controlled, y_t, u_t are respectively, the system's output and the control signal. d_t represents the unmeasured disturbance.

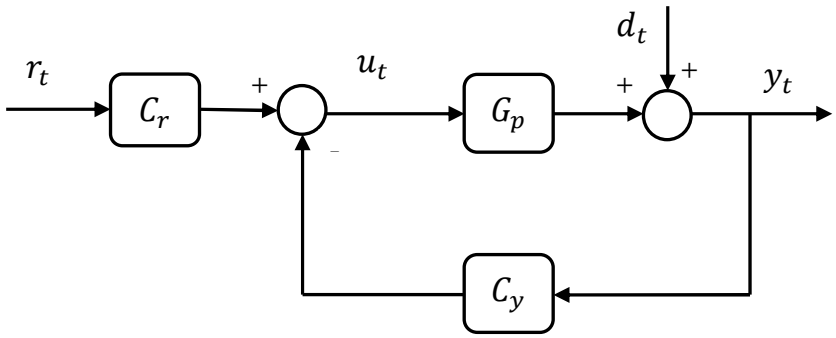

Figure 3.6 Block Diagram Illustrating IFT Method for PID Tuning

It follows from the feedback control system block diagram that the controller to be used is described by:

$$u_t = C_r(\rho)r_t - C_y(\rho)y_t \tag{3.18}$$

Where $C_r(\rho)$ and $C_y(\rho)$ are linear invariant transfer functions parametrized by some parameter vector ρ and which can have a common parameters, r_t is the external reference signal independent of the signal d_t.

For a controller of some fixed structure and parametrized by the vector ρ, the iterative feedback tuning (IFT) method consists of iteratively obtaining the setting vector ρ that minimizes the following cost function:

$$J(\rho) = \frac{1}{2N} E\left[\sum_{t=1}^{N}(L_y\tilde{y}_t(\rho))^2 + \lambda\sum_{t=1}^{N}(L_u u_t(\rho))^2\right] \tag{3.19}$$

Where $\tilde{y}_t(\rho)$ denotes the error signal between the reference signal and the measured output.

The right hand side first term in (3.19) is weighted by a filter *Ly* and is known as the frequency error between the desired response and the achieved response. The second term in this side is the penalty on the control effort which is frequency

weighted by a filter L_u. The filters L_y, and L_u, can of course be set to 1, but they give added flexibility to the design.

The objective of the criterion (3.19) is to tune the system response to a desired deterministic response of finite length $\boldsymbol{N}$ in a mean square sense [72], and the minimum solution to the cost function is obtained by evaluating the gradient $\frac{\partial J}{\partial \rho}$, which, at the same time, represents the important ingredient of the design criterion. Using the IFT method, this gradient is estimated using data from multiple experiments during iterations and the controller parameters found give the optimal solution to the performance criterion [73].

In comparison with the available methods for PID controllers tuning, IFT requires typically more data and experiments. However, it offers several advantages: the achieved responses are typically faster than those obtained with other model-free methods (features based tuning methods). Moreover, the control objective is clearly expressed, thereby giving the control engineer a confidence for the tuning of critical loops that he cannot have with some commercially available loop tuners that behave more like "dark grey box" systems. A more theory, applications and advantages of the method applied to controller tuning of mechanical systems and chemical plants are covered in [74].

3.5.3.2 Integral Based Minimum Criteria Tuning Methods

These are methods based on integrating the tracking error of feedback control system to tune and synchronize the controller parameters following the disturbance or set point change. The principle involves searching for the minimum of the cost function $J(\rho)$ over the controller parameter vector ρ, which can be stated in the general form as [31]:

$$J(\rho) = \int_0^\infty t^n f[e(t)]dt \tag{3.20}$$

Where $e(t)$ represents the tracking error signal.

There are several criteria that can be derived from the general form (3.20), this is usually depending on the particular choice of the function f and the exponent n. Particularly we can have the following criteria:

- ***Integral of Error (IE)***: obtained by setting $f[e(t)] = e(t),\ n = 0$;
- ***Integral of Absolute Error (IAE)***: obtained by setting $f[e(t)] = |e(t)|, n = 0$;
- ***Integral of Time multiplied by Absolute Error (ITAE)***: obtained by setting $f[e(t)] = |e(t)|, n = 1$;
- ***Integral of Squared Error (ISE)***: obtained by setting $f[e(t)] = e^2(t), n = 0$;
- ***Integral of Time multiplied by Square of Error (ITSE)***: obtained by setting $f[e(t)] = e^2(t),\ n = 1$;
- ***Integral of Time squared multiplied by Square of Error (IT^2SE)***: obtained by setting $f[e(t)] = e^2(t), n = 2$.

Of these, the IE or IAE, ITAE and ISE are the most common used criteria in designing and tuning the PID controller [75, 76], where the optimum parameters are found by minimizing the penalty function *J*; implying that its partial derivatives with respect to the controller parameters are equal to zero. Traditionally, this is done by numerically solving the following three equations:

$$\frac{\partial J}{\partial K_p} = 0 \tag{3.21}$$

$$\frac{\partial J}{\partial K_I} = 0 \tag{3.22}$$

$$\frac{\partial J}{\partial K_d} = 0 \tag{3.23}$$

To solve this criterion based minimization control problems, many methods, in fact, are found in literature. K. J. Astrom, H. Panagopoulos and T. Hagglund, in [77, 78], have presented their optimization approach to minimize the integrated error signal under the constraint that the maximum sensitivity should not exceed a certain desired value, guaranteeing the desired robustness and giving good load disturbance response.

The Linear Quadratic Regulator (LQR) algorithm is, on the other hand, used by Argelaguet [79] to minimize the ISE criterion to obtain the PID controller parameters used with FOPDT process model type. In [80], a method named the Extremum

Seeking Optimization is used to obtain the optimal settings of PID controller through minimization of ISE based cost function.

Recently, under the availability of different software packages, PID based control system models can be simulated and the controller parameters are tuned using any one of the previous integral based minimization criteria, which are unique for set point or load disturbances. Therefore, when a disturbance is applied to a process, the control loop responds and attempts to compensate for that disturbance. Until the system is brought back under control, there exists an error at any instant of time between the control point and the set point. The integrating criterion method attempts to minimize the sum of errors over any specified period of time. Resulting is controller tuning parameters of set point change, which are different of that of load disturbance change [31].

Up to now, the aim was to emphasize and overview PI and PID tuning methods found in literature. But only a selection is discussed, since it is impossible to include them all. However, these are the most popular methods and many others are also available in literature, all of them have been used to achieve improvement of operating performance of a given PI or PID based industrial process via an appropriate selection of the controller parameters. For instance, by referring to [81]-[86], it is used the Fuzzy Logic Control (FLC) method to optimally tune the parameters of PID controller. In [87], Lee has used a method based on gain and phase margins specifications to tune the PID controller parameters for stable and unstable processes. This method has been also used in [88]-[93]. The Genetic Algorithm (GA), Particle Swarm Optimization (PSO) and the hybrid fuzzy neural network methods were also reported as optimization techniques for controller parameters determination for different applications [94]-[97].

On the other hand, the classification of the tuning methods discussed in the previous sections of this chapter does not set an artificial boundary because some methods applied in practice may belong to more than one category. Overall, an excellent summary on the methods of PID parameters tuning can be found by referring to [22], [98], [99] and [100].

In our work, we propose the Mini-Max as a novel and alternative optimization approach to optimally tune the parameters of PI speed controller based DC motor drive system. The main aim is to enhance the performance properties of the electromechanical speed response and, consequently, an amelioration of product quality of paper and steel rolling mills, as a vital industrial sector, can be achieved without any additional equipment.

3.6 Tuning PI Parameters using Mini-Max Optimization Approach

The Mini-Max approach takes its meaning from the nonlinear multi-objective Mini-Max optimization problem, which, in general, can be formulated by letting X be the set of all solutions to the problem and S be the set of all possible available scenarios. If the objective function $F(x, s)$ is the performance of a solution $x \in X$ in scenario $s \in S$, then the Mini-Max optimization problem is the task of finding the optimal solution that has the best performance and which is the same as minimizing (over all the solution set) the maximum performance (over all the scenarios). Mathematically, this is expressed as [101]:

$$Min_{x \in X} \; Max_{s \in S} \; F(x, s) \tag{3.24}$$

This type of optimization problem is originally formulated by game theorists [102] and is encountered in numerous fields including engineering design, optimal control and many game theory applications.

In our case, the Mini-Max optimization problem consists of determining (over a set of solutions) the parameters of the PI speed controller that minimize (over a given time interval) the maximum value of speed tracking error, defined as the difference between the estimated system output and set point desired response. With analogy to (3.24) and according to [103] and [104], we formulate the problem as:

$$Min_{K} \; Max_{t \in [t_0, t_f]} \; \{e(K, t)\} \tag{3.25}$$

In other words, we seek to minimize with respect to PI speed controller parameter vector $K = [k_p, k_i]$ the maximum tracking error $e(t)$ from an initial instant t_0 to a given final time instant t_f as it is depicted in Fig.3.7 [105].

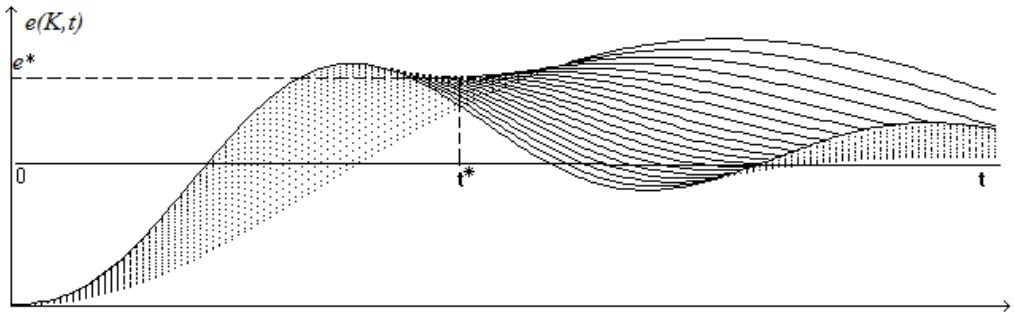

Figure 3.7 Variation of Tracking Error Function with respect to PI Parameter Vector and Time

To solve this problem, we propose the Mini-Max approach, where we have used the "fminimax" MATLAB function from optimization toolbox [106]. To generate the optimal solution, this function uses the Sequential Quadratic Programming algorithm to, iteratively, run the SIMULINK model, evaluate the cost function and modify the line search as well as the Hessian cost function.

3.6.1 Simulation Results of Dynamic Performance Improvement

In this section, we present the results on the improvements in dynamic and steady state performances of the control system due to the optimal selection of PI speed controller parameters using the Mini-Max approach, defined earlier. In order to show the superiority of the proposed approach, the results are compared with those obtained using the commonly used integral based performance minimization criteria, namely: IAE, ISE and ITAE, where the optimal parameters of speed controller generated by these criteria are obtained, respectively, as follows:

For **I.A.E.**, we solve**:** $min_K[\int_0^{t_f}|e(K,\ t)|dt]$ (3.26)

For **I.S.E.**, we solve: $min_K[\int_0^{t_f} e^2(K,t)dt]$ (3.27)

For **I.T.A.E.**, we solve: $\min_K[\int_0^{t_f} t.|e(K,t)|dt]$ (3.28)

where $e(t)$ and $K = [k_p, k_i]$ are the error signal and the parameter vector of the PI speed controller to be tuned.

Of course, this study will cover independently all the available drive models previously defined in chapter 2. In other words, we will apply the Mini-Max approach to tune the parameters of PI speed controller of models having single controller, but those models where this controller is doubled, the optimization tuning will concern only the first PI.

In order to mention the effect of viscous friction coefficient on the optimized response, the simulation results showing the speed and tracking error step responses of each drive model are given by taking into account the effect of this parameter.

3.6.1.1 System Model with 1PI Speed Controller and State Observer of Order 2

a) Case of $\boldsymbol{\beta = 0}$

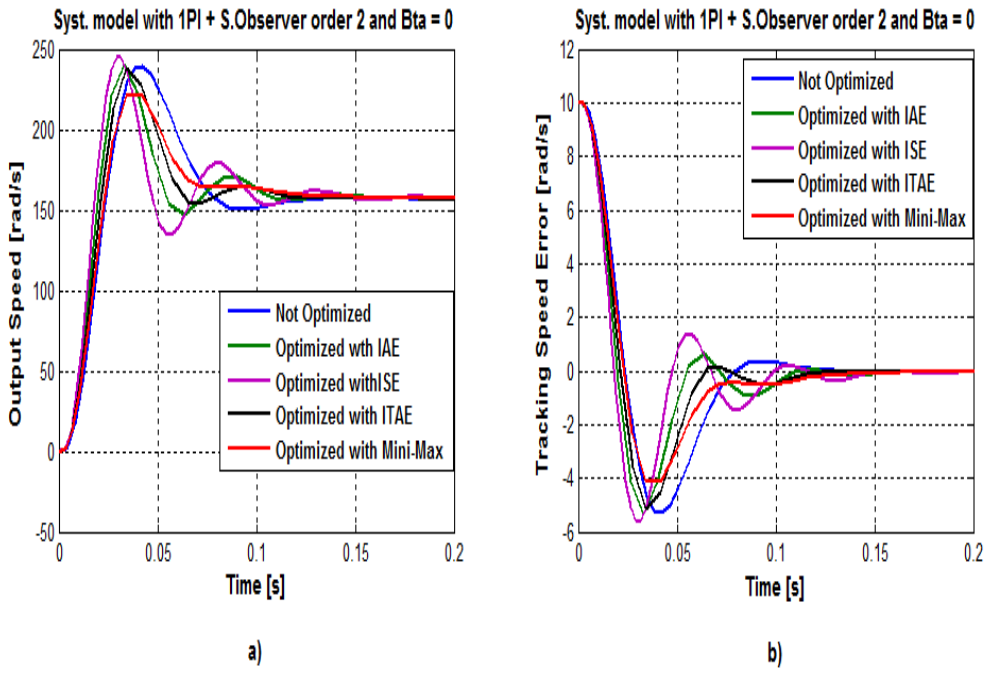

Figure 3.8 Responses as Optimized with Mini-Max, I.A.E., I.S.E., I.T.A.E. and Compared to not Optimized Response for the Model with 1PI Speed Controller, State Observer of order 2 and $\boldsymbol{\beta = 0}$; **a)** Output Speed, **b)** Tracking Speed Error.

b) Case of $\beta > 0$

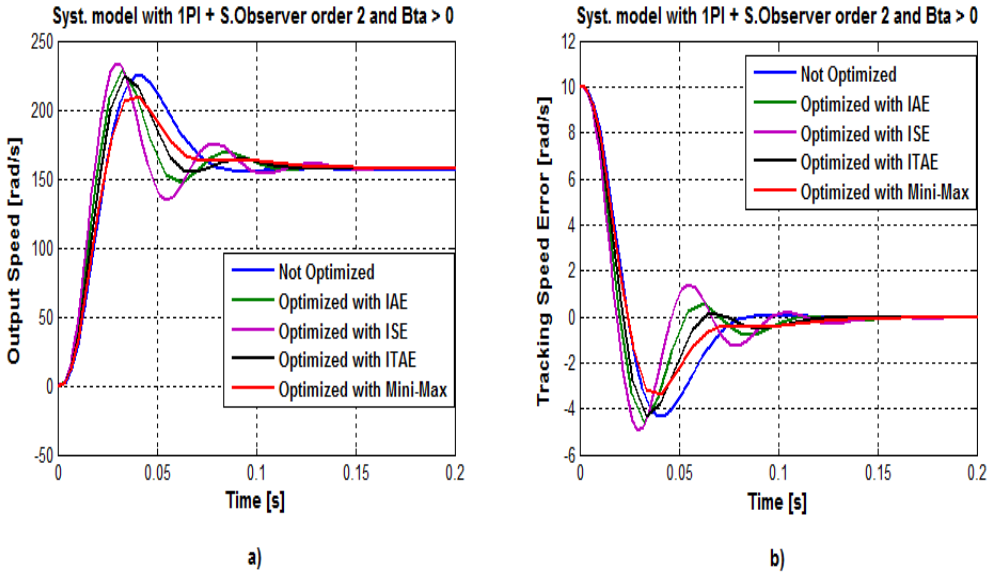

Figure 3.9 Responses as Optimized with Mini-Max, I.A.E., I.S.E., I.T.A.E. and Compared to not Optimized Response for the Model with 1PI Speed Controller, State Observer of order 2 and $\beta > 0$; **a)** Output Speed, **b)** Tracking Speed Error.

c) Case of $\beta < 0$

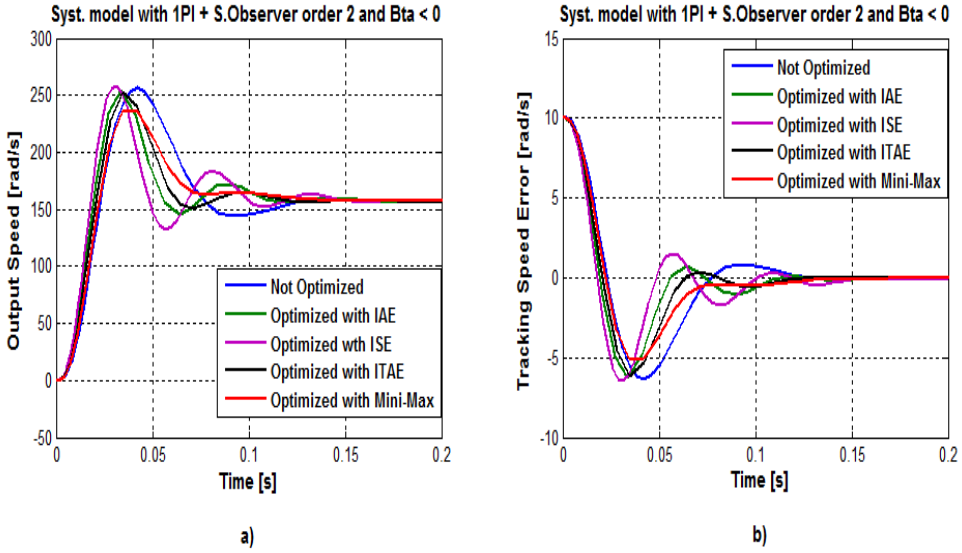

Figure 3.10 Responses as Optimized with Mini-Max, I.A.E., I.S.E., I.T.A.E. and Compared to not Optimized Response for the Model with 1PI Speed Controller, State Observer of order 2 and $\beta < 0$; **a)** Output Speed, **b)** Tracking Speed Error.

d) Comparison plots for Responses Optimized with Mini-Max only

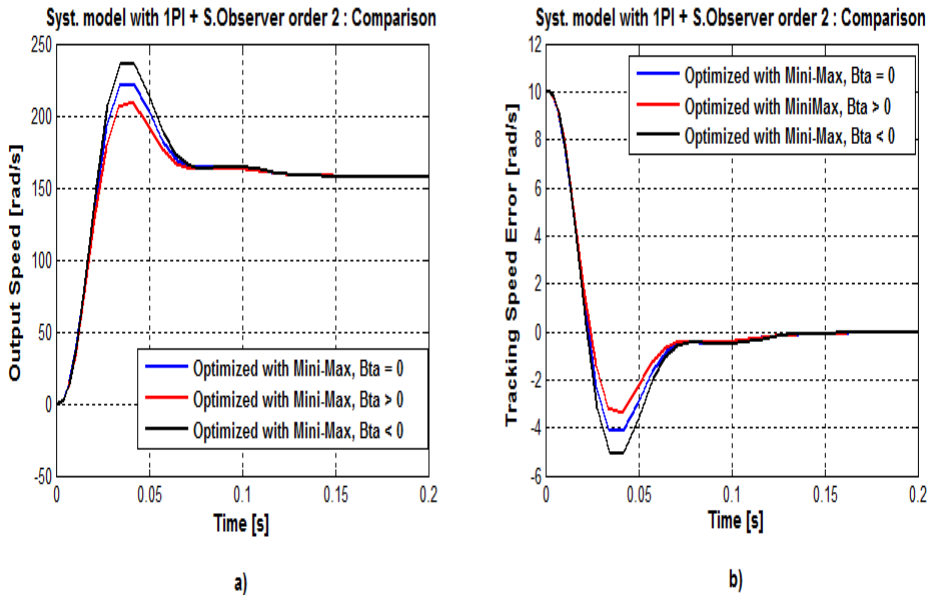

Figure 3.11 Responses Showing the Effect of β when Optimized with Mini-Max for the Model with 1PI Speed Controller and State Observer of order 2; **a)** Output Speed, **b)** Tracking Speed Error.

Numerically, we summarize the above graphical results for this model in the following tables according to the values of viscous friction coefficient.

Table 3.5 Numerical Results of Dynamic Performance Improvement as Optimized with Mini-Max, I.A.E., I.S.E., I.T.A.E. and Compared to not Optimized Response for the Model with 1PI Speed Controller, State Observer of order 2 and $\boldsymbol{\beta = 0}$.

Characteristics	**Not Optimized**	**IAE**	**ISE**	**ITAE**	**Mini-Max**
% peak Overshoot	53,06	53,60	56,03	51,62	40,30
Settling time [s]	0,094	0,0987	0,0931	0,0974	0,0906
Rise time [s]	0,022	0,0185	0,0171	0,0198	0,0213
Improvement in Mp [%]	-	-	-	2.71	24.05

Table 3.6 Numerical Results of Dynamic Performance Improvement as Optimized with Mini-Max, I.A.E., I.S.E., I.T.A.E. and Compared to not Optimized Response for the Model with 1PI Speed Controller, State Observer of order 2 and $\boldsymbol{\beta} > 0$.

Characteristics	**Not Optimized**	**IAE**	**ISE**	**ITAE**	**Mini-Max**
% peak Overshoot	43,18	45,26	48,56	43,67	33,43
Settling time [s]	0,0958	0,0953	0,0904	0,0931	0,0899
Rise time [s]	0,01471	0,01198	0,01108	0,013	0,0147
Improvement in Mp [%]	-	-	-	-	22.56

Table 3.7 Numerical Results of Dynamic Performance Improvement as Optimized with Mini-Max, I.A.E., I.S.E., I.T.A.E. and Compared to not Optimized Response for the Model with 1PI Speed Controller, State Observer of order 2 and $\boldsymbol{\beta} < 0$.

Characteristics	**Not Optimized**	**IAE**	**ISE**	**ITAE**	**Mini-Max**
% peak Overshoot	63,50	61,99	63,58	58,63	50,50
Settling time [s]	0,1101	0,102	0,132	0,1008	0,0954
Rise time [s]	0,01366	0,0114	0,01055	0,01208	0,01322
Improvement in Mp [%]	-	2.38	-	7.67	20.45

Table 3.8 Numerical Results of Peak Overshoot Improvement as achieved with Mini-Max Optimization and affected by the Viscous Friction Coefficient for the Model with 1PI Speed Controller and State Observer of order 2.

Viscous coefficient $\boldsymbol{\beta}$	$\boldsymbol{\beta = 0}$	$\boldsymbol{\beta} > 0$	$\boldsymbol{\beta} < 0$
Δ. **Peak Overshoot**	240 - 220	224.5 – 209.22	256.37 - 236

3.6.1.2 System Model with 2PI Speed Controller and State Observer of Order 2

a) Case of $\boldsymbol{\beta = 0}$

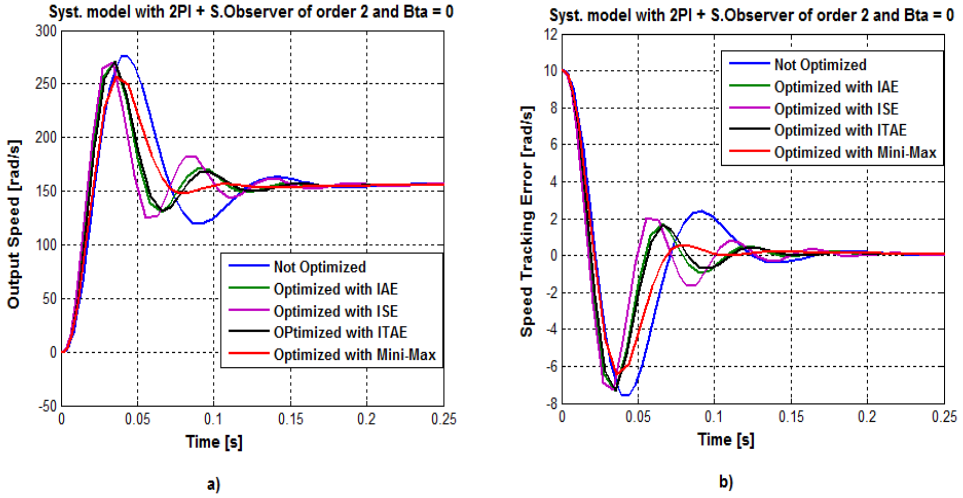

Figure 3.12 Responses as Optimized with Mini-Max, I.A.E., I.S.E., I.T.A.E. and Compared to not Optimized Response for the Model with 2PI Speed Controller, State Observer of order 2 and $\boldsymbol{\beta = 0}$; **a)** Output Speed, **b)** Tracking Speed Error.

b) Case of $\boldsymbol{\beta} > 0$

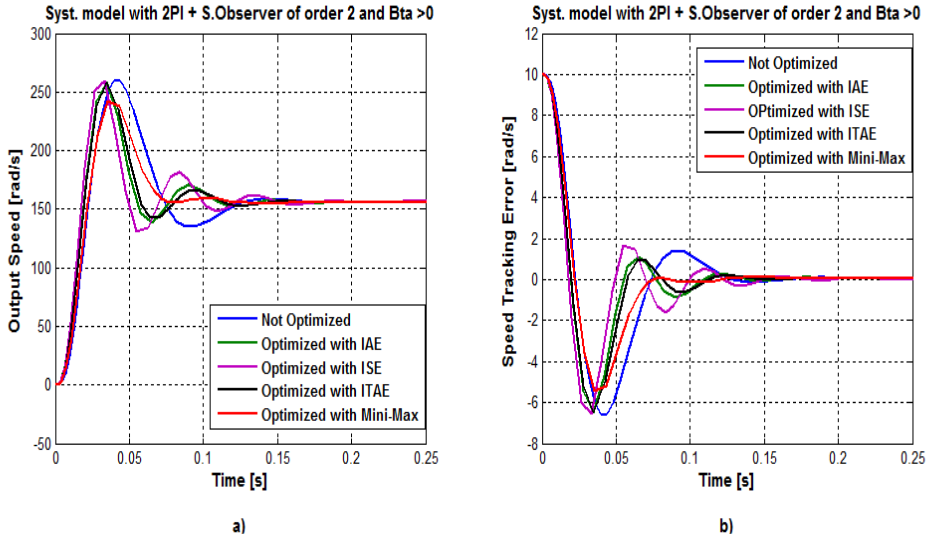

Figure 3.13 Responses as Optimized with Mini-Max, I.A.E., I.S.E., I.T.A.E. and Compared to not Optimized Response for the Model with 2PI Speed Controller, State Observer of order 2 and $\boldsymbol{\beta} > 0$; **a)** Output Speed, **b)** Tracking Speed Error.

c) Case of $\beta < 0$

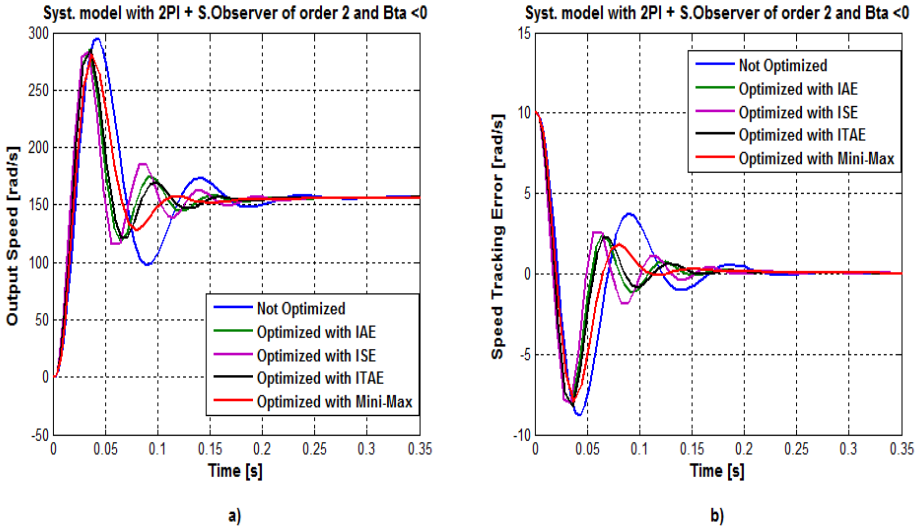

Figure 3.14 Responses as Optimized with Mini-Max, I.A.E., I.S.E., I.T.A.E. and Compared to not Optimized Response for the Model with 2PI Speed Controller, State Observer of order 2 and $\beta < 0$; **a)** Output Speed, **b)** Tracking Speed Error.

d) Comparison plots for Responses Optimized with Mini-Max only

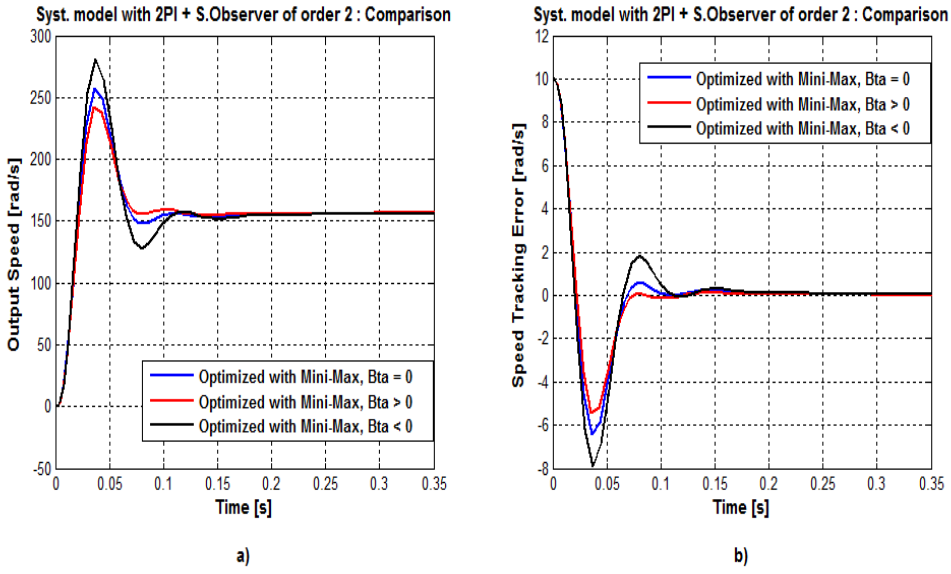

Figure 3.15 Responses showing the effect of β when Optimized with Mini-Max for the Model with 2PI Speed Controller and State Observer of order 2; **a)** Output Speed, **b)** Tracking Speed Error.

Table 3.9 Numerical Results of Dynamic Performance Improvement as Optimized with Mini-Max, I.A.E., I.S.E., I.T.A.E. and Compared to not Optimized Response for the Model with 2PI Speed Controller, State Observer of order 2 and $\boldsymbol{\beta = 0}$.

Characteristics	**Not Optimized**	**IAE**	**ISE**	**ITAE**	**Mini-Max**
% peak Overshoot	75.84	72.93	72.51	70.78	64,16
Settling time [s]	0,1394	0,1019	0,097	0,1031	0,0656
Rise time [s]	0,01313	0,0109	0,0103	0,0111	0,01253
Improvement in Mp [%]	-	3.84	4.39	6.67	15.40

Table 3.10 Numerical Results of Dynamic Performance Improvement as Optimized with Mini-Max, I.A.E., I.S.E., I.T.A.E. and Compared to not Optimized Response for the Model with 2PI Speed Controller, State Observer of order 2 and $\boldsymbol{\beta} > 0$.

Characteristics	**Not Optimized**	**IAE**	**ISE**	**ITAE**	**Mini-Max**
% peak Overshoot	65,82	64,52	65,18	63,71	54,34
Settling time [s]	0,0706	0,0999	0,095	0,1	0,067
Rise time [s]	0,01358	0,0113	0,0105	0,0116	0,0131
Improvement in Mp [%]	-	1.97	0.97	3.20	17.44

Table 3.11 numerical results of dynamic performance improvement as Optimized with Mini-Max, I.A.E., I.S.E., I.T.A.E. and Compared to not Optimized Response for the Model with 2PI Speed Controller, State Observer of order 2 and $\boldsymbol{\beta} < 0$.

Characteristics	**Not Optimized**	**IAE**	**ISE**	**ITAE**	**Mini-Max**
% peak Overshoot	87.95	81.95	80.64	81,27	75,94
Settling time [s]	0,1565	0,1038	0,0985	0,1062	0,0631
Rise time [s]	0,01276	0,01062	0,01003	0,011	0,0122
Improvement in Mp [%]	-	6.62	7.67	7.59	13.65

Table 3.12 Numerical Results of Peak Overshoot Improvement as achieved with Mini-Max optimization and affected by the Viscous Friction Coefficient for the Model with 2PI Speed Controller and State Observer of order 2.

Viscous coefficient β	$\beta = 0$	$\beta > 0$	$\beta < 0$
Δ. **Peak Overshoot**	275.72 – 257.40	260 - 242	294.63 - 275.80

3.6.1.3 System Model with 1PI Speed Controller and State Observer of Order 5

a) Case of $\beta = 0$

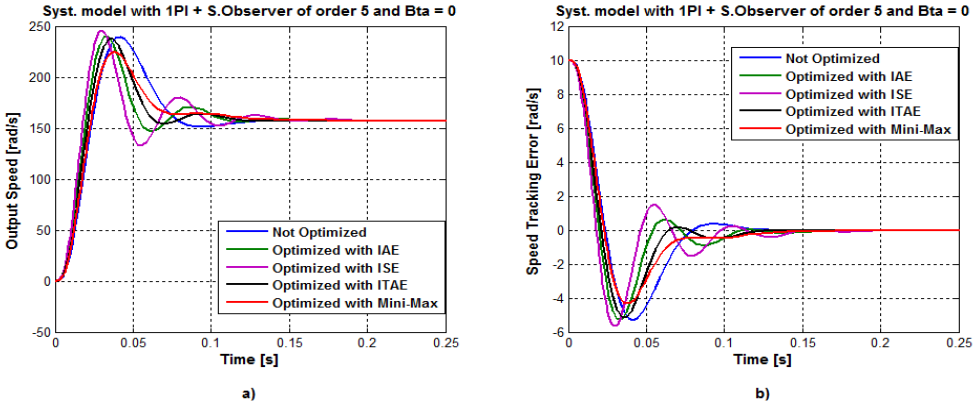

Figure 3.16 Responses as Optimized with Mini-Max, I.A.E., I.S.E., I.T.A.E. and Compared to not Optimized Response for the Model with 1PI Speed Controller, State Observer of order 5 and $\beta = 0$; **a)** Output Speed, **b)** Tracking Speed Error.

b) Case of $\beta > 0$

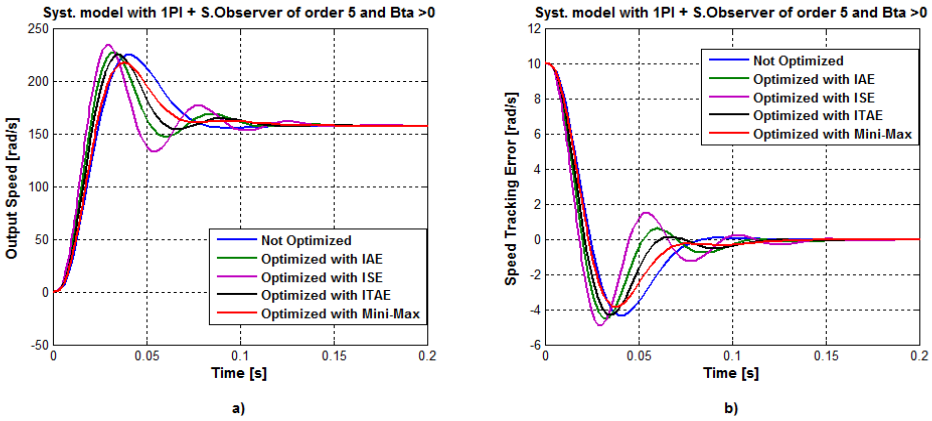

Figure 3.17 Responses as Optimized with Mini-Max, I.A.E., I.S.E., I.T.A.E. and Compared to not Optimized Response for the Model with 1PI Speed Controller, State Observer of order 5 and $\beta > 0$; **a)** Output Speed, **b)** Tracking Speed Error.

c) Case of $\beta < 0$

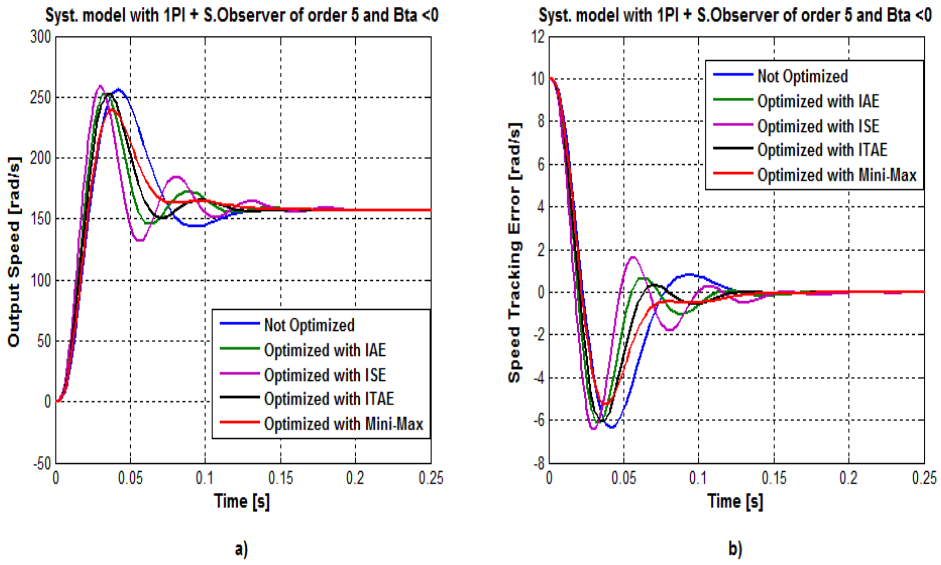

Figure 3.18 Responses as Optimized with Mini-Max, I.A.E., I.S.E., I.T.A.E. and Compared to not Optimized Response for the Model with 1PI Speed Controller, State Observer of order 5 and $\beta < 0$; **a)** Output Speed, **b)** Tracking Speed Error.

d) Comparison plots for Responses Optimized with Mini-Max only

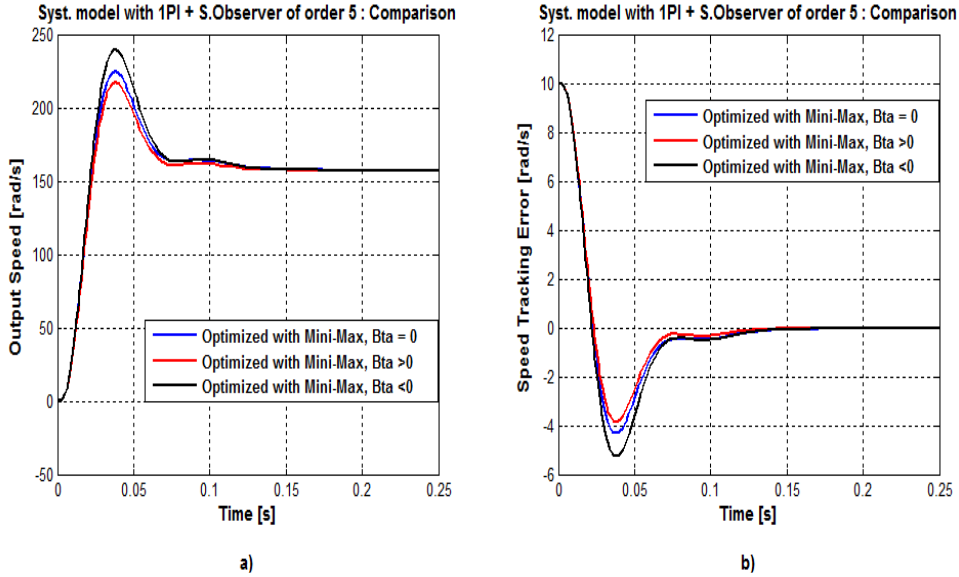

Figure 3.19 Responses showing the effect of β when Optimized with Mini-Max for the Model with 1PI Speed Controller and State Observer of order 5; **a)** Output Speed, **b)** Speed Tracking Error.

Table 3.13 Numerical Results of Dynamic Performance Improvement as Optimized with Mini-Max, I.A.E., I.S.E., I.T.A.E. and Compared to not Optimized Response for the Model with 1PI Speed Controller, State Observer of order 5 and $\boldsymbol{\beta = 0}$.

Characteristics	**Not Optimized**	**IAE**	**ISE**	**ITAE**	**Mini-Max**
% peak Overshoot	53,06	53,17	55,93	51,47	42,86
Settling time [s]	0,073	0,0985	0,0921	0,094	0,0931
Rise time [s]	0,01415	0,0116	0,0106	0,01255	0,01372
Improvement in Mp [%]	-	-	-	2.99	19.22

Table 3.14 Numerical Results of Dynamic Performance Improvement as Optimized with Mini-Max, I.A.E., I.S.E., I.T.A.E. and Compared to not Optimized Response for the Model with 1PI Speed Controller, State Observer of order 5 and $\boldsymbol{\beta} > 0$.

Characteristics	**Not Optimized**	**IAE**	**ISE**	**ITAE**	**Mini-Max**
% peak Overshoot	43,36	45,41	49,04	43,35	36,64
Settling time [s]	0,0725	0,095	0,0893	0,0912	0,0667
Rise time [s]	0,01462	0,0119	0,01082	0,0128	0,01412
Improvement in Mp [%]	-	-	-	-	15.52

Table 3.15 Numerical Results of Dynamic Performance Improvement as Optimized with Mini-Max, I.A.E., I.S.E., I.T.A.E. and Compared to not Optimized Response for the Model with 1PI Speed Controller, State Observer of order 5 and $\boldsymbol{\beta} < 0$.

Characteristics	**Not Optimized**	**IAE**	**ISE**	**ITAE**	**Mini-Max**
% peak Overshoot	63,58	61,17	64,12	61,15	52,59
Settling time [s]	0,1089	0,1016	0,0132	0,1015	0,0965
Rise time [s]	0,01367	0,01121	0,01035	0,01206	0,01312
Improvement in Mp [%]	-	3.79	-	3.82	17.28

Table 3.16 Numerical Results of Peak Overshoot Improvement as achieved with Mini-Max optimization and affected by the viscous friction coefficient for the Model with 1PI Speed Controller and State Observer of order 5.

Viscous coefficient β	$\beta = 0$	$\beta > 0$	$\beta < 0$
Δ. **Peak Overshoot**	240 - 224	224.80 – 214.25	256.50 – 239.26

3.6.1.4 System Model with 2PI Speed Controller and State Observer of Order 6

a) Case of $\beta = 0$

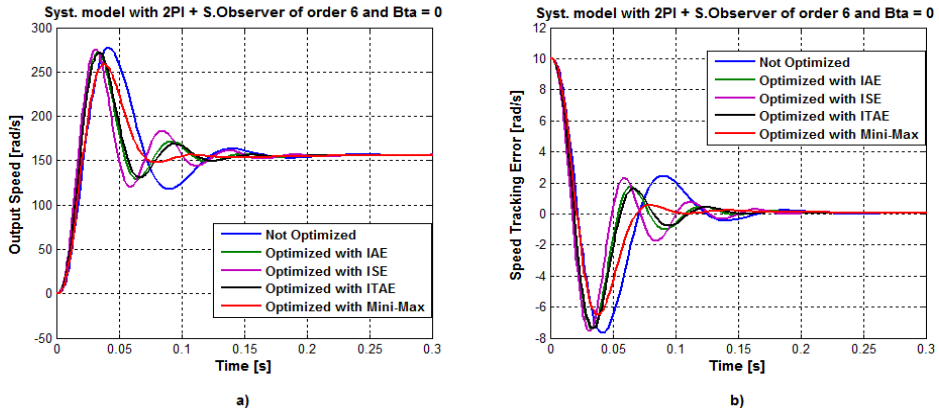

Figure 3.20 Responses as Optimized with Mini-Max, I.A.E., I.S.E., I.T.A.E. and Compared to not Optimized Response for the Model with 2PI Speed Controller, State Observer of order 6 and $\beta = 0$; **a)** Output Speed, **b)** Tracking Speed Error.

b) Case of $\beta > 0$

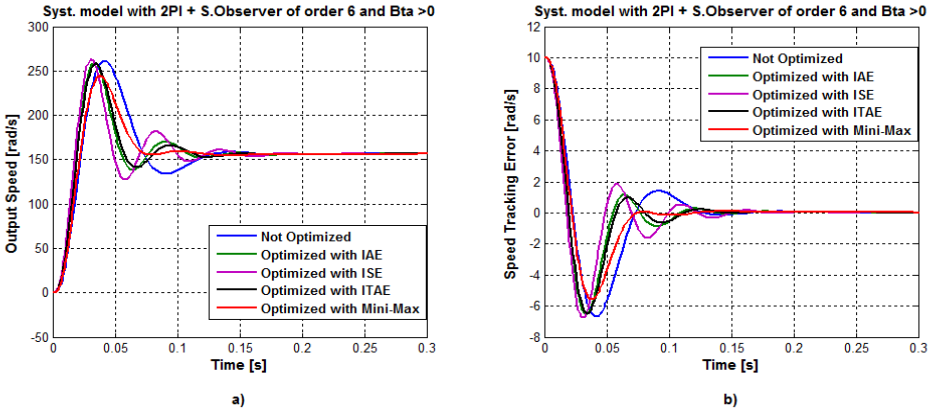

Figure 3.21 Responses as Optimized with Mini-Max, I.A.E., I.S.E., I.T.A.E. and Compared to not Optimized Response for the Model with 2PI Speed Controller, State Observer of order 6 and $\beta > 0$; **a)** Output Speed, **b)** Tracking Speed Error.

c) Case of $\beta < 0$

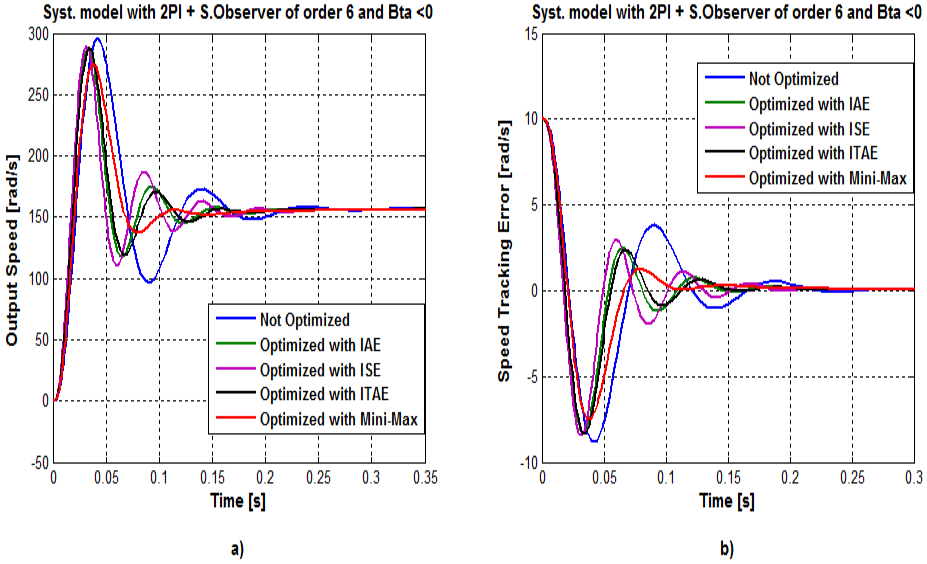

Figure 3.22 Responses as Optimized with Mini-Max, I.A.E., I.S.E., I.T.A.E. and Compared to not Optimized Response for the Model with 1PI Speed Controller, State Observer of order 5 and $\beta < 0$; **a)** Output Speed, **b)** Tracking Speed Error.

d) Comparison Plots for Responses Optimized with Mini-Max only

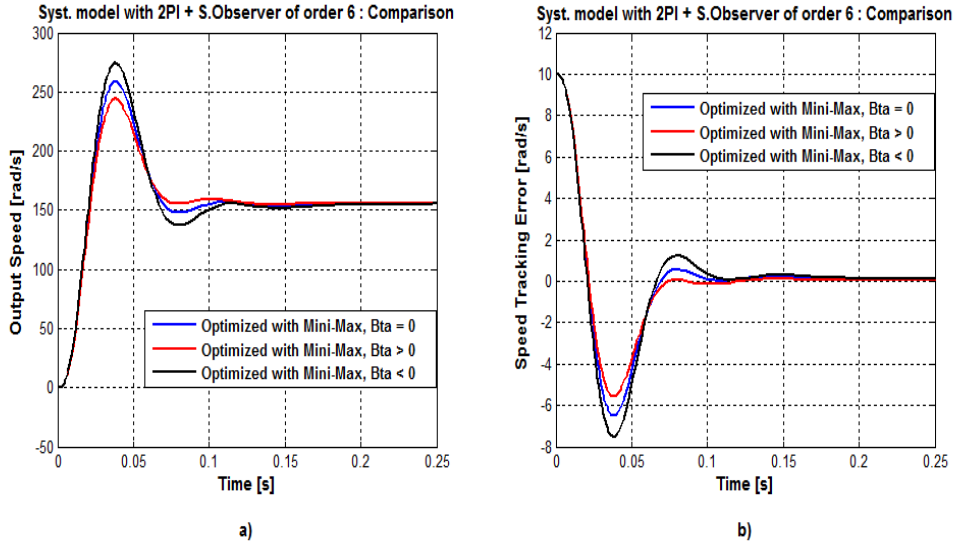

Figure 3.23 Responses showing the effect of β when Optimized with Mini-Max for the Model with 1PI Speed Controller and State Observer of order 5; **a)** Output Speed, **b)** Speed Tracking Error.

Table 3.17 Numerical Results of Dynamic Performance Improvement as Optimized with Mini-Max, I.A.E., I.S.E., I.T.A.E. and Compared to not Optimized Response for the Model with 2PI Speed Controller, State Observer of order 6 and $\boldsymbol{\beta = 0}$.

Characteristics	**Not Optimized**	**IAE**	**ISE**	**ITAE**	**Mini-Max**
% peak Overshoot	76.90	74.12	75.68	73.77	64.20
Settling time [s]	0.1974	0.1353	0.1733	0.1396	0.1516
Rise time [s]	0.0209	0.0176	0.0167	0.018	0.0199
Improvement in Mp [%]	-	3.61	1.58	4.07	16.52

Table 3.18 Numerical Results of Dynamic Performance Improvement as Optimized with Mini-Max, I.A.E., I.S.E., I.T.A.E. and Compared to not Optimized Response for the Model with 2PI Speed Controller, State Observer of order 6 and $\boldsymbol{\beta} > 0$.

Characteristics	**Not Optimized**	**IAE**	**ISE**	**ITAE**	**Mini-Max**
% peak Overshoot	66.66	65.11	67.52	64.82	55.07
Settling time [s]	0.1430	0.1055	0.1425	0.1078	0.1001
Rise time [s]	0.0213	0.0181	0.0169	0.0185	0.0204
Improvement in Mp [%]	-	2.32	-	2.76	17.38

Table 3.19 Numerical Results of Dynamic Performance Improvement as Optimized with Mini-Max, I.A.E., I.S.E., I.T.A.E. and Compared to not Optimized Response for the Model with 2PI Speed Controller, State Observer of order 6 and $\boldsymbol{\beta} < 0$.

Characteristics	**Not Optimized**	**IAE**	**ISE**	**ITAE**	**Mini-Max**
% peak Overshoot [%]	88.47	83.51	84.68	83.47	74.28
Settling time [s]	0.211	0.1901	0.1802	0.1894	0.171
Rise time [s]	0.0205	0.0173	0.0164	0.0177	0.0194
Improvement in Mp [%]	-	5.60	4.28	5.65	16.04

Table 3.20 Numerical Results of Peak Overshoot Improvement as achieved with Mini-Max optimization and affected by the viscous friction coefficient for the Model with 2PI Speed Controller and State Observer of order 6.

Viscous coefficient β	$\boldsymbol{\beta = 0}$	$\boldsymbol{\beta > 0}$	$\boldsymbol{\beta < 0}$
Δ. **Peak Overshoot**	277.2 – 257.3	261.16 - 243	295.33 – 273.10

3.7 Results Interpretation and Discussion

These simulation results indicate that both Mini-Max approach and the integral-based minimization methods have led to a moderate improvement in settling and rise time of the system response for all the studied models. However, the Mini-Max optimization approach has given a significant improvement in percent overshoot when compared with the small percentage of improvement achieved using the other methods for some models. The results have, also, mentioned that the application of integral based minimization criteria on some models has led to no reduction of percent overshoot performance index, which is the case of the models that employ 1PI speed controller and, respectively, state observers of order 2 and 5. Regarding these minimization criteria, the interpretation of both graphical and numerical results indicates the bad responses in terms of peak overshoot are those given when ISE optimization criterion is used.

For the effect of viscous friction coefficient on the dynamic performance improvement and amelioration, the simulation results are very closer whether this coefficient is taken into account or neglecting its incorporation in the drive model structure. This means that its effect on the dynamic performance of system response is not significant.

By referring to the explanation given at the beginning of this chapter, which concerns the relationship between the peak overshoot and stability margins of the system, we can say, based on the obtained results, that the use of Mini-Max approach has allowed us to achieve an important amelioration in system stability margin without losing the speed and accuracy performance of the control system.

3.8 Conclusion

In this chapter, we have presented the results of an optimization study that we have performed to perfecting the control performance of cascade PI speed controller and state observer-based DC drive system models, which are elaborated for implementation particularly in paper and steel rolling mill industries. The results concern the application of Mini-Max optimization approach to optimally selecting the parameters of PI speed controller for which improvements in dynamic and stability performance are achieved. The simulation results have shown that an improvement in transient response characteristics (e.g., rise time, settling time and % overshoot) is evident, especially with a significant improvement in percent overshoot and a minor effect of viscous friction coefficient.

These results are compared to those obtained with IAE, ISE and ITAE integral-based minimization methods. This comparison has shown the superiority of the Mini-Max approach over the other methods in giving an important amelioration in system stability margin without losing the speed and accuracy performance of the control system’s steady-state response.

Chapter 4

Improving Accuracy Performance and Order of Astatism of DC Drive using Feed-Forward Compensation

4.1 Introduction

Feedback control systems are built to modify the behavior of a process so it behaves in a specific desirable way over time. In other words, the primary objective of feedback system is to make the system's output trajectories follow the imposed input trajectories. The DC drive systems, widely used in paper and steel rolling mill industries, are considered as high performance motion control systems which are characterized by their good dynamic and steady state input reference tracking and load disturbance rejection requirements [107]. The PI controller is particularly extensively used to build the feedback system where the drive motor speed should be precisely controlled to give the desired performance. This is found highly effective if both set point and load disturbance changes are small. However, in event of substantial speed and /or torque variation, as the case of rolling mill plants, these conventional systems become unable alone to track accurately these variations and preventing, therefore, the deviation from the desired performance. Since the quality of product in these plants is closely related to the steady state accuracy performance, the improvement of these performances in presence of external variations and change is crucial.

In this chapter, we intend to study and investigate the steady state performance of those systems in response to input reference and load torque changes, where an

appropriate feed-forward compensating transfer function is applied to enhance their order of astatism without inserting additional integrators in the forward path of the closed loop system and therefore achieving improvement of the corresponding tracking error accuracy performance.

4.2 Preliminaries

Before we start discussing the accuracy performance analysis and improvement of the system at hand, which is the core idea of this chapter, we find it necessary to know, first, the basic signals used to carry out this study.

4.2.1 Typical Standard Signals for Accuracy Analysis

The accuracy performance of any system is estimated by its ability to follow accurately with a smallest possible error a given input signal. Consequently, in order to study and analyze the accuracy performance property of the feedback control system, it is used to employ the test standard signals, expressed in the time domain by the polynomial of degree q as follows [108]:

$$r(t) = \frac{t^q}{q!}u(t) = K_q\, t^q u(t), \qquad t \geq 0 \tag{4.1}$$

With K_q is an arbitrary constant and $u(t)$ represents the unit step input function defined as:

$$u(t) = \begin{cases} 0\ ,\ t < 0 \\ \\ 1\ ,\ t \geq 0 \end{cases} \tag{4.2}$$

The corresponding Laplace transform of the reference signal is defined by:

$$R(s) = \frac{K_q}{s^{q+1}} \tag{4.3}$$

However, when this system is being analyzed for its accuracy, it does not make any sense to stimulate it with all manner of input functions. Instead, it is in analyzer's

best interest to test the system with a set of standard and simple reference functions. These are step, ramp and parabolic input stimulating signals of which we give the following brief description [109].

4.2.1.1 Step Function Signal

The step signal is defined by the piecewise function as follows:

$$r(t) = \begin{cases} 0\,, & t < 0 \\ K_0\,, & t \geq 0 \end{cases} \tag{4.4}$$

In term of unit step function defined by (4.2), the step function can be re-expressed as follows:

$$r_0(t) = K_0 u(t) \tag{4.5}$$

Its corresponding Laplace transform is given by:

$$R_0(s) = \frac{K_0}{s} \tag{4.6}$$

This step function is an important signal, not only its usefulness in determining the transient (dynamic) performance properties in control systems engineering from the step response characteristics, but also in signal processing, systems analysis, and all branches of engineering. Moreover, if the step function is input to a system, the output of the system is known as the step response and it can be defined using the inverse Laplace transform as:

$$r(t) = r_0(t) = K_0\, u(t) \xrightarrow{yields}$$

$$y(t) = L^{-1}\left\{ G(s) \,\middle|\, R(s) = {K_0}/{s} \right\} = L^{-1}\left\{ G(s)\frac{K_0}{s} \right\} \tag{4.7}$$

Where: $G(s)$ being the system's transfer function.

4.2.1.2 The Ramp Function

The ramp signal is defined in terms of unit step function by the following expression:

$$r_1(t) = K_1 t\, u(t) \tag{4.8}$$

Using the inverse Laplace transform, the corresponding ramp response of a system defined by its transfer function $G(s)$ is described by the following:

$$r(t) = r_1(t) = K_1\, t\, u(t) \xrightarrow{yields}$$

$$y(t) = L^{-1}\left\{G(s)\left|R(s) = {K_1}/{s^2}\right.\right\} = L^{-1}\left\{G(s)\frac{K_1}{s^2}\right\} \tag{4.9}$$

This response is also used to study the performance properties in steady state regime.

4.2.1.3 Parabolic Function

The parabolic signal is also typical and standard used basically to stimulate a system for accuracy performance analysis. It is defined in terms of unit step function by the following:

$$\mathrm{r_2(t) = K_2\, t^2\, u(t)} \tag{4.10}$$

Similarly, the parabolic response is given by:

$$r(t) = r_2(t) = K_2\, t^2\, u(t) \xrightarrow{yields}$$

$$y(t) = L^{-1}\left\{G(s)\left|R(s) = {K_2}/{s^3}\right.\right\} = L^{-1}\left\{G(s)\frac{K_2}{s^3}\right\} \tag{4.11}$$

4.3 System's Accuracy Performance Assessment for Variable Set Point

Besides the interest of having good dynamic performance properties, the steady state performance is also of paramount concern when designing and analyzing a control system. This performance is fully described by the accuracy property of the control system response. It means that, not only we require the transient regime to be short with the desired dynamic performance specifications, but also we need the system to be accurately enough at steady state regime.

The accuracy of a closed loop control system is fully quantified in terms of steady state error, which is defined, in the time domain, as the difference between the reference signal and the measured controlled signal as time tends to infinity.

Based on this definition, our theoretical evaluation and analysis of system accuracy performance due to assumed set point changes is performed by considering the separately excited DC drive system being represented by the general block diagram of Fig.4.1.

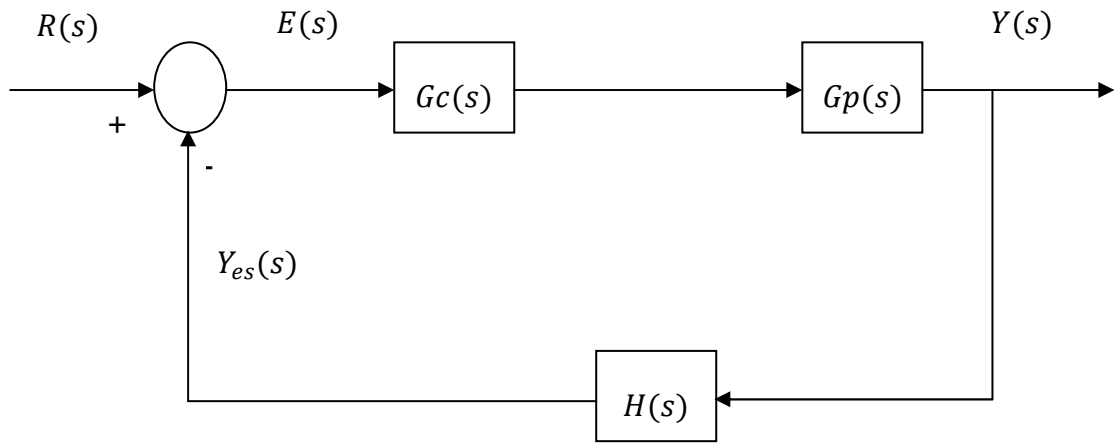

Figure 4.1 General Block Diagram of DC Drive Control System without Load Disturbance Signal.

With $R(s)$ represents the reference input signals.

$Y(s)$ and $Y_{es}(s)$ are, respectively, the actual and estimated output speed signals.

$E(s)$ is the tracking error signal of closed loop system.

$G_C(s), G_P(s)\ and\ H(s)$ are, respectively, the corresponding transfer functions of the controller, the controlled system (motor + power converter) and the state observer (the feedback element) defined by the general forms as follows:

$$G_C(s) = \frac{N_c(s)}{s^{\alpha_C} D_c(s)} = \frac{b_{mc}\, s^{mc} + b_{mc-1}\, s^{mc-1} + \cdots + b_{1c}\, s + b_{0c}}{s^{\alpha_c}\,(a_{nc}\, s^{nc} + a_{nc-1}\, s^{nc-1} + \cdots + a_{1c}\, s + a_{0c})},\ \alpha_c \geq 0,\ (\alpha_c + nc) \geq mc$$

(4.12)

$$G_P(s) = \frac{N_p(s)}{s^{\alpha_p} D_p(s)} = \frac{b_{mp}\, s^{mp} + b_{mp-1}\, s^{mp-1} + \cdots + b_{1p}\, s + b_{0p}}{s^{\alpha_p}\,(a_{np}\, s^{np} + a_{np-1}\, s^{np-1} + \cdots + a_{1p}\, s + a_{0p})},\ \alpha_p \geq 0,\ (\alpha_p + np) \geq mp$$

(4.13)

$$H(s) = \frac{N_h(s)}{s^{\alpha_h} D_h(s)} = \frac{b_{mh}\, s^{mh} + b_{mh-1}\, s^{mh-1} + \cdots + b_{1h}\, s + b_{0h}}{s^{\alpha_h}\,(a_{nh}\, s^{nh} + a_{nh-1}\, s^{nh-1} + \cdots + a_{1h}\, s + a_{0h})},\ \alpha_h \geq 0,\ (\alpha_h + nh) \geq mh$$

(4.14)

Based on this general representation, the previously defined steady state tracking error of the system is expressed, in time domain, as:

$$e_{ss} = \lim_{t\to\infty}(r(t) - y_{es}(t)) \tag{4.15}$$

It is known that this steady state error is a standard measure of performance that is widely used in assessing the accuracy of control system [62]; therefore, it is obvious that an accurate control system is that of ideally zero steady state error.

4.3.1 Calculation of System's Steady State Error

By referring to the general block diagram representation of Fig.4.1, in frequency domain, the control tracking error is defined as the difference between the reference signal $R(s)$ and the estimated output signal $Y_{es}(s)$ as follows:

$$E(s) = R(s) - H(s)Y(s) \tag{4.16}$$

Since:

$$Y(s) = G_C(s)G_P(s)E(s) \tag{4.17}$$

It results that:

$$E(s) = R(s) - H(s)G_c(s)G_p(s)E(s) \tag{4.18}$$

Hence:

$$E(s) = \frac{1}{1+H(s)G_C(s)G_P(s)} R(s) \tag{4.19}$$

Based on the definitions (4.12), (4.13) and (4.14), we define the control system's open loop transfer function to be:

$$G_{OL}(s) = H(s)G_C(s)G_P(s) = \frac{N_h(s)N_c(s)N_p(s)}{s^{(\alpha_h+\alpha_c+\alpha_p)}D_h(s)D_c(s)D_p(s)} \tag{4.20}$$

Or:

$$G_{OL}(s) = \frac{N_{ol}(s)}{s^{\alpha}D_{ol}(s)} \tag{4.21}$$

Where:

$$N_{ol}(s) = N_h(s)N_c(s)N_p(s) = K_{ol}(1 + b_1 s + b_2 s^2 + \cdots + b_m s^m) \tag{4.22}$$

$$D_{ol}(s) = D_h(s)D_c(s)D_p(s) = (1 + a_1 s + a_2 s^2 + \cdots + a_n s^n) \tag{4.23}$$

And

$$\alpha = \alpha_h + \alpha_c + \alpha_p \tag{4.24}$$

The constant: $K_{ol} = \frac{b_0}{a_0}$ in the polynomial expression (4.22) is known as the steady state gain of the open loop transfer function. The parameter α defined by (4.24) is known as the ***order of astatism (type)*** of the system's open loop transfer function, which represents the number of integrators in the forward path of the feedback control loop. Therefore, the tracking error is rewritten under the following expression:

$$E(s) = \frac{1}{1+G_{OL}(s)} R(s) = \frac{s^{\alpha} D_{ol}(s)}{N_{ol}(s)+s^{\alpha} D_{ol}(s)} R(s) \quad (4.25)$$

If the control system is stable [109], the final value of the tracking error in the time domain ($t \to \infty$), which is the steady state error, is calculated using the final value theorem as follows:

$$e_{ss}(\infty) = \lim_{t\to\infty} e(t) = \lim_{s\to 0} s\, E(s) = \lim_{s\to 0} s \frac{1}{1+G_{OL}(s)} R(s) \quad (4.26)$$

Or:

$$e_{ss}(\infty) = \lim_{s\to 0} \frac{s^{\alpha+1} D_{ol}(s)}{N_{ol}(s)+s^{\alpha} D_{ol}(s)} R(s) \quad (4.27)$$

By referring to expressions (4.22) and (4.23), we obtain:

$$\lim_{s\to 0} N_{ol}(s) = K_{ol} \quad (4.28)$$

$$\lim_{s\to 0} D_{ol}(s) = 1 \quad (4.29)$$

Consequently, the expression of steady state error becomes:

$$e_{ss}(\infty) = \lim_{s\to 0} \frac{s^{\alpha+1}}{K_{ol}+s^{\alpha}} R(s) \quad (4.30)$$

If we substitute the input reference signal $R(s)$ by its general expression (4.3) in (4.30), we obtain:

$$e_{ss}(\infty) = \lim_{s\to 0} \frac{K_q\, s}{s^{q+1}(1+\frac{K_{ol}}{s^{\alpha}})} = \lim_{s\to 0} \frac{K_q\, s^{\alpha-q}}{s^{\alpha}+K_{ol}} \tag{4.31}$$

It is clear from expression (4.31) that the final value of the steady state error depends simultaneously on the system's order of astatism and the form of reference signal $R(s)$ (the value of q in the expression). Using the previously defined standard input signals, this final value can be distinguished as follows:

- ***Position steady state error*** when the system is stimulated using ***step*** input signal and is characterized by the position error coefficient K_p defined by:

$$K_p = \lim_{s\to 0} G_{OL}(s) \tag{4.32}$$

- ***Speed steady state error*** when the system is stimulated using ***ramp*** input signal and is characterized by the speed error coefficient K_v defined as:

$$K_v = \lim_{s\to 0}\ s\ G_{OL}(s) \tag{4.33}$$

- ***Acceleration steady state error*** when the system is stimulated using ***parabolic*** input signal and is characterized by the acceleration error coefficient K_a defined as:

$$K_a = \lim_{s\to 0} s^2\ G_{OL}(s) \tag{4.34}$$

These coefficients enter implicitly in the definition of the steady state error expression, where their knowledge determines the quality and accuracy of a given automatic control system when it is being excited by a determined standard input reference signal.

4.3.2 Relationship between System Accuracy and its Order of Astatism

From the above, we deduce that there is a correlation between the system's order of astatism and its accuracy represented by the final value of steady state error. This

fact is summarized in the Table 4.1 that mentions the steady state error evaluated for different order of astitism and stimulated with the standard input signals.

Table 4.1 Values of Steady State Error due to Step, Ramp and Parabolic Set Point Changes and its Relation to System's Order of Astatism.

System's type	**System Input Reference Signal**		
	Step $(\boldsymbol{q = 0})$	***Ramp*** $(\boldsymbol{q = 1})$	***Parabolic*** $(\boldsymbol{q = 2})$
0	$e_{ss} = \dfrac{K_0}{1 + K_p}$	$e_{ss} = \infty$	$e_{ss} = \infty$
1	$e_{ss} = 0$	$e_{ss} = \dfrac{K_1}{K_v}$	$e_{ss} = \infty$
2	$e_{ss} = 0$	$e_{ss} = 0$	$e_{ss} = \dfrac{K_2}{K_a}$
> 2	$e_{ss} = 0$	$e_{ss} = 0$	$e_{ss} = 0$

From these theoretical results, we notice that if the system is stable and of order of astatism (type) α, then it has a zero steady-state error for polynomial reference inputs of order less than α, a nonzero finite steady-state error for an input of order equals to α, and an infinite steady-state error for inputs of order greater than α. Therefore, we have:

- ***A type 0*** system has a nonzero but finite steady-state error for a step reference input, and an infinite steady-state error for ramp and higher-order inputs.
- ***A type 1*** system has zero steady-state error for a step input, a finite steady-state error for a ramp input, and infinite steady-state error for inputs of order two or higher.
- ***A type 2*** system has zero steady-state error for step and ramp inputs, a finite steady-state error for a second-order input, and infinite steady-state error for inputs of order three or higher.

4.3.3 Simulation Results

In this subsection, we shall apply the above theoretical facts to analyze and assess the quality of the drive speed response in terms of accuracy performance and order of astatism. We will follow the same procedure previously worked out for all studied models. Each model is being stimulated using step, ramp, and parabolic or higher order polynomial functions (depending on the model order of astatism) as reference input signals. In order to investigate the effect of viscous friction coefficient (β), the obtained simulation results of the speed tracking error response are depicted according to the value of this coefficient.

4.3.3.1 System Model with 1PI Speed Controller and State Observer of order 2

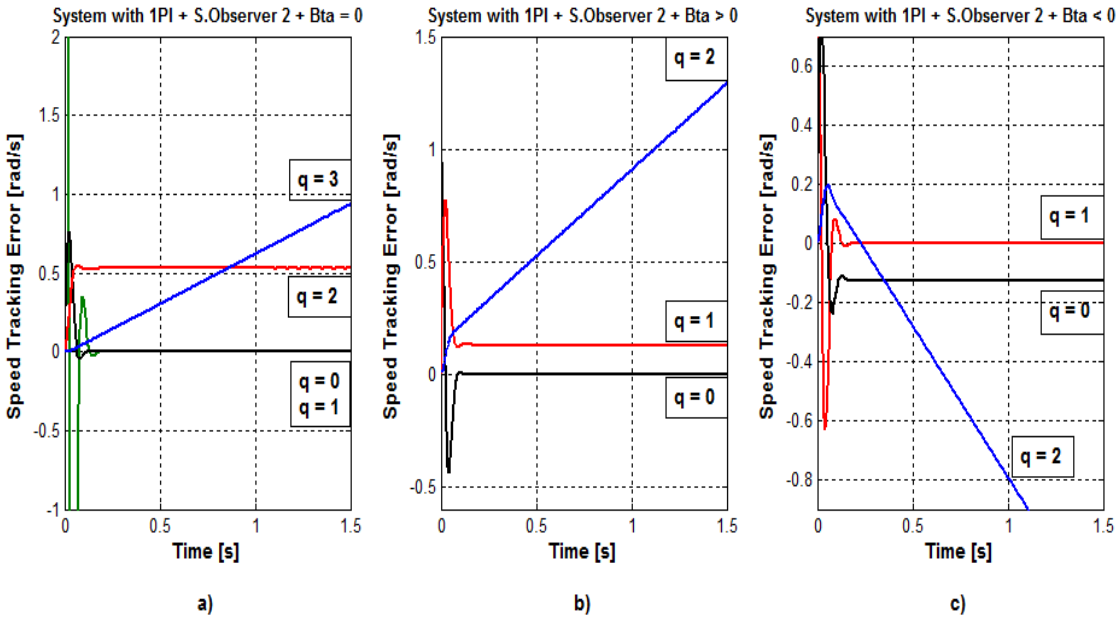

Figure 4.2 Speed Tracking Error Response of System Model with 1PI Speed Controller and State Observer of order 2 due to Input Set Point Changes; **a)** case of $\beta = 0$, **b)** case of $\beta > 0$, **c)** case of $\beta < 0$.

4.3.3.2 System Model with 2PI Speed Controller and State Observer of order 2

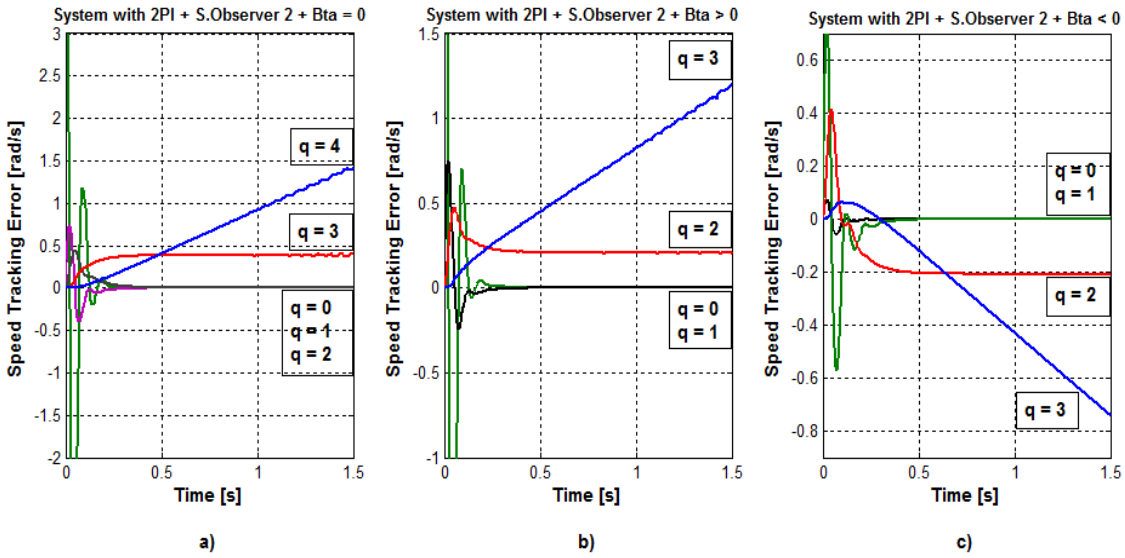

Figure 4.3 Speed Tracking Error Response of System Model with 2PI Speed Controller and State Observer of order 2 due to Input Set Point Changes; **a)** case of $\beta = 0$, **b)** case of $\beta > 0$, **c)** case of $\beta < 0$.

4.3.3.3 System Model with 1PI Speed Controller and State Observer of order 5

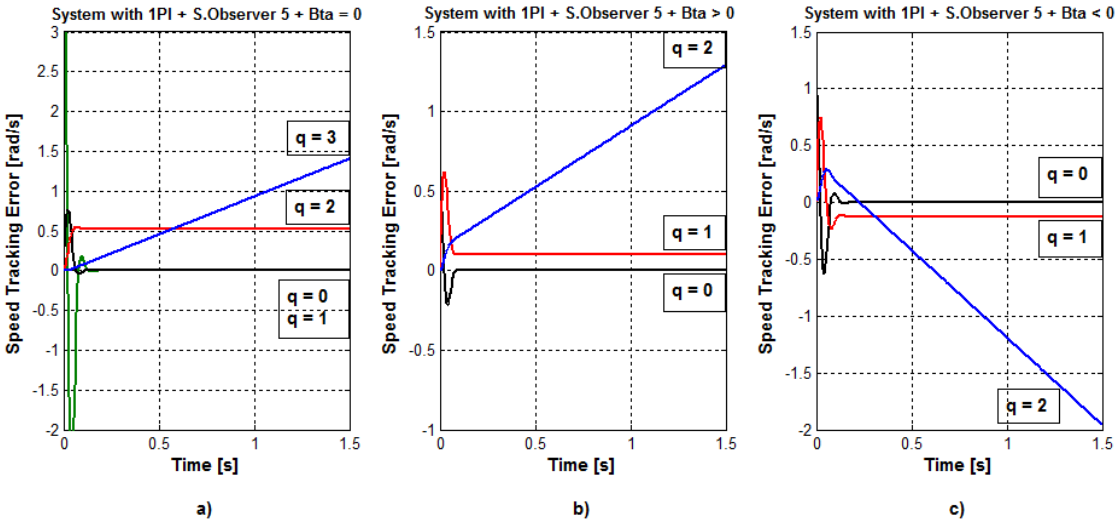

Figure 4.4 Speed Tracking Error Response of System Model with 1PI Speed Controller and State Observer of order 5 due to Input Set Point Changes; **a)** case of $\beta = 0$, **b)** case of $\beta > 0$, **c)** case of $\beta < 0$.

4.3.3.4 System Model with 2PI Speed Controller and State Observer of order 6

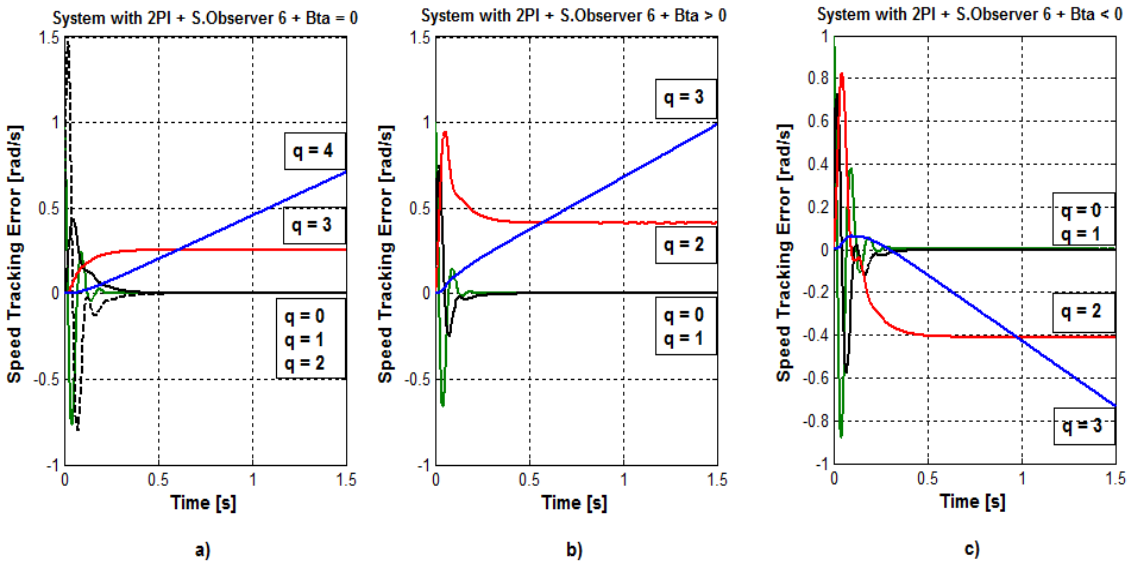

Figure 4.5 Speed Tracking Error Response of System Model with 2PI Speed Controller and State Observer of order 6 due to Input Set Point Changes; **a)** case of $\beta = 0$, **b)** case of $\beta > 0$, **c)** case of $\beta < 0$.

4.3.4 Results Interpretation and Discussion

Obviously, the graphical simulation results mention that the four studied models respond differently to input set point changes, where the final value of steady state error depends on the order of astatism of each model. Moreover, the results show that the models which incorporate double PI speed controller, acquire higher order of astatism, hence they have better accuracy performance in response to set point change than those models of only single PI controller. It is also noticeable that the models simulated with disregarding the coefficient of viscous friction ($\beta = 0$) have higher order of astatism than the case of taking this coefficient different of zero.

Overall, all the models exhibit the ability to improve their accuracy performance and order of astatism by zeroing their constant steady state errors due to a given input set point stimulation.

4.4. Accuracy Performance Improvement using Feed-Forward Compensation

The above simulation results give us a good picture about the accuracy performance quality of the PI based speed controller DC drive system when it is stimulated using basically a different input reference signals. The results mention, for all the different models studied, the failure of PI and double PI speed controller alone to withstand the substantial speed variation and maintaining the desired tracking performance.

In order to overcome this problem, a lot of work has been done by many researchers to find control methods and techniques that are capable of achieving improvement in accuracy performance of control systems under variable input reference conditions.

4.4.1 Previous Work

To solve this control problem, particularly arisen in paper and steel rolling mill industries, many methods are proposed in the literature. Traditionally, it is used to improve the accuracy performance of a closed loop control system by the proportional gain method [41], which consists of exploiting the inverse proportionality relationship that exists between the system steady state error and the loop static gain and reducing the former by increasing the loop gain. This method, although efficient of allowing obtaining a speed response with a very small steady state error, it degrades the system's transient performance by increasing the percent overshoot. Another method known as integral control [110] is also used to improve both systems' order of astatism and accuracy by modifying the control structure and adding integral terms in the forward path of the control loop. The main drawback of this method is that these added integrators may lead to instability of the system.

The sliding mode control (SMC) is used with PI controller in [111, 112] as a robust and simple control technique to ensure stability and desired tracking performance for especially systems characterized by uncertainties and disturbance variation. Although its effectiveness in achieving the performance objectives, this method suffers from a major drawback of chattering phenomenon, which can be reduced using other techniques. Due to the fact that SMC method exhibits robustness

and high disturbance rejection capability, it is used alone in [113] to replace the PID controller and improving the accuracy performance affected by the cutting forces of the machine tool systems.

In an attempt of combining the advantages of sliding mode control and the adaptive control approach, the method named as adaptive sliding mode control is proposed in [114] to compensate model uncertainties of flexible-joint manipulator nonlinear dynamic systems and ensuring robust stability and accuracy performance. An accurate steady state response with zero error is also obtained using this combined technique in [115], where the control chattering is thereafter eliminated.

An adaptive neural network (NN) control scheme is also used in [116] to study and improve the tracking performance of induction motor speed control drive systems under variable reference input signal. The achieved performance is judged satisfactory using both simulation and experimental laboratory results even in the presence of much strong mechanical friction and other non linear characteristics. The method is also applied in [117] for the same purpose on the speed and position controlled DC motor drive system.

The hybrid fuzzy-neural networks controller is, on the other hand, applied in [118], to adaptively improve both robustness and accuracy performance of induction motor speed control system. The tracking performance of the system was satisfactorily illustrated under a variable load torque with the external disturbance introduced by disturbing the load during trajectory control. The same approach is also used in [119] to improve the control performance of the DC drive under transient and steady state conditions.

4.4.2 Application of Feed-Forward Compensation Technique

The feed-forward compensation is an alternative approach widely employed to enhance the quality and performance of control system in different engineering branches. It consists of altering the structure of the control system by adding a compensating branch in the forward path of the closed loop system. Many techniques have used this approach to improve the tracking and accuracy performance of feedback control systems. In the literature, the Neural Network (NN) based feed-

forward method is used in [120] to ameliorate the accuracy performance of PID based nonlinear control systems characterized with an input disturbance.

The obtained results have mentioned a satisfactory reduction of the steady state error after a certain learning number. The Fuzzy logic control combined with PI controller has also been used in [121] as a feed-forward compensator to improve the already implemented sliding mode based positioning control system. For more reading in this topic, we can refer to [122] where other forms of feed-forward compensators are studied.

In our work we will use this feed-forward compensating technique according to the structure depicted by the simulink block diagram of Fig.4.6 and applied, typically, on the system model with 1PI and state observer of order 2.

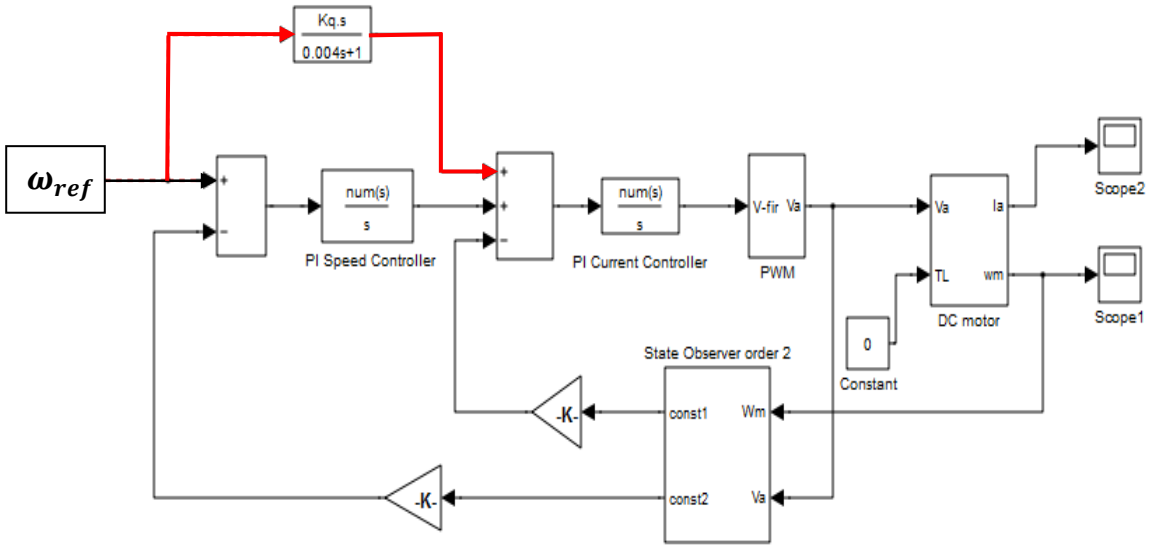

Figure 4.6 Typical Block Diagram of System Model with 1PI and State Observer of order 2 Incorporating Feed-Forward Compensation Technique.

Accordingly, we aim of using the feed-forward compensation to improve both accuracy and order of astatism of the drive system by reducing the finite steady state error via the identification of the proposed feed-forward transfer function, which we define it to have the following form:

$$T_{FF}(s) = \frac{K_q s}{0.004s+1} \tag{4.35}$$

Where the constant K_q is determined by solving the square of error based minimization problem described as:

$$Min_{K_q}\, K_q e^2(t) \tag{4.36}$$

In order to solve the function (4.36), we use the MATLAB function "fminsearch" from optimization tool box [106]. The output of the minimization process gives the optimal value of the constant K_q, which identifies completely the transfer function of the used feed-forward compensator that corresponds to the improved accuracy performance for each simulink model representing the system at hand.

The simulation results showing improvements of both accuracy performance and order of astatism that are achieved with each of four studied models are illustrated consecutively in the following subsequent figures.

4.4.2.1 System Model with 1PI Speed Controller and State Observer of order 2

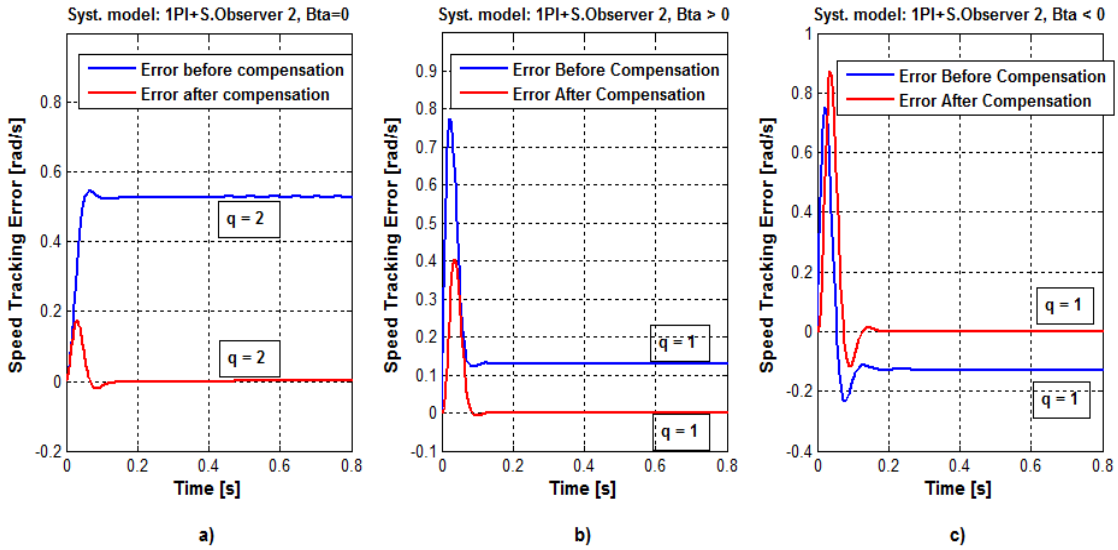

Figure 4.7 Steady State Error and order of Astatism Improvement with Feed-Forward Compensation of System Model with 1PI and State Observer of order 2 under Input Set Point Changes; a) case of $\beta = 0$, b) case of $\beta > 0$, c) case of $\beta < 0$

4.4.2.2 System Model with 2PI Speed Controller and State Observer of order 2

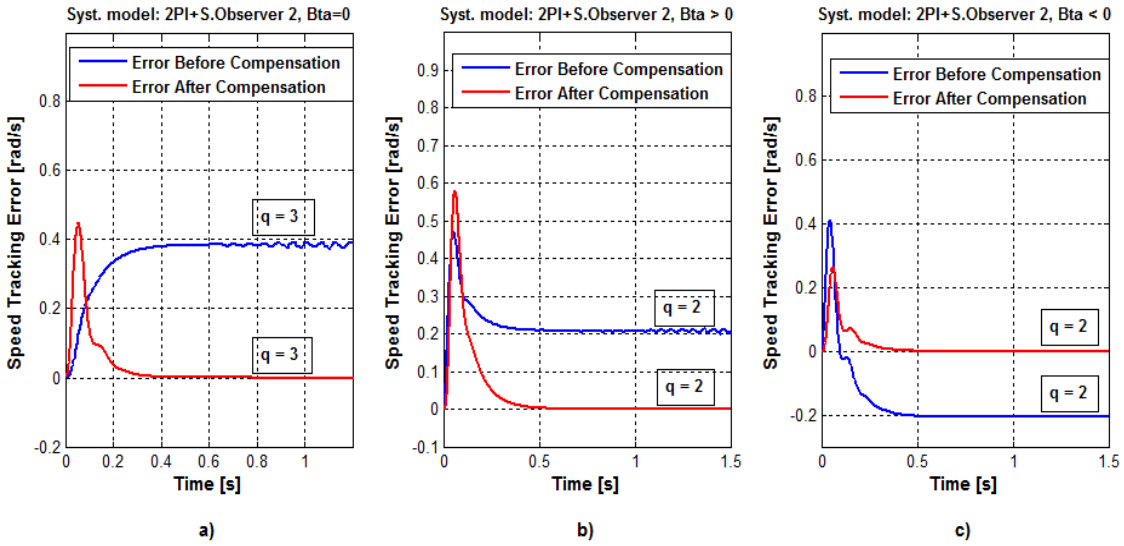

Figure 4.8 Steady State Error and order of Astatism Improvement with Feed-Forward Compensation of System Model with 2PI and State Observer of order 2 under Input Set Point Changes; a) case of $\beta = 0$, b) case of $\beta > 0$, c) case of $\beta < 0$

4.4.2.3 System Model with 1PI Speed Controller and State Observer of order 5

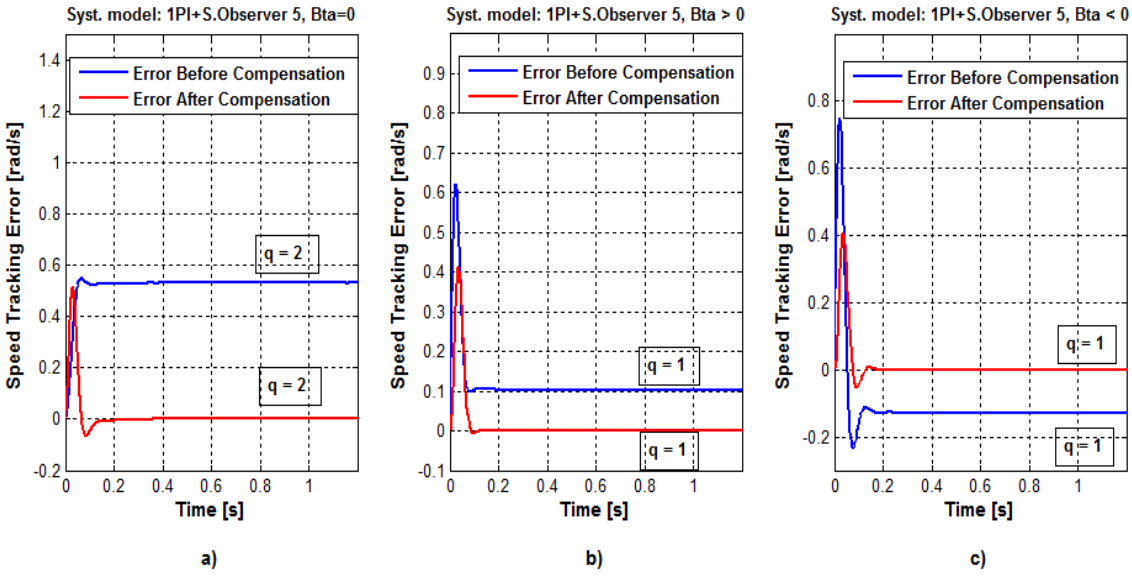

Figure 4.9 Steady State Error and order of Astatism Improvement with Feed-Forward Compensation of System Model with 1PI and State Observer of order 5 under Input Set Point Changes; a) case of $\beta = 0$, b) case of $\beta > 0$, c) case of $\beta < 0$

4.4.2.4 System Model with 2PI Speed Controller and State Observer of order 6

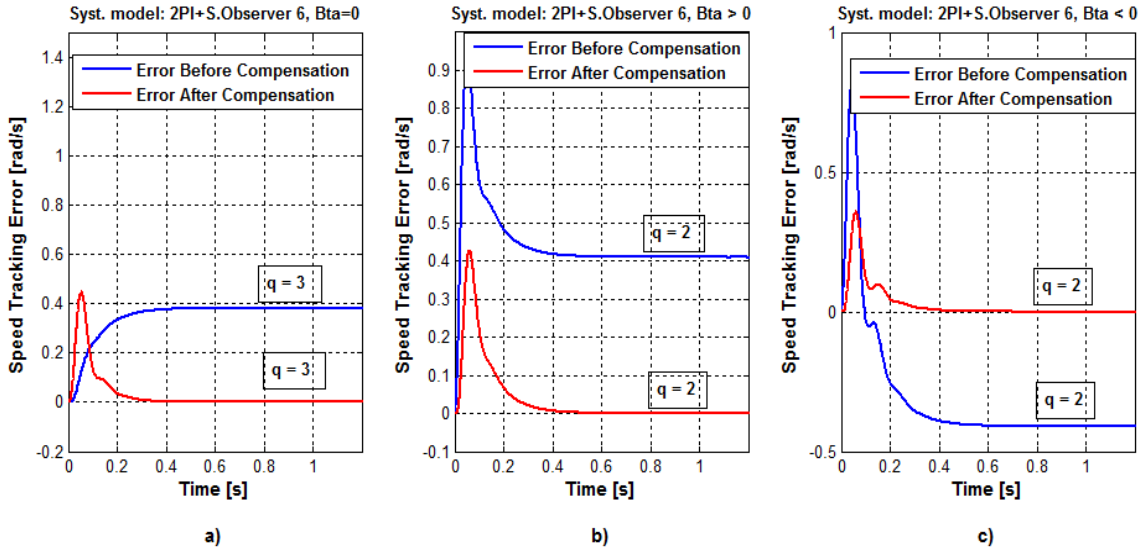

Figure 4.10 Steady State Error and order of Astatism Improvement with Feed-Forward Compensation of System Model with 2PI and State Observer of order 6 under Input Set Point Changes; a) case of $\beta = 0$, b) case of $\beta > 0$, c) case of $\beta < 0$

4.4.3 Results Interpretation and Discussion

The simulation results mention clearly that the use of optimized feed-forward transfer function compensation has allowed improvement of accuracy performance of all the models subjected to input set point changes, in such a way that a response with constant steady state error before compensation has perfectly followed, after compensation, the change occurred in the input reference. Consequently, regardless the value of viscous friction coefficient, an improvement of accuracy is achieved for all models and their order of astatism has been augmented by one.

4.5 Improving System's Accuracy under Load Disturbance Effect

In a drive system, the task of a speed controller is to generate the torque reference that drives the output speed towards the set point value and keeps the speed error as small as possible, preferably zero. The speed error is caused either by the input disturbance (i.e., the speed reference) or by changes in the load torque T_L. in this section we study the effect of load torque disturbance on the accuracy performance of the drive speed response where an improvement is being inspired.

4.5.1 Load Disturbance Steady State Error Evaluation

To calculate the steady state error due load torque disturbance, we consider the following general block diagram representation of our drive system.

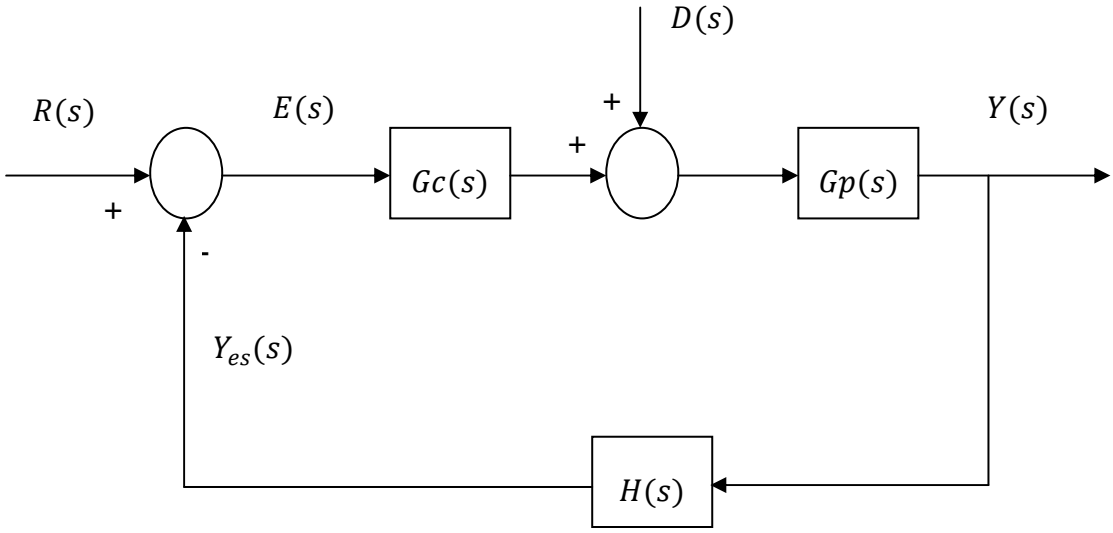

Figure 4.11 General Block Diagram of DC Drive Control System with Load Disturbance Signal Account

With $D(s)$ represents the load torque disturbance signal.

In frequency domain, the control tracking error $E(s)$ is defined as the difference between the reference signal $R(s)$ and the estimated output signal $Y_{es}(s)$ as follows:

$$E(s) = R(s) - H(s)Y(s) \tag{4.37}$$

Since:

$$Y(s) = [G_C(s)E(s) + D(s)]G_P(s) \tag{4.38}$$

It results that:

$$E(s) = R(s) - H(s)G_c(s)G_P(s)E(s) - H(s)G_p(s)D(s) \tag{4.39}$$

Hence:

$$E(s) = \frac{1}{1+H(s)G_C(s)G_P(s)} R(s) - \frac{H(s)G_p(s)}{1+H(s)G_c(s)G_P(s)} D(s) \tag{4.40}$$

Or:

$$E(s) = E_R(s) + E_D(s) \tag{4.41}$$

Where:

$E_R(s) = \frac{1}{1+H(s)G_C(s)G_P(s)}\ R(s)$ is the tracking error due to the input reference signal, and: $E_D(s) = -\frac{H(s)G_p(s)}{1+H(s)G_c(s)G_P(s)}\ D(s)$ is error due to the load disturbance signal.

This is can be verified by rearranging the block diagram of Fig.4.11 in the following two forms:

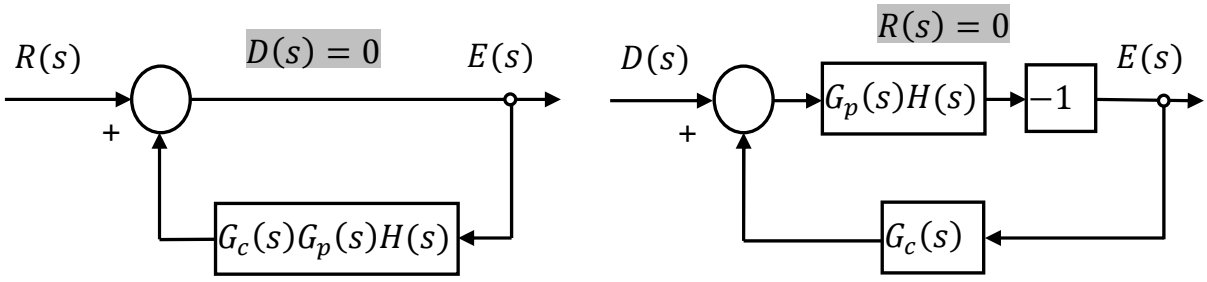

a) **b)**

Figure 4.12 Equivalent Block Diagram of DC Drive System under the Independent effect of Set Point (a) and Load Disturbance (b) Variations.

We shall only consider the evaluation of the steady state error caused by the variation and change of load torque disturbance according to Fig.4.12 (b).

Therefore, by using the definitions (4.12), (4.13) and (4.14) given, respectively to the transfer functions $G_C(s), G_P(s)$ and $H(s)$ with the expression (4.21) defining the open loop transfer function of the system, the control tracking error due to disturbance can, finally, be given as the following:

$$E_D(s) = -\frac{s^{\alpha_c} D_c(s)N_p(s)N_h(s)}{N_{ol}(s)+s^{\alpha} D_{ol}(s)}\ D(s) \tag{4.42}$$

The steady state error is calculated using the final value theorem as follows:

$$e^{D}{}_{ss}(\infty) = \lim_{t\to\infty} e^{D}(t) = \lim_{s\to 0} s\, E_D(s) = \lim_{s\to 0} -\frac{s^{\alpha_c+1}\, D_c(s) N_p(s) N_h(s)}{N_{ol}(s)+s^{\alpha}\, D_{ol}(s)}\, D(s) \qquad (4.43)$$

With $e^{D}(t)$ is the tracking error due to the load disturbance expressed in the time domain, and $e^{D}{}_{ss}(\infty)$ is its corresponding steady state value.

If we define:

$$K_c = \frac{b_{0c}}{a_{0c}} \qquad (4.44)$$

$$K_p = \frac{b_{0p}}{a_{0p}} \qquad (4.45)$$

$$K_h = \frac{b_{0h}}{a_{0h}} \qquad (4.46)$$

As being, respectively, the static gains of the corresponding transfer functions $G_c(s)$, $G_p(s)$ and $H(s)$;

And if we use the expression (4.3) to define a variable load torque disturbance as:

$$D(s) = \frac{K_q}{s^{q+1}} \qquad (4.47)$$

After developing the equation (4.43), the final value of the steady state error reflecting the effect of load torque disturbance can be given as:

$$e^{D}{}_{ss}(\infty) = \lim_{s\to 0} -\frac{K_q\, K_p K_h\, s^{\alpha_c}}{s^{q}(s^{\alpha}+K_c\, K_p K_h)} = \lim_{s\to 0} -\frac{K_q\, K_p K_h\, s^{\alpha_c}}{s^{q}(s^{\alpha}+K_{ol})} \qquad (4.48)$$

With: $K_{ol} = K_c\, K_p K_h$

Based on the above theoretical background, we summarize in Table 4.2 the values of the steady state error corresponding to the different standard test signals of the load torque disturbance.

By comparing the two forms of the equivalent circuit of Fig.4.12, we can deduce that the parameters of the controller's transfer function (α_c, K_c) are basic in

determining the steady state error value as well as the number of integrators at origin or astatism order of the system due to load torque disturbance.

We summarize these values according to the type of the applied load disturbance signal in Table 4.2.

Table 4.2 Values of Steady State Error due to Step, Ramp and Parabolic Load Torque Disturbance

System type	**Load Torque Disturbance Signal**		
	$K_0\, u(t)$ $(q = 0)$	$K_1 t\, u(t)$ $(q = 1)$	$K_2\, t^2\, u(t)$ $(q = 2)$
0	$e^D{}_{ss}(\infty) = -\dfrac{K_0 K_p K_h}{1 + K_c K_p K_h}$	$e^D{}_{ss}(\infty) = \infty$	$e^D{}_{ss}(\infty) = \infty$
1	$e^D{}_{ss}(\infty) = 0$	$e^D{}_{ss}(\infty) = -\dfrac{K_1}{K_c}$	$e^D{}_{ss}(\infty) = \infty$
2	$e^D{}_{ss}(\infty) = 0$	$e^D{}_{ss}(\infty) = 0$	$e^D{}_{ss}(\infty) = -\dfrac{K_2}{K_c}$
> 2	$e^D{}_{ss}(\infty) = 0$	$e^D{}_{ss}(\infty) = 0$	$e^D{}_{ss}(\infty) = 0$

4.5.2 Simulation Results of Steady State Error under Load Disturbance

We will explore this theoretical assessment of steady state error due to load torque disturbance by simulation. To do so, we make zero the input set point signal and applying a variable load torque polynomial signal of standard step, ramp and parabolic basis.

The results are given consecutively for each model and according to the value of viscous friction coefficient in the following figures.

4.5.2.1 System Model with 1PI Speed Controller and State Observer of order 2

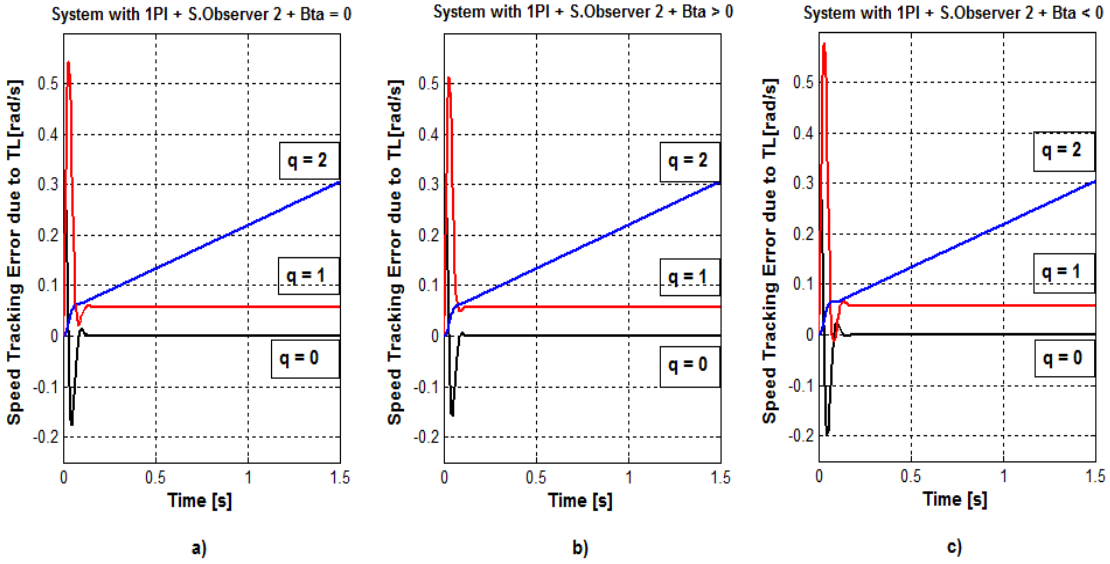

Figure 4.13 Speed Tracking Error Response of System Model with 1PI Speed Controller and State Observer of order 2 due to Load Torque Disturbance; **a)** case of $\beta = 0$, **b)** case of $\beta > 0$, **c)** case of $\beta < 0$.

4.5.2.2 System Model with 2PI Speed Controller and State Observer of order 2

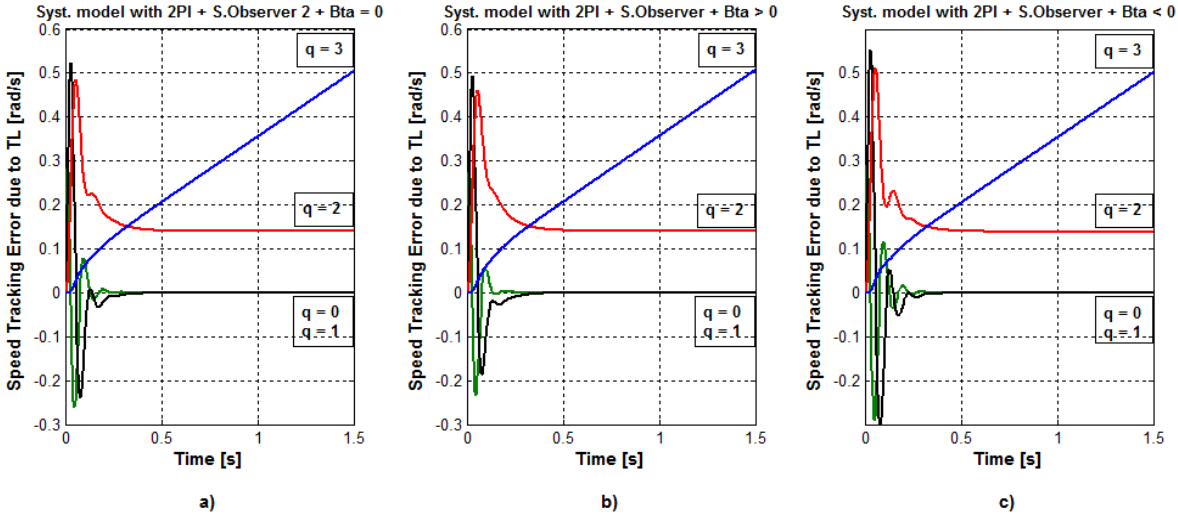

Figure 4.14 Speed Tracking Error Response of System Model with 2PI Speed Controller and State Observer of order 2 due to Load Torque Disturbance; **a)** case of $\beta = 0$, **b)** case of $\beta > 0$, **c)** case of $\beta < 0$.

4.5.2.3 System Model with 1PI Speed Controller and State Observer of order 5

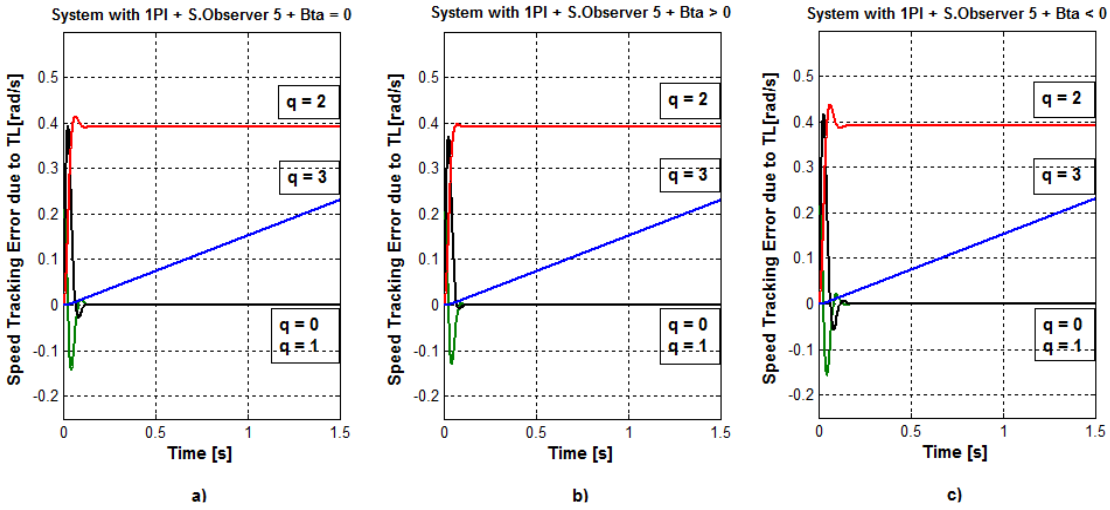

Figure 4.15 Speed Tracking Error Response of System Model with 1PI Speed Controller and State Observer of order 5 due to Load Torque Disturbance; **a)** case of $\beta = 0$, **b)** case of $\beta > 0$, **c)** case of $\beta < 0$.

4.5.2.4 System Model with 2PI speed controller and State Observer of order 6

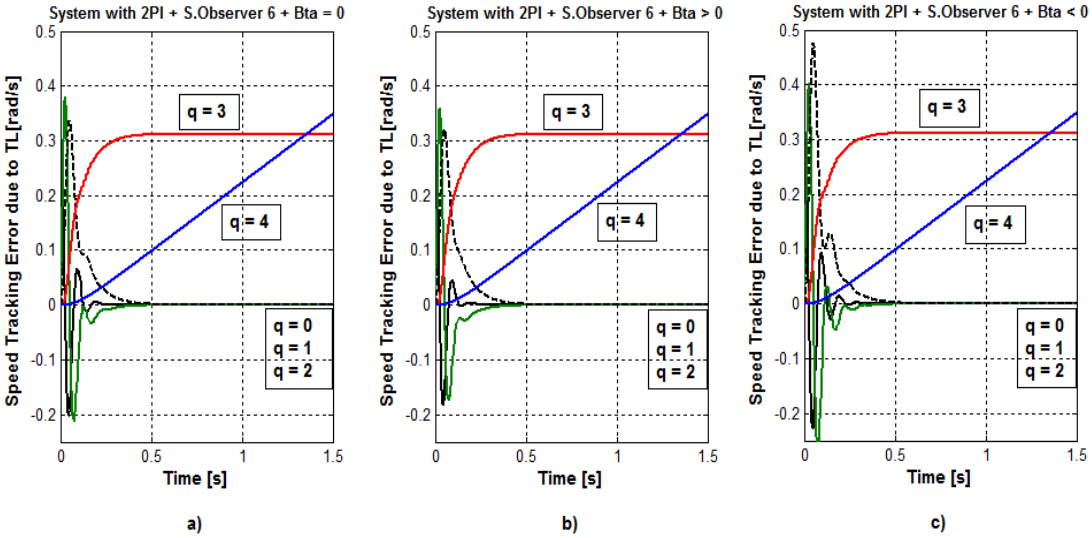

Figure 4.16 Speed Tracking Error Response of System Model with 2PI Speed Controller and State Observer of order 6 due to Load Torque Disturbance; **a)** case of $\beta = 0$, **b)** case of $\beta > 0$, **c)** case of $\beta < 0$.

4.5.3 Results Interpretation and Discussion

These results, which reflect the effect of load torque variation on the accuracy performance of the drive system, illustrate the discrepancy between the models in responding the different stimulating signals as load torque. Unlike the case of set point effect on the value of steady state error, here, the results obtained for the final value of this accuracy parameter have nothing to do with neither the number of PI speed controller nor the consideration of the value of viscous friction coefficient. However, all the models exhibit the ability to improve their accuracy performance and by zeroing their constant steady state errors produced due to a given load torque disturbance.

4.5.4 Load Torque Disturbance Suppression using Feed-Forward Compensation

In this section, we present the same Feed-Forward compensation technique to suppress the effect of load torque disturbance and achieving improvement of accuracy performance of the system. A typical structure that illustrates the employment of this compensator with system model constituted of 1PI speed controller and state observer of order two is depicted by the block diagram of Fig.4.16.

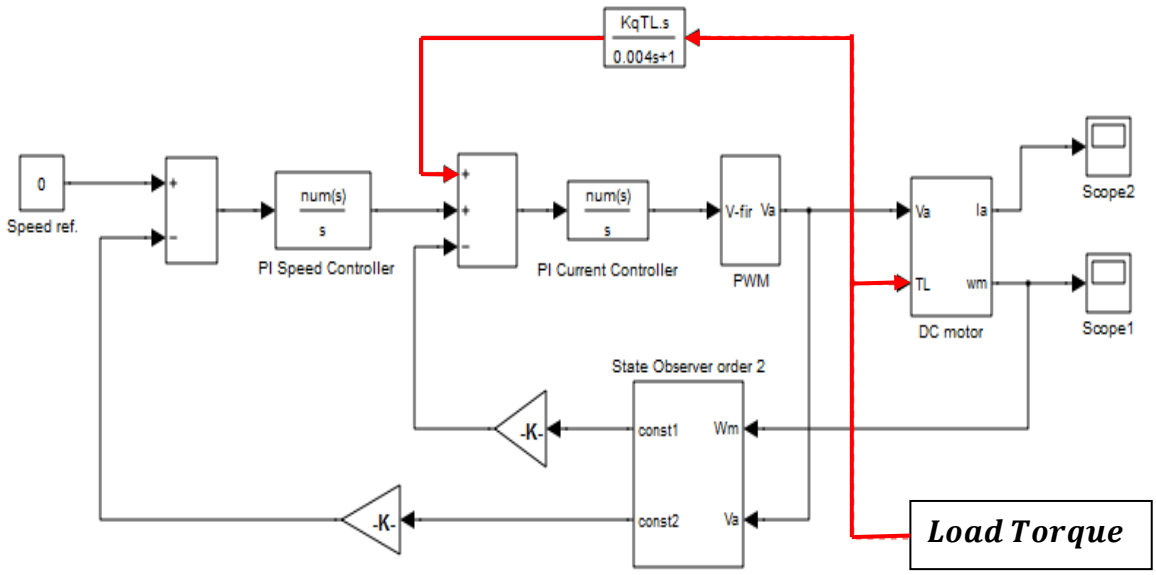

Figure 4.17 Typical Block Diagram of System Model with 1PI and State Observer of order 2 Incorporating Feed-Forward Load Torque Disturbance Compensation.

By applying this structure on all the studied models, the simulation results are given consecutively in the following figures.

4.5.4.1 System Model with 1PI Speed Controller and State Observer of order 2

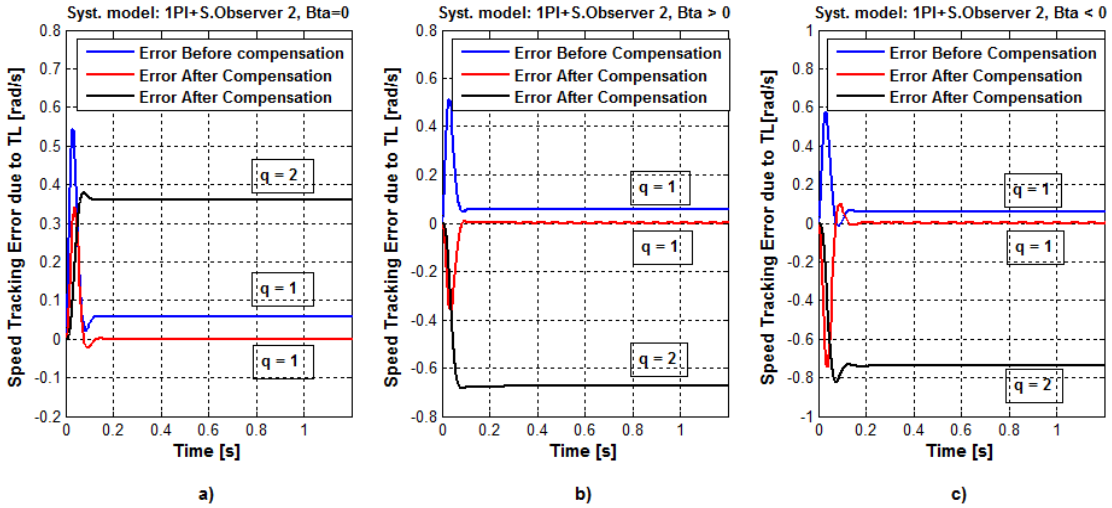

Figure 4.18 Steady State Error Improvement with Feed-Forward Compensation of System Model with 1PI and State Observer of order 2 under Load Torque Disturbance; a) case of $\beta = 0$, b) case of $\beta > 0$, c) case of $\beta < 0$

4.5.4.2 System Model with 2PI Speed Controller and State Observer of order 2

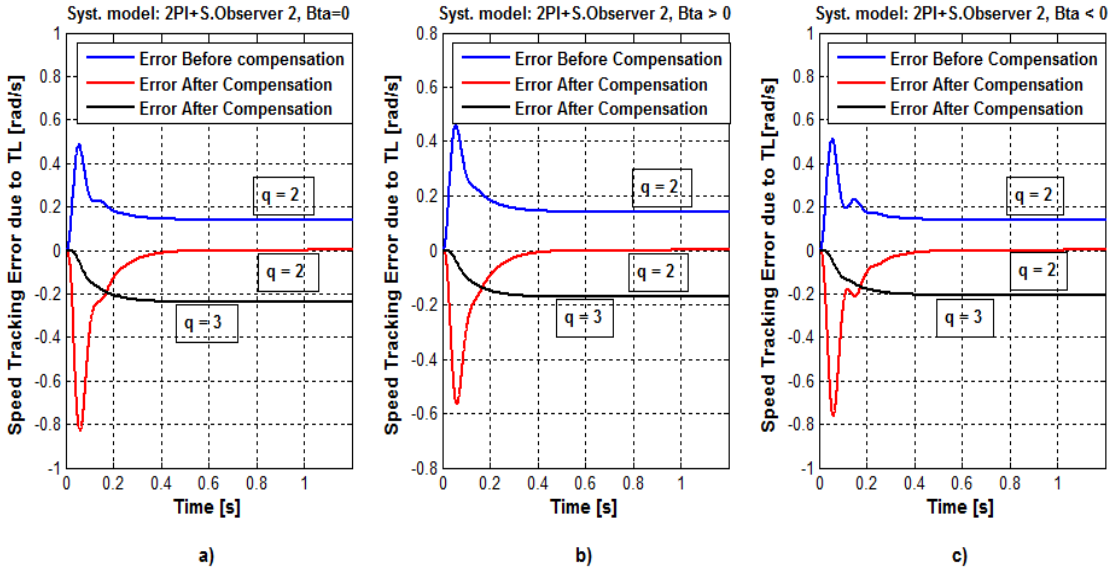

Figure 4.19 Steady State Error Improvement with Feed-Forward Compensation of System Model with 2PI and State Observer of order 2 under Load Torque Disturbance; a) case of $\beta = 0$, b) case of $\beta > 0$, c) case of $\beta < 0$

4.5.4.3 System Model with 1PI Speed Controller and State Observer of order 5

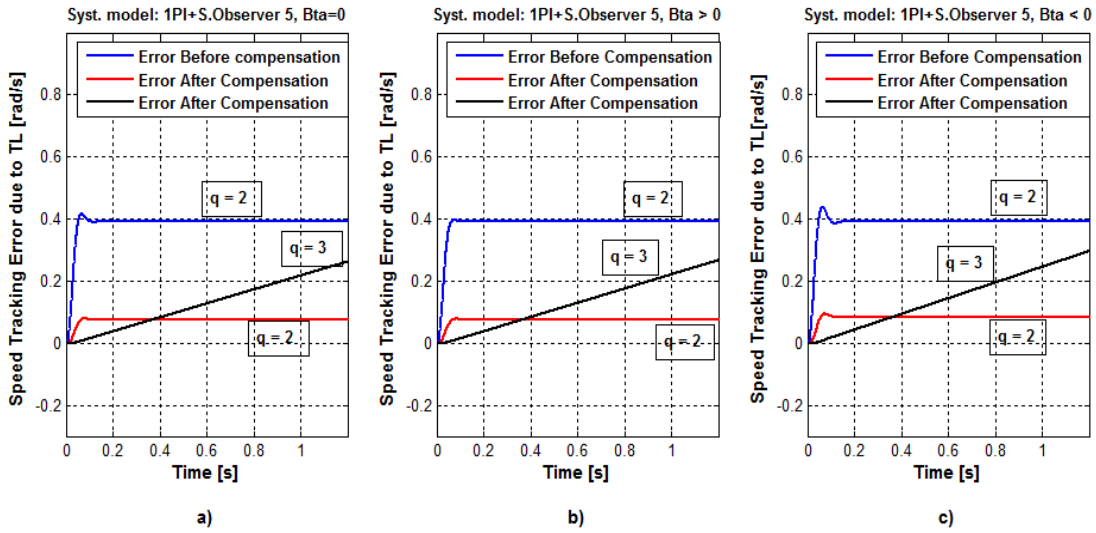

Figure 4.20 Steady State Error Improvement with Feed-Forward Compensation of System Model with 1PI and State Observer of order 5 under Load Torque Disturbance; a) case of $\beta = 0$, b) case of $\beta > 0$, c) case of $\beta < 0$

4.5.4.4 System Model with 2PI Speed Controller and State Observer of order 6

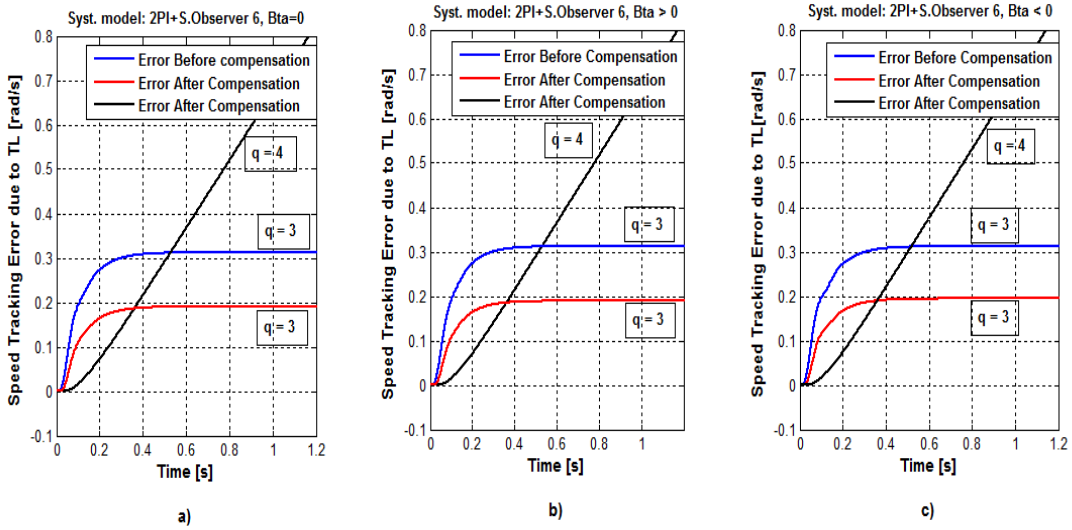

Figure 4.21 Steady State Error Improvement with Feed-Forward Compensation of System Model with 2PI and State Observer of order 6 under Load Torque Disturbance; a) case of $\beta = 0$, b) case of $\beta > 0$, c) case of $\beta < 0$

4.5.5 Results Interpretation and Discussion

The above simulation results show clearly that the use of feed-forward technique has allowed improvement in accuracy performance and order of astatism of all simulated models by full compensation of steady state error due to set point changes. This is not, however, similarly achieved for the case of suppressing the effect of load torque disturbance, where, the results mention that the application of this technique for load torque disturbance compensation has allowed the reduction to zero of steady state error for the two models with state observer of order two and only reduced the steady state error to a value smaller than that before compensation for the other two ones without any increase in order of astatism for all models.

4.6 Conclusion

In this chapter, a theoretical analysis and assessment of the drive accuracy performance under the effect of input set point change is first given, where the correlation existing between the accuracy performance of the system and its order of astatism is mentioned. In order to verify this by simulation, we have used the standard signals (step, ramp, parabolic) to simulate the models at hand for set point profile tracking capability, where for the models which are characterized by an inherent higher order of astatism; case of double PI speed controller based models, it was necessary to use higher order polynomials than the parabolic signal to stimulate the model for accuracy performance evaluation and assessment.

The simulation results have shown different order of astatism and accuracy levels of these models, where the use of feed-forward technique has allowed full compensation by eliminating the finite value of steady state error due to input reference signal change and hence, increasing model order of astatism by one. It is also concluded, based on the obtained results, that the use of such technique did not, in general, satisfactorily neither compensate for steady state error nor improve the order of astatism due load torque disturbance for the studied models although a bit reduction of the finite value of steady state error is achieved. This is understood because of the fact that this mechanical parameter variation is inherently accounted for by the use of state observer in each model.

Chapter 5

Study of Nonlinearity and Parameters Variation Effects on System Performance

5.1 Introduction

The major problems in applying a conventional control algorithm in a speed controller are the effects of nonlinearity in a DC motor. The nonlinear characteristics of a DC motor such as saturation and friction could degrade the performance of conventional controller [123], [124]. There are alternative control approaches which are proposed to overcome drawbacks of conventional PI controller and solving nonlinear effects in electric drives, particularly, in DC drives. The Fuzzy Logic (FL) [7], [9], Neural Network (NN) [5], the hybrid Fuzzy Neural controller [11], Linear Quadratic Regulator (LQR) [4], Sliding Mode Control (SMC) [125] and others, are such methods. In this chapter, we will discuss in details this inherent phenomenon highly pronounced when the PI controller is used to control the speed of the DC drive system. Furthermore, the sensitivity of the achieved dynamic and steady state performance of the system against parameters variation is being investigated and analyzed.

5.2 Drive Systems with Input Saturation Nonlinearities

Practically, all electric drives are equipped with actuators, which are manipulated by the controller output signal. These actuators, which have limitation constraints to limit the drive speed and/or torque, cause a nonlinear effect in these engineering systems and are often modeled with a nonlinear element having saturation characteristics (u_{min}, u_{max}) at the input of the actuator as it is shown in Fig.5.1.

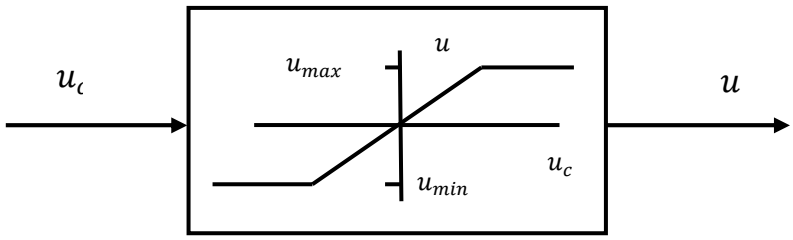

Figure 5.1 Typical Actuator Saturation Characteristic.

This saturation function is mathematically defined as follows [126], [127]:

$$For\ u\ \in \mathbb{R},\ sat(u) = u(t) = \begin{cases} u_{max}, & if\ \ u_c(t) > u_{max} \\ u_c, & if\ \ u_{max} \leq u_c(t) \leq u_{min} \\ u_{min}, & if\ \ u_c(t) < u_{min} \end{cases} \quad (5.1)$$

Therefore, if it happens that the controller output signal $u_c(t)$ exceeds the actuator upper limit u_{max}, or when it falls below its lower limit u_{min} of the linear operating range (case for instance of input reference change or abrupt external disturbance [128], [129]), the saturation state is attained and the controller output will not coincide with the process input $u(t)$. As a result, the feedback loop is broken leading the system to run under an open loop condition for a given time because the actuator will remain at its maximum (or minimum) limit independently of the process output value.

For control system where the controller involves an integral term, such as PID and PI based controlled plants, in case of saturation, the tracking control error takes a time to attain again the normal operating state because it decreases more slowly as in the ideal case (where there is no saturation limits). During this time, the integral part output becomes large and it ***winds up***, hence the name of wind up phenomenon. Thus, even when the value of the process variable attains that of the reference signal, the controller still saturates due to this phenomenon, which causes a serious degradation of system's response performance appearing mainly in large overshoot, long settling time and even may lead to instability of the system [22], [127], [130], [131].

5.3 Simulation Results of Actuator Saturation Effects

In this section we focus on studying the effect of actuator saturation limits on response quality and drive operational performances. In order to do this, the studied

models are intentionally being excited using two amplitude set point changes, which are 8.2 V and 10 V respectively. The simulation results are illustrated consecutively for each model and according to the value of viscous friction coefficient in the following.

5.3.1 System Model with 1PI Speed Controller and State Observer of Order 2

- **Case of $\beta = 0$**

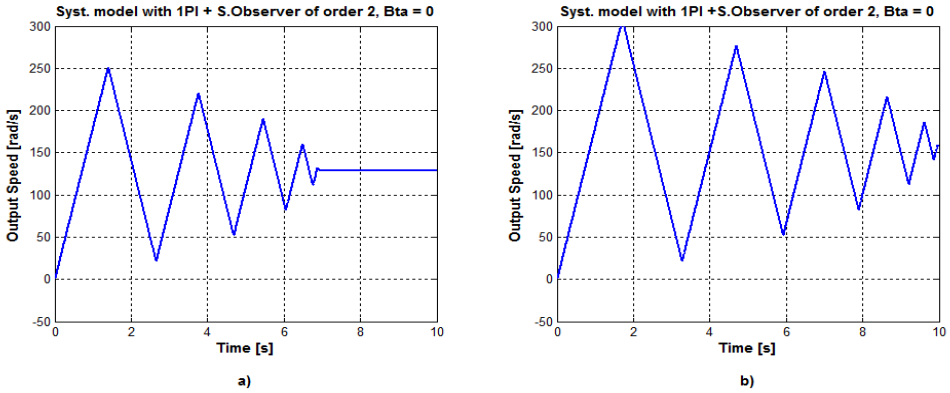

Figure 5.2 Speed Response of System Model with 1PI, State Observer of order 2 and $\beta = 0$ in presence of Actuator Saturation: **a)** using Speed Set Point Value: 8.2V and **b)** using Speed Set Point Value: 10 V.

- **Case of $\beta > 0$**

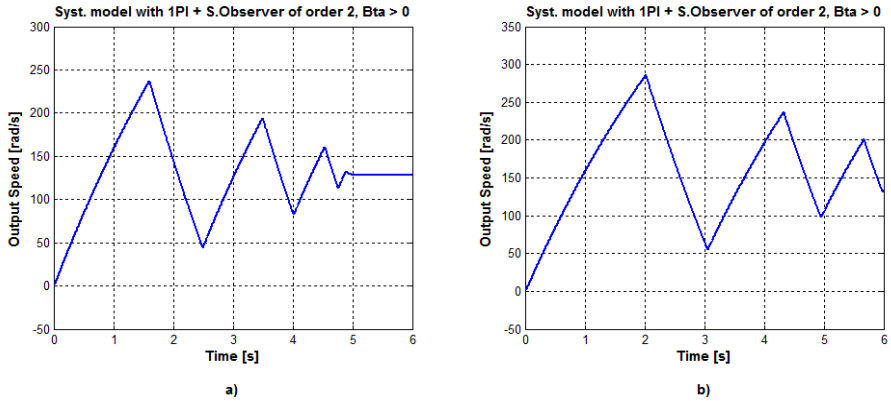

Figure 5.3 Speed Response of System Model with 1PI, State Observer of order 2 and $\beta > 0$ in presence of Actuator Saturation: **a)** using Speed Set Point Value: 8.2V and **b)** using Speed Set Point Value: 10 V.

- **Case of $\beta < 0$**

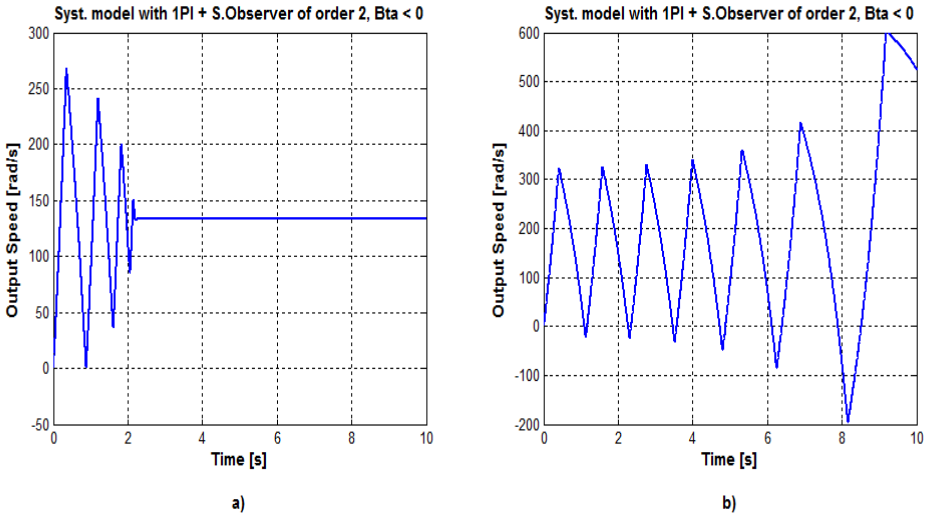

Figure 5.4 Speed Response of System Model with 1PI, State Observer of order 2 and $\beta < 0$ in presence of Actuator Saturation: **a)** using Speed Set Point Value: 8.2V and **b)** using Speed Set Point Value: 10 V.

5.3.2 System Model with 2PI Speed Controller and State Observer of Order 2

- **Case of $\beta = 0$**

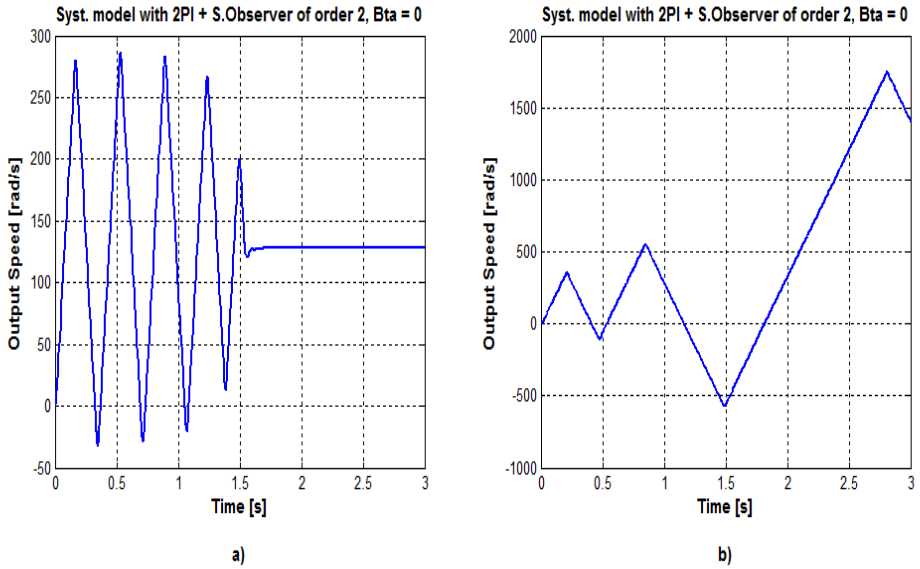

Figure 5.5 Speed Response of System Model with 2PI, State Observer of order 2 and $\beta = 0$ in presence of Actuator Saturation: **a)** using Speed Set Point Value: 8.2V and **b)** using Speed Set Point Value: 10 V.

- **Case of $\beta > 0$**

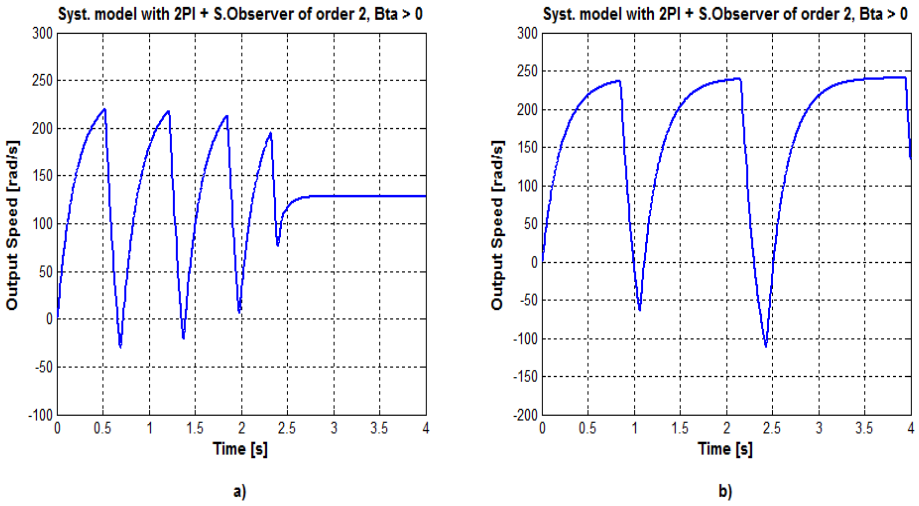

Figure 5.6 Speed Response of System Model with 2PI, State Observer of order 2 and $\beta > 0$ in presence of Actuator Saturation: **a)** using Speed Set Point Value: 8.2V and **b)** using Speed Set Point Value: 10 V.

- **Case of $\beta < 0$**

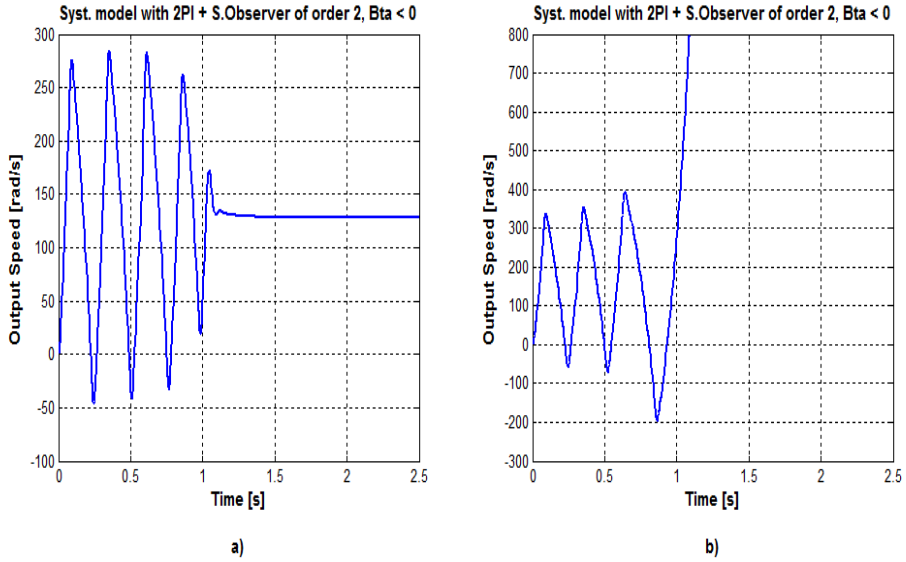

Figure 5.7 Speed Response of System Model with 2PI, State Observer of order 2 and $\beta < 0$ in presence of Actuator Saturation: **a)** using Speed Set Point Value: 8.2V and **b)** using Speed Set Point Value: 10 V.

5.3.3 System Model with 1PI Speed Controller and State Observer of Order 5

- **Case of $\beta = 0$**

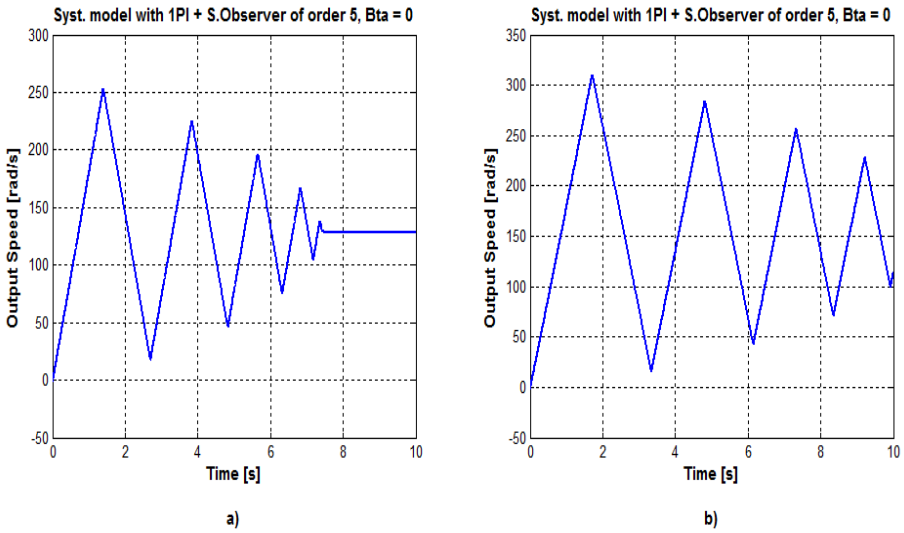

Figure 5.8 Speed Response of System Model with 1PI, State Observer of order 5 and $\beta = 0$ in presence of Actuator Saturation: **a)** using Speed Set Point Value: 8.2V and **b)** using Speed Set Point Value: 10 V.

- **Case of $\beta > 0$**

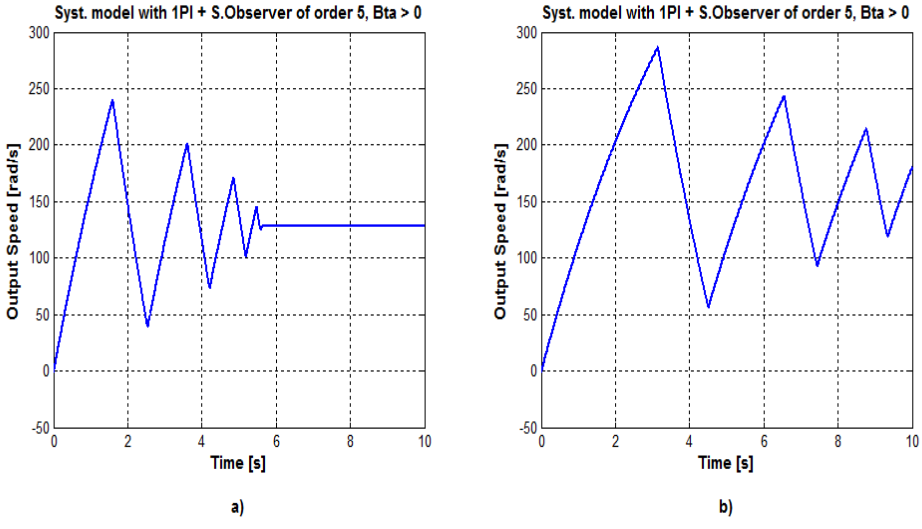

Figure 5.9 Speed Response of System Model with 1PI, State Observer of order 5 and $\beta > 0$ in presence of Actuator Saturation: **a)** using Speed Set Point Value: 8.2V and **b)** using Speed Set Point Value: 10 V.

- **Case of $\beta < 0$**

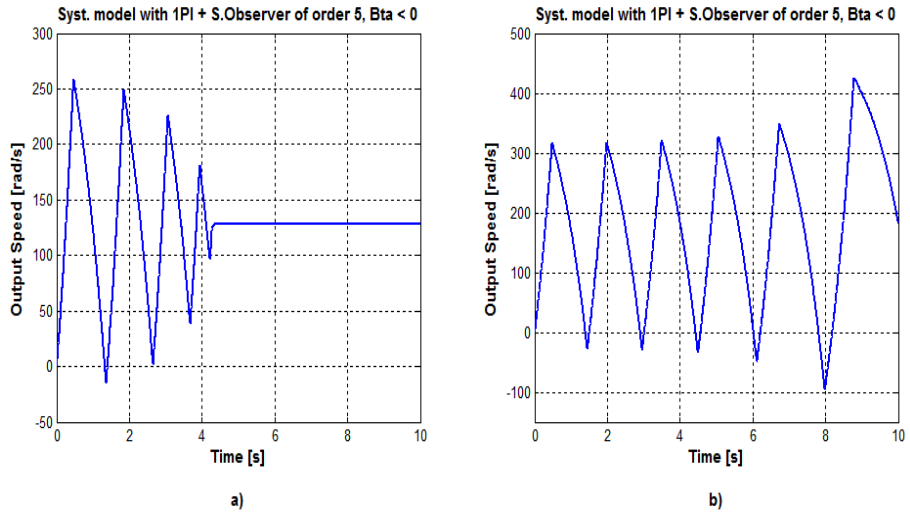

Figure 5.10 Speed Response of System Model with 1PI, State Observer of order 5 and $\beta < 0$ in presence of Actuator Saturation: **a)** using Speed Set Point Value: 8.2V and **b)** using Speed Set Point Value: 10 V.

5.3.4 System Model with 2PI Speed Controller and State Observer of Order 6

- **Case of $\beta = 0$**

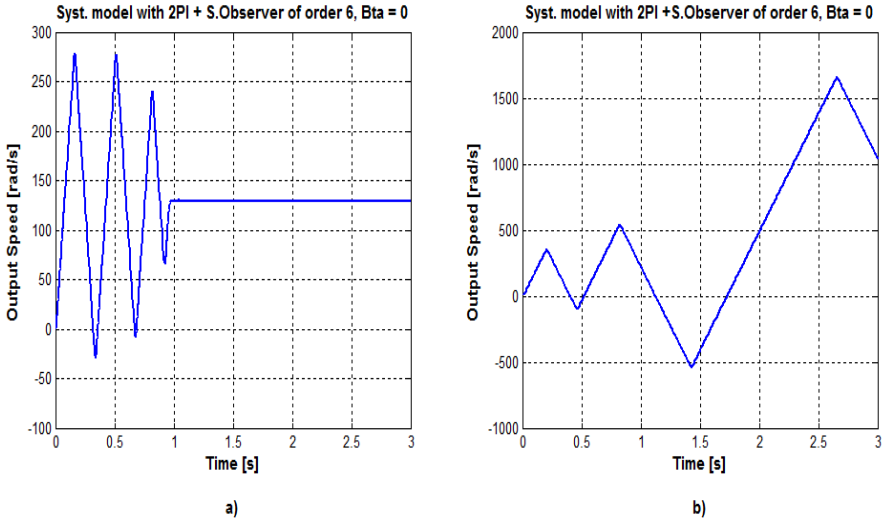

Figure 5.11 Speed Response of System Model with 2PI, State Observer of order 6 and $\beta = 0$ in presence of Actuator Saturation: **a)** using Speed Set Point Value: 8.2V and **b)** using Speed Set Point Value: 10 V.

- **Case of $\beta > 0$**

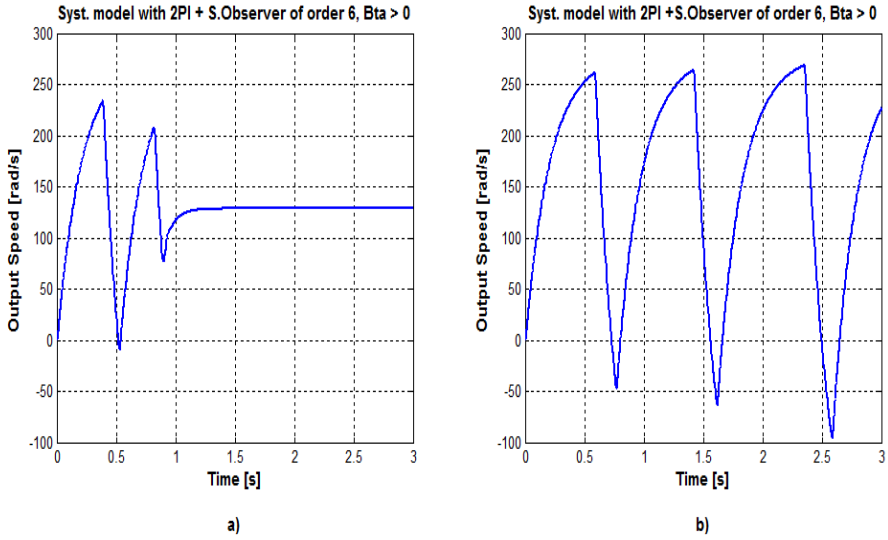

Figure 5.12 Speed Response of System Model with 2PI, State Observer of order 6 and $\beta > 0$ in presence of Actuator Saturation: **a)** using Speed Set Point Value: 8.2V and **b)** using Speed Set Point Value: 10 V.

- **Case of $\beta < 0$**

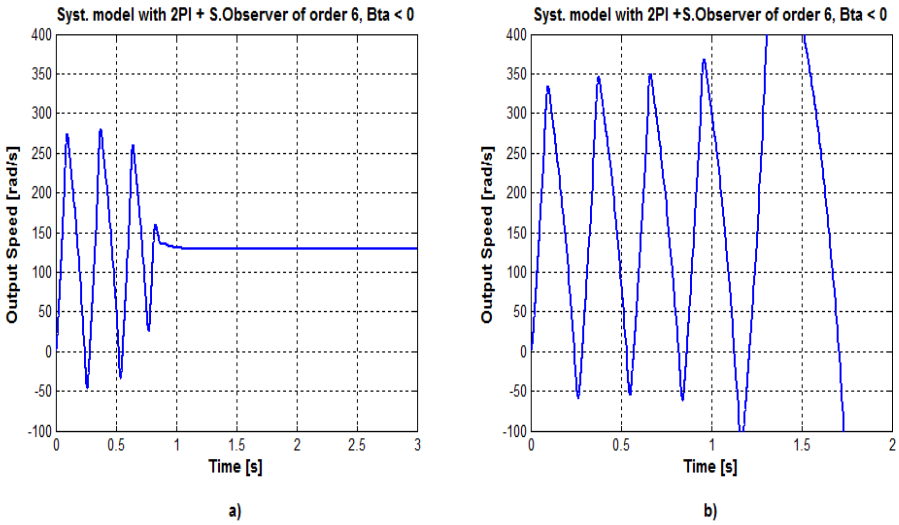

Figure 5.13 Speed Response of System Model with 2PI, State Observer of order 6 and $\beta < 0$ in presence of Actuator Saturation: **a)** using Speed Set Point Value: 8.2V and **b)** using Speed Set Point Value: 10 V.

5.3.5 Results Interpretation and Discussion

From the above simulation results, we see that the nonlinear dynamics of the actuator is detrimental for the system performance. Obviously, the system responds badly to the amplitude set point changes in presence of actuator saturation as nonlinearity; where the shape of the response begins to be deformed for the first value of set point amplitude and it becomes fully oscillatory divergent for 10 V of amplitude, indicating the instability state of the system.

5.4 DC Drive Performance Improvement by Saturation Compensation

5.4.1 Saturation Compensation Techniques

In order to cope with the presence of the actuator saturation, two design approaches can, in general, be followed. In the first one, the nonlinearity is considered explicitly from the beginning of the design phase and the control law is derived in the context of nonlinear control theory. Although this is a more rigorous approach, it might be too complicated to be applied in practical cases where the cost (and the fast commissioning) of the controller is of primary importance [132]. In other words, the advantages provided by the use of a standard PID control law are no more exploited.

In the second approach, on the other hand, the control law is designed disregarding the actuator nonlinearity, so that a PID controller can be adopted. Then, the detrimental effects due to the integrator windup are compensated by conveniently adopting an additional functionality designed for this purpose [133], [129]. This approach is called in control literature as the anti wind up compensation control, where the idea is to mitigate the effects of the integrator continuing to integrate due to the nonlinear saturation effect. The first approach is beyond the scope of this work, where the second will be briefly discussed to explore the different anti wind up techniques that have been used to compensate of actuator saturation effects in PI based control systems. Broadly speaking, these are classified representatively into the following categories.

5.4.1.1 Limiting Integrator Anti-Windup Techniques [134], [135]

This is a very simple approach to reduce the effects of integral windup. A feedback signal is created from the integrator output by feeding the integrator output through a dead zone with a high gain in order to reduce the integrator input and guarantee an operation in the linear range. The function is depicted by the block diagram of Fig.5.14.

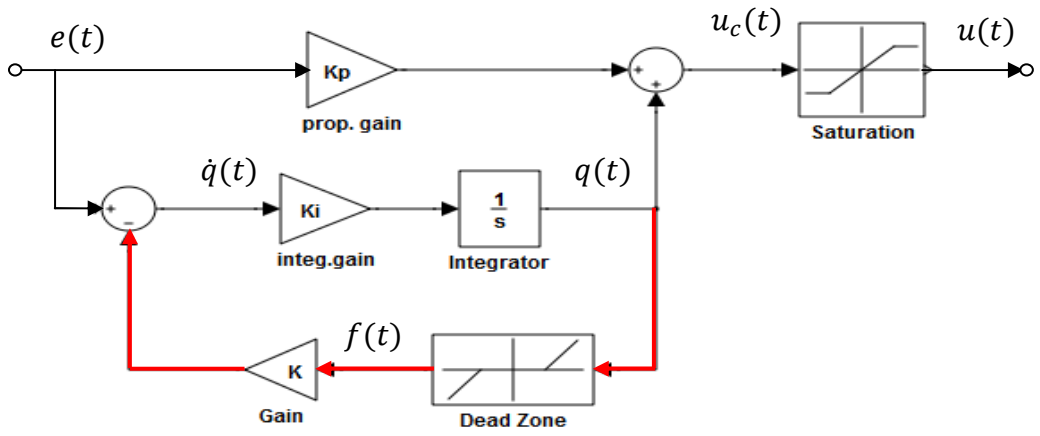

Figure 5.14 PI Controller with Dead Zone Limiting Integrator Anti-Windup Scheme

Where the dead zone block is characterized by its range: $R = [-R,\ +R]$, and the gain b. To allow the full linear range of the actuator, the dead zone range has to be the same as the linear range of the actuator. Therefore, when the integrator value is out of the dead zone range, a feedback signal of magnitude:

$$f(t) = b(q(t) - R) \tag{5.2}$$

is generated to reduce the integrator output by acting upon the integrator input, where the gain K is used for further adjustment. If the dead zone gain b is sufficiently high ($b > 10$) [136], the integrator output will effectively be limited to the range R.

The main drawback of this anti–windup scheme may, possibly, appear due to integrator's limit, which works independently of the Saturation element, so if the limit value of the dead zone is not correctly adjusted, the PI could have problems, such as large overshoot or undershoot as if the integral part wasn't working.

5.4.1.2 Tracking Back Calculation Ant-Windup Techniques

The principle of operation of this compensator is illustrated by the block diagram of Fig.5.15.

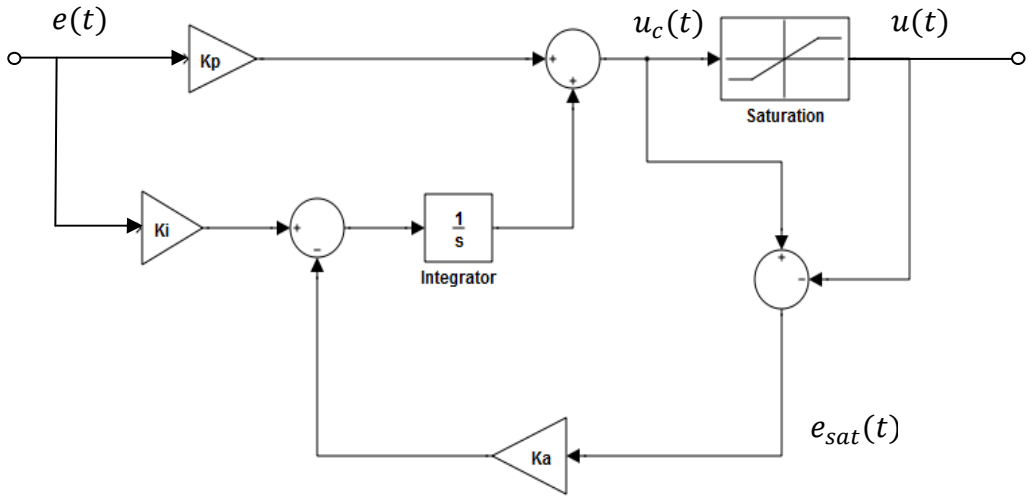

Figure 5.15 PI Controller with Tracking Back Calculation Anti-Windup Scheme

The approach, which is firstly proposed by Fertik and Ross [137], is based on the calculation of the difference between the saturated and the unsaturated control input signals, which is used to generate a feedback signal $e_{sat}(t)$ for properly controlling the integral state in the saturation range. This is performed according to the expression:

$$\begin{cases} u(t) = K_p e(t) + K_i \int e(t) & if \quad u_c = u \\ u(t) = K_p e(t) + \int [K_i e(t) - K_a (u_c(t) - u(t))] & if \quad u_c \neq u \end{cases} \tag{5.3}$$

Obviously, the extra feedback signal used to control the value of the integral term is zero when there is no saturation and in this case it will not have any effect on the normal operation. However, when the actuator saturates, this signal will be different from zero and is fed back to the integrator through the gain K_a, which should be properly chosen in such a way to reduce the input to the integrator until e_{sat} is zero. This reduces the controller output so it equals the saturation limit and stops the wind up.

The main drawback of this anti wind up compensator scheme consists in the fact that, in case of saturation, the reset of the integrator cannot be happened instantaneously but dynamically with a time constant $T_t = \frac{1}{K_a}$, which is known as tracking time constant [22], [127], [138]-[141]. The value of this parameter determines how quickly the integral term is reset and, obviously, its selection has a visible and considerable effect on the plant performance, in such a way that the transient performance properties, particularly: the overshoot and settling time depend heavily upon the feedback gain of the control difference rather than the PI gains [142]. For PI controller, the rule of thumb is to choose the starting value of this parameter equal to the integral time constant T_i and then it may be increased or decreased manually in order to achieve a fine tuning.

Another way in setting the parameter T_t is that it can be searched by running a global search algorithm through a properly chosen cost function
[143]. In general, this method can, conveniently, be applied for processes where the instantaneous reset of the integral term is not crucial.

5.4.1.3 Conditional Integration Anti-Windup Compensation Techniques

This anti wind up compensator is represented for PI controller by the block diagram of Fig.5.16.

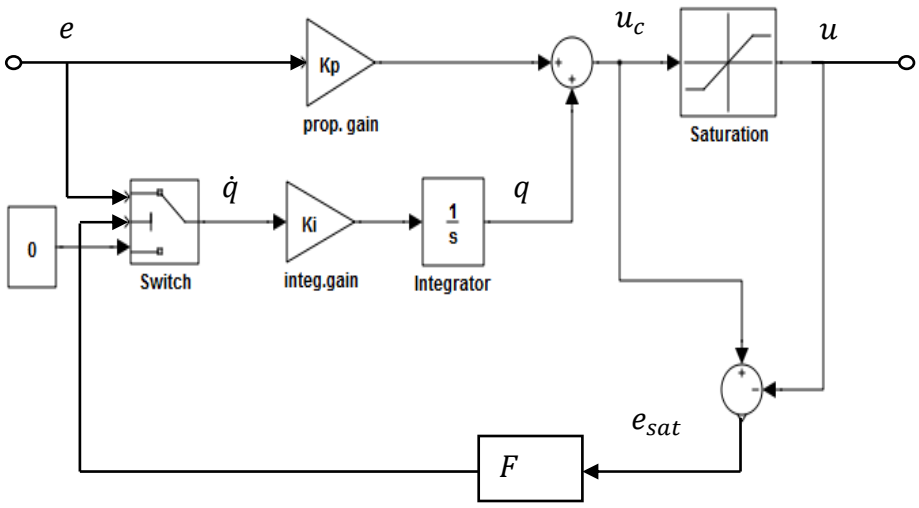

Figure 5.16 PI Controller with Conditional Integration Anti-Windup Scheme

This technique is based on the principle that the integral action is suspended when the control input is saturated and the P control only is activated, therefore the PI control is only effective when the control input lies within the saturation limit [141], [144], [145]. In other words, the integral action is switched on or off depending on the linear range or the saturation range according to the description below [127], [147]

$$\dot{q} = \begin{cases} e & if \quad u_c = u \\ 0 & if \quad u_c \neq u \end{cases} \tag{5.4}$$

with q is the integral term output, defined as:

$$q = \int K_i e(t) dt \tag{5.5}$$

The switching action of the integral term will be activated only when certain conditions are fulfilled, such as when the control error is large or during saturation of the controller; otherwise, it is kept constant**.**

This method is criticized of having the disadvantage that the controller may get stuck at a non-zero control error if the integral term has a large value at the time of switch off [22], [148]. However, for some applications with large change of set point or in case of start up, speed up, speed down, this method may be appropriate.

These are, in general, the most classes and approaches of ant-windup compensation. Under each class, several schemes exist and have been proposed to overcome the drawbacks and compensate effectively for the actuator saturation effects that characterize, in particular, the PI based control system. Other methods are also proposed, but we cannot go through all of them. For more reading in the topic, we refer to [149], [150].

5.4.2 Novel Conditional Integration Anti-Windup Compensator

In our work, we have proposed a novel conditional integration for compensating the actuator saturation effects in the PI speed controlled DC drive system. When it is used with a single PI speed controller based drive system, this technique is illustrated

by the block diagram of Fig.5.17. Whereas the block diagram illustrating its use with the double PI speed controller based system is mentioned in Fig.5.18.

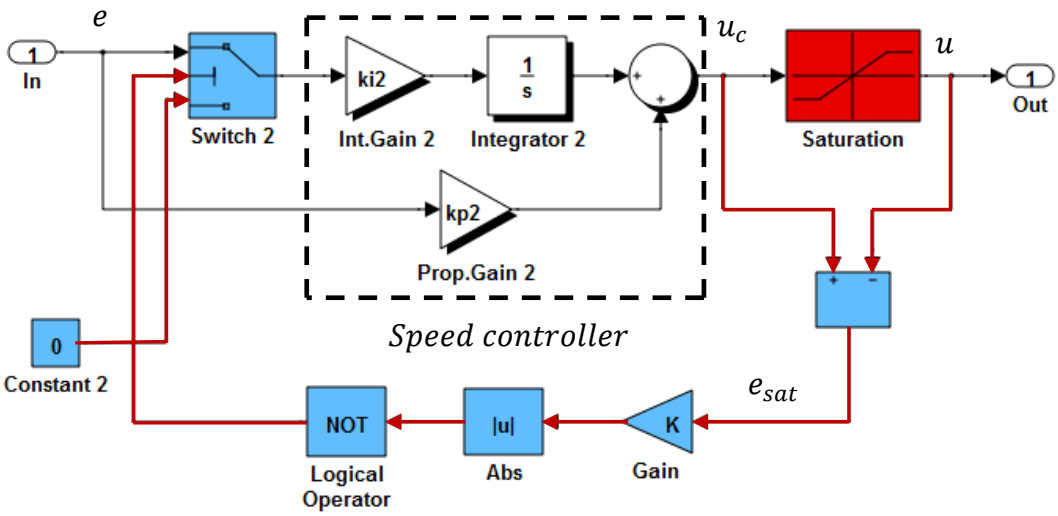

Figure 5.17 Block Diagram of Single PI Speed Controller incorporating the proposed Conditional Integration Anti-Windup Compensator.

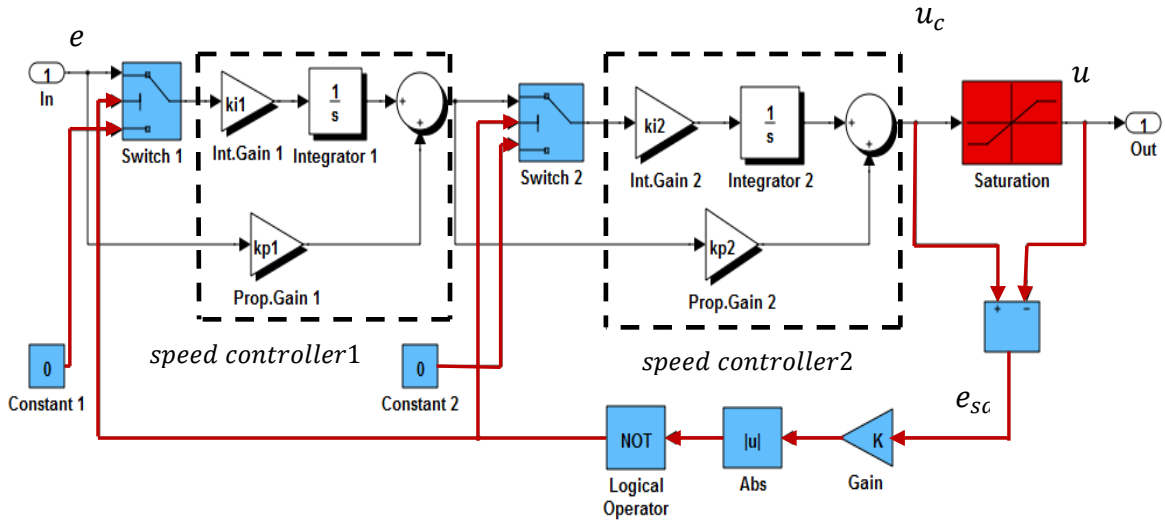

Figure 5.18 Block Diagram of Double PI Speed Controller incorporating the proposed Conditional Integration Anti-Windup Compensator.

The compensator belongs to the conditional integration techniques for overcoming the effects of saturation occurrence. It consists of switching off the integration process of PI speed controller (s) whenever the control signal has been saturated. As it can be seen from Fig.5.17 and Fig.5.18, the new controller structure that incorporates this technique has an extra feedback path that is generated by measuring the actual actuator output and forming an error signal $e_{sat}\ (t)$ as the difference between the controller output $u_c(t)$ and the actuator output $u(t)$. This error signal $e_{sat}\ (t)$ is multiplied by the design gain constant K and the resultant absolute value is fed to the logic function block "NOT". The output is then used to control the operation of the switch or the two switches "switch 1" and "switch 2" through which the integral term (s) of the speed controller(s) is (are) disabled in case of saturation occurrence. Therefore, this supplementary feedback path becomes only active during saturation and stabilizes the control system when the main feedback loop is opened due to saturation.

Particularly, in this method, the insertion logic function allows the integration process to be stopped immediately when saturation occurs. This matches with the real case requirements of the rolling mill PI based cascaded DC drive control system, where, in case of control signal saturation, the integration process is switched off. If we do not intervene, the system dynamic will behave badly under the influence of its inertia and could provoke, in addition to worsening the product quality, a serious personal injuries and disaster material damage.

5.4.3 Simulation Results of Compensated Actuator Saturation

In an attempt of improving DC drive operational performances in presence actuator saturation nonlinearity, we will apply this compensator according to the schemes mentioned in Fig.5.17 and Fig.5.18 on the different models that we have covered in this study. The obtained simulation results are given consecutively for each model and according to the value of viscous friction coefficient in the following.

5.4.3.1 System Model with 1PI Speed Controller and State Observer of Order 2

- **Case of $\beta = 0$**

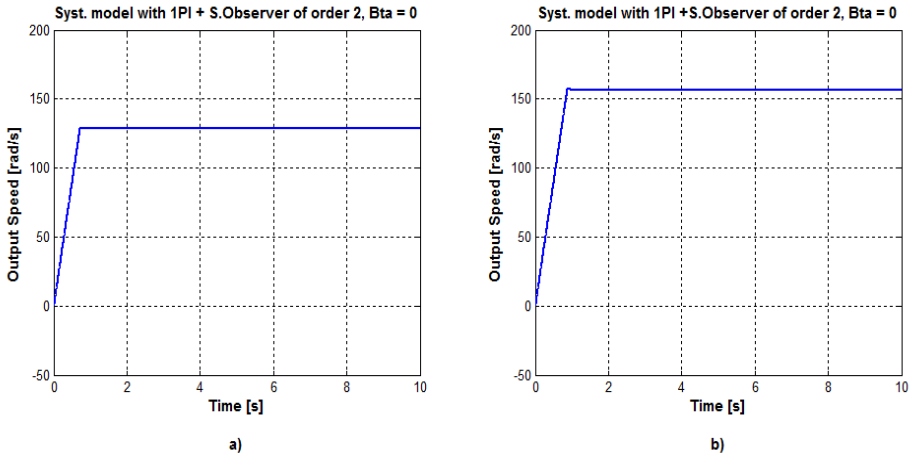

Figure 5.19 Speed Response of System Model with 1PI, State Observer of order 2 and $\beta = 0$ incorporating the Novel Conditional Integration Anti-Windup Compensator: **a)** using Speed Set Point Value: 8.2V and **b)** using Speed Set Point Value: 10 V.

- **Case of $\beta > 0$**

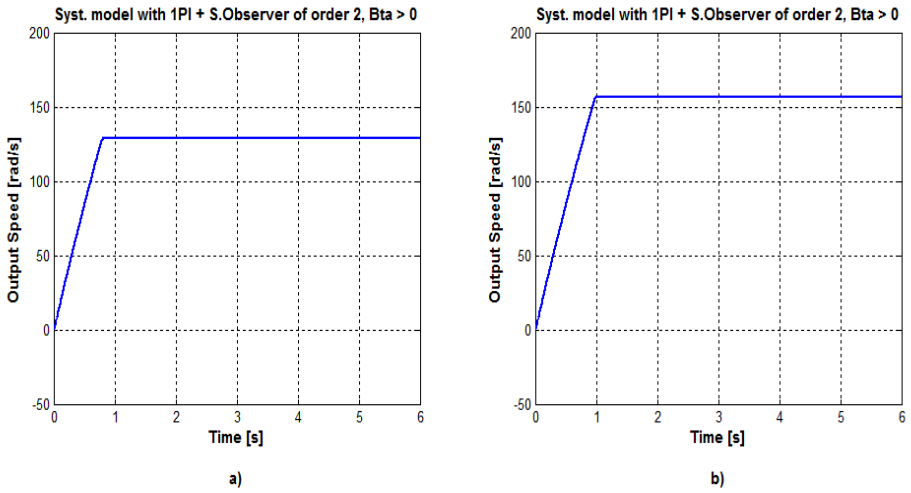

Figure 5.20 Speed Response of System Model with 1PI, State Observer of order 2 and $\beta > 0$ incorporating the Novel Conditional Integration Anti-Windup Compensator: **a)** using Speed Set Point Value: 8.2V and **b)** using Speed Set Point Value: 10 V.

- **Case of $\beta < 0$**

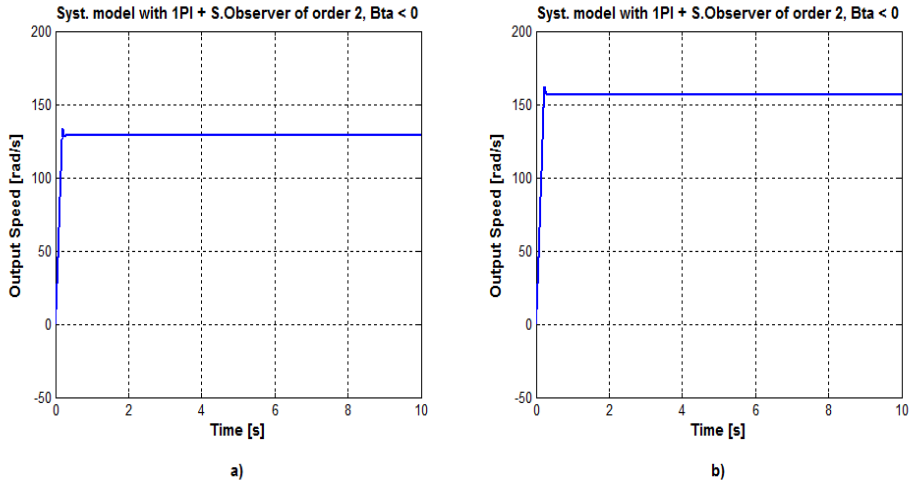

Figure 5.21 Speed Response of System Model with 1PI, State Observer of order 2 and $\beta < 0$ incorporating the Novel Conditional Integration Anti-Windup Compensator: **a)** using Speed Set Point Value: 8.2V and **b)** using Speed Set Point Value: 10 V.

5.4.3.2 System Model with 2PI Speed Controller and State Observer of Order 2

- **Case of $\beta = 0$**

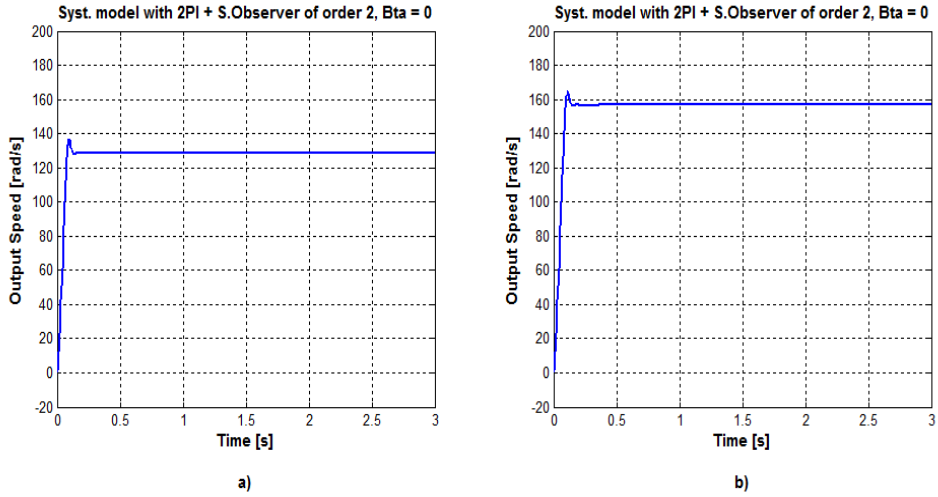

Figure 5.22 Speed Response of System Model with 2PI, State Observer of order 2 and $\beta = 0$ incorporating the Novel Conditional Integration Anti-Windup Compensator: **a)** using Speed Set Point Value: 8.2V and **b)** using Speed Set Point Value: 10 V.

- **Case of $\boldsymbol{\beta} > 0$**

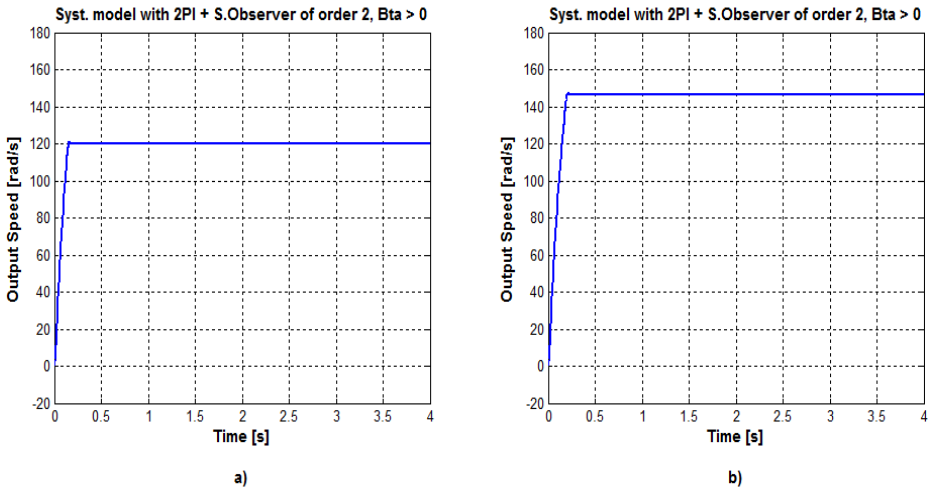

Figure 5.23 Speed Response of System Model with 2PI, State Observer of order 2 and $\beta > 0$ incorporating the Novel Conditional Integration Anti-Windup Compensator: **a)** using Speed Set Point Value: 8.2V and **b)** using Speed Set Point Value: 10 V.

- **Case of $\boldsymbol{\beta} < 0$**

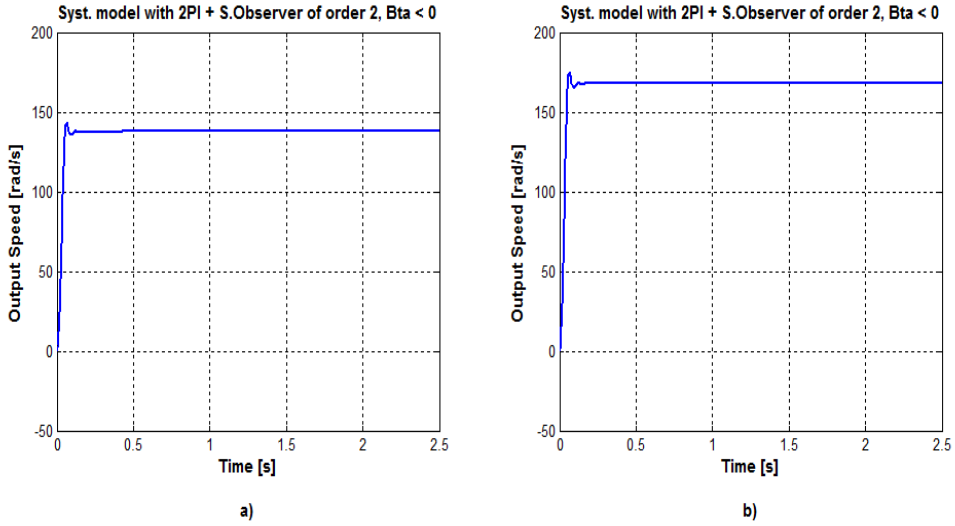

Figure 5.24 Speed Response of System Model with 2PI, State Observer of order 2 and $\beta < 0$ incorporating the Novel Conditional Integration Anti-Windup Compensator: **a)** using Speed Set Point Value: 8.2V and **b)** using Speed Set Point Value: 10 V.

5.4.3.3 System Model with 1PI Speed Controller and State Observer of Order 5

- **Case of $\beta = 0$**

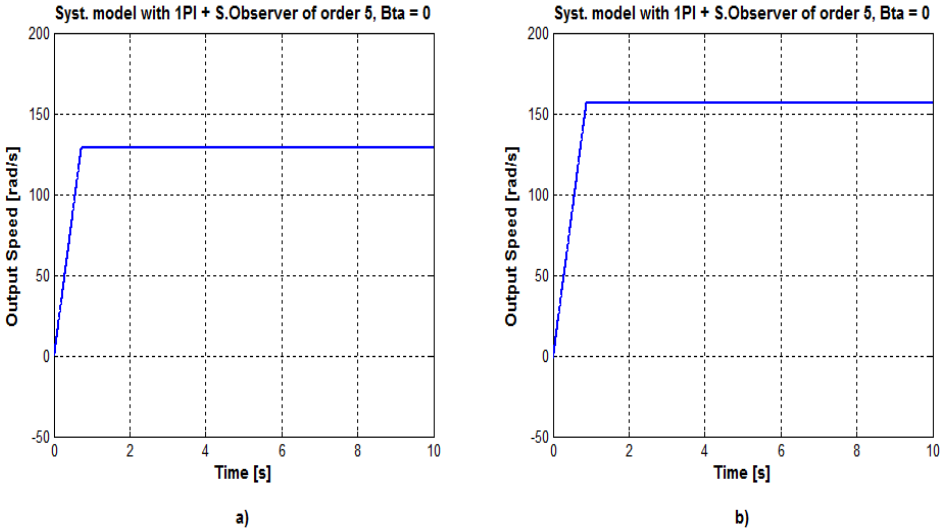

Figure 5.25 Speed Response of System Model with 1PI, State Observer of order 5 and $\beta = 0$ incorporating the Novel Conditional Integration Anti-Windup Compensator: **a)** using Speed Set Point Value: 8.2V and **b)** using Speed Set Point Value: 10 V.

- **Case of $\beta > 0$**

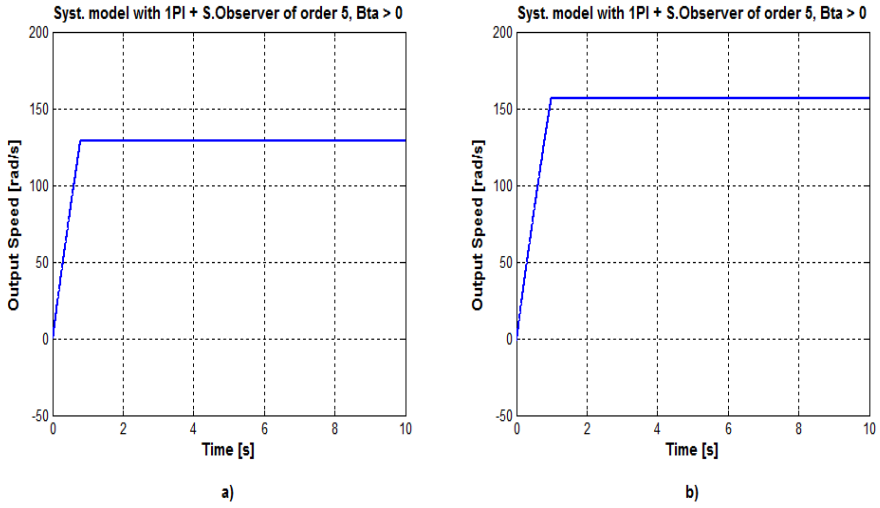

Figure 5.26 Speed Response of System Model with 1PI, State Observer of order 5 and $\beta > 0$ incorporating the Novel Conditional Integration Anti-Windup Compensator: **a)** using Speed Set Point Value: 8.2V and **b)** using Speed Set Point Value: 10 V.

- **Case of $\beta < 0$**

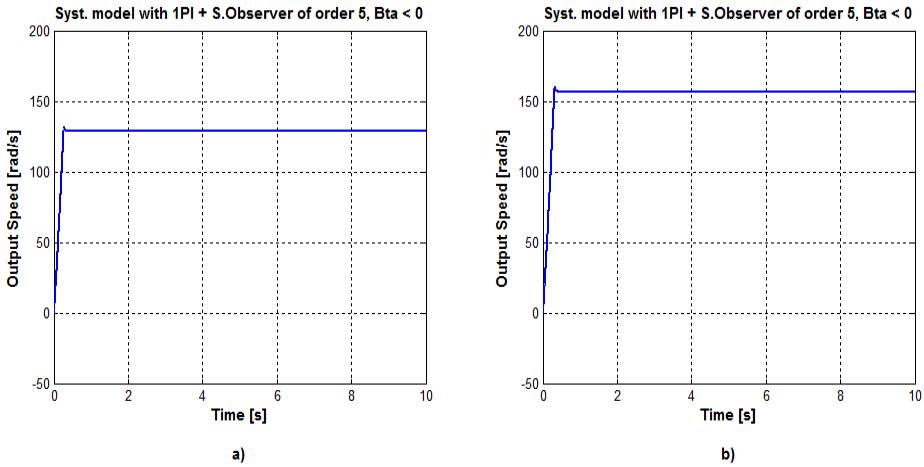

Figure 5.27 Speed Response of System Model with 1PI, State Observer of order 5 and $\beta < 0$ incorporating the Novel Conditional Integration Anti-Windup Compensator: **a)** using Speed Set Point Value: 8.2V and **b)** using Speed Set Point Value: 10 V.

5.4.3.4 System Model with 2PI Speed Controller and State Observer of Order 6

- **Case of $\beta = 0$**

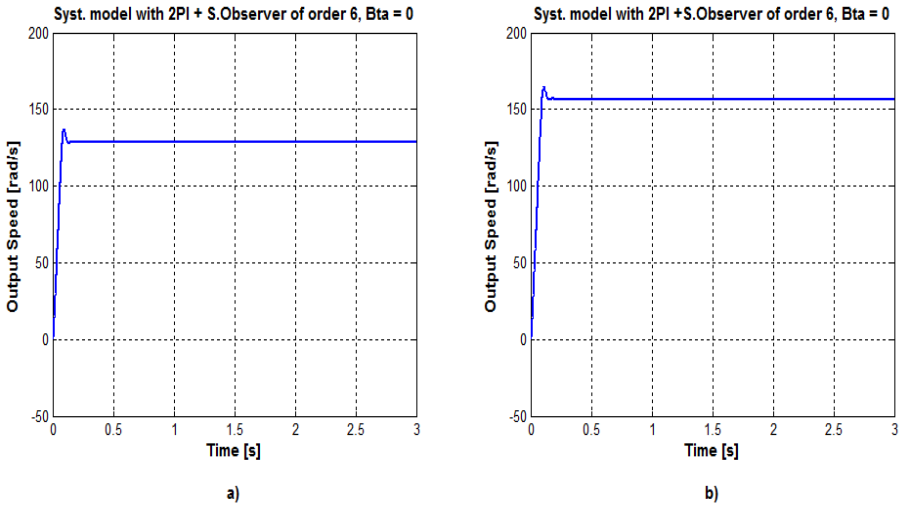

Figure 5.28 Speed Response of System Model with 2PI, State Observer of order 6 and $\beta = 0$ incorporating the Novel Conditional Integration Anti-Windup Compensator: **a)** using Speed Set Point Value: 8.2V and **b)** using Speed Set Point Value: 10 V.

- **Case of $\beta > 0$**

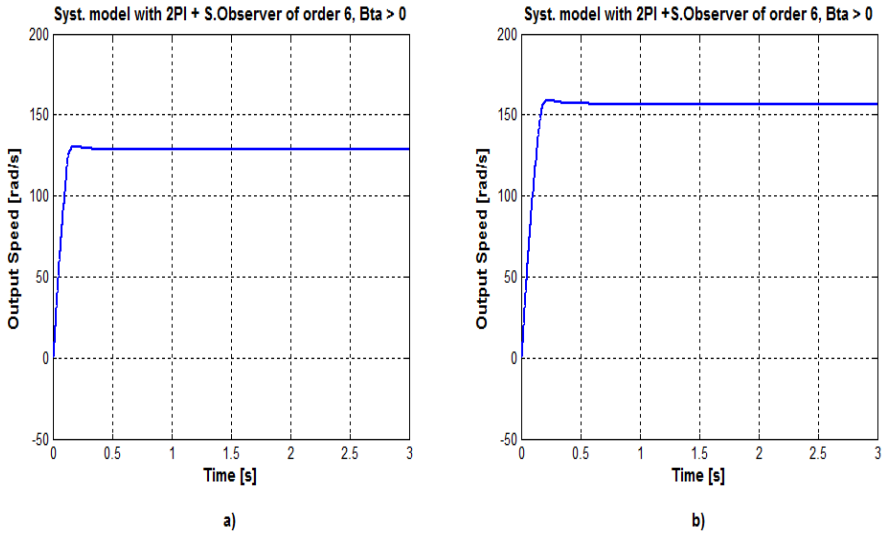

Figure 5.29 Speed Response of System Model with 2PI, State Observer of order 6 and $\beta > 0$ incorporating the Novel Conditional Integration Anti-Windup Compensator: **a)** using Speed Set Point Value: 8.2V and **b)** using Speed Set Point Value: 10 V.

- **Case $\beta < 0$**

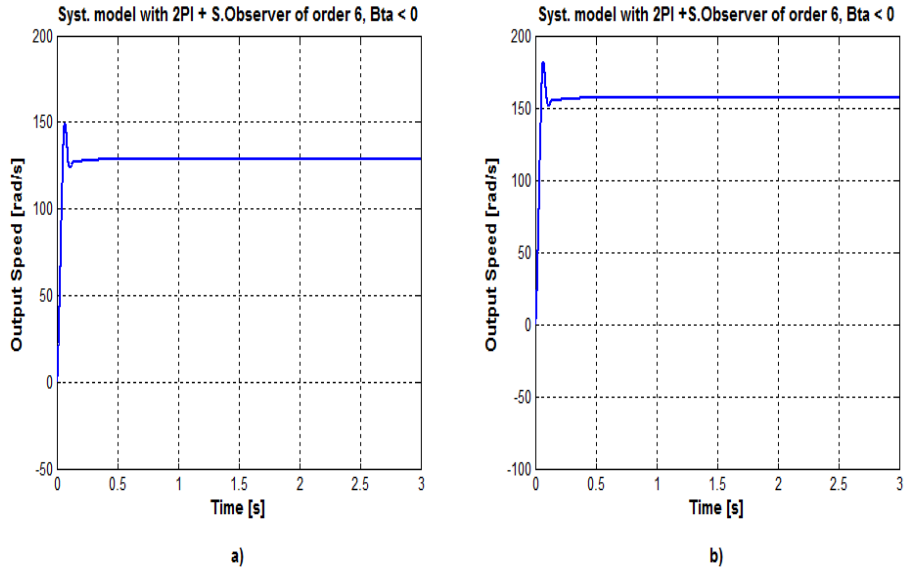

Figure 5.30 Speed Response of System Model with 2PI, State Observer of order 6 and $\beta < 0$ incorporating the Novel Conditional Integration Anti-Windup Compensator: **a)** using Speed Set Point Value: 8.2V and **b)** using Speed Set Point Value: 10 V.

5.4.4 Results Interpretation and Discussion

These results show, for all the system models, that the response is significantly improved than when the conditional integration compensator is not used. Also, we have a response with highly improved overshoot and much faster settling time, irrespective of the value of viscous friction coefficient. These results are equivalent to a significant improvement in system's dynamic and steady-state performance.

5.5 Study of Drive Performance Sensitivity to Parameters Variation

In this section, we want to consider the extent to which changes in system parameters affect the behavior of a system through its speed response. Ideally, parameter changes due to heat or other causes should not appreciably affect a system's performance. In system engineering and design, Sensitivity is the term given to the degree to which changes in system parameters affect system performance. Therefore, an ideal system has zero sensitivity where the internal parameters variation has no effect on its performance.

In order to quantify the system's sensitivity, we first formalize it as being the ratio of the fractional change in the function representing the system performance to the fractional change in the parameter as the fractional change of the parameter approaches zero [41], [151]. That is:

$$S_{F:P} = \lim_{\Delta P \to 0} \frac{Fractional\ change\ in\ the\ function,\ F}{Fractional\ change\ in\ the\ parameter,\ P}$$

$$S_{F:P} = \lim_{\Delta P \to 0} \frac{\frac{\Delta F}{F}}{\frac{\Delta P}{P}} = \lim_{\Delta P \to 0} \frac{P\ \Delta F}{F\ \Delta P} \tag{5.6}$$

This reduces to:

$$S_{F:P} = \frac{P\ \delta F}{F\ \delta P} \tag{5.7}$$

With $S_{F:P}$ is the concerned sensitivity function due to parameter variation.

5.5.1 Simulation Results

To demonstrate the parameters variation robustness of the system performance improvement, which has been achieved and mentioned previously, we assume that the parameters of armature resistance R_a and load inertia J have been perturbed from their nominal values by, respectively, 20 % and 10%. The simulation results showing the effect of this variation are given subsequently for each model and according to the value of viscous friction coefficient in the following plots.

5.5.1.1 System Model with 1PI Speed Controller and State Observer of order 2

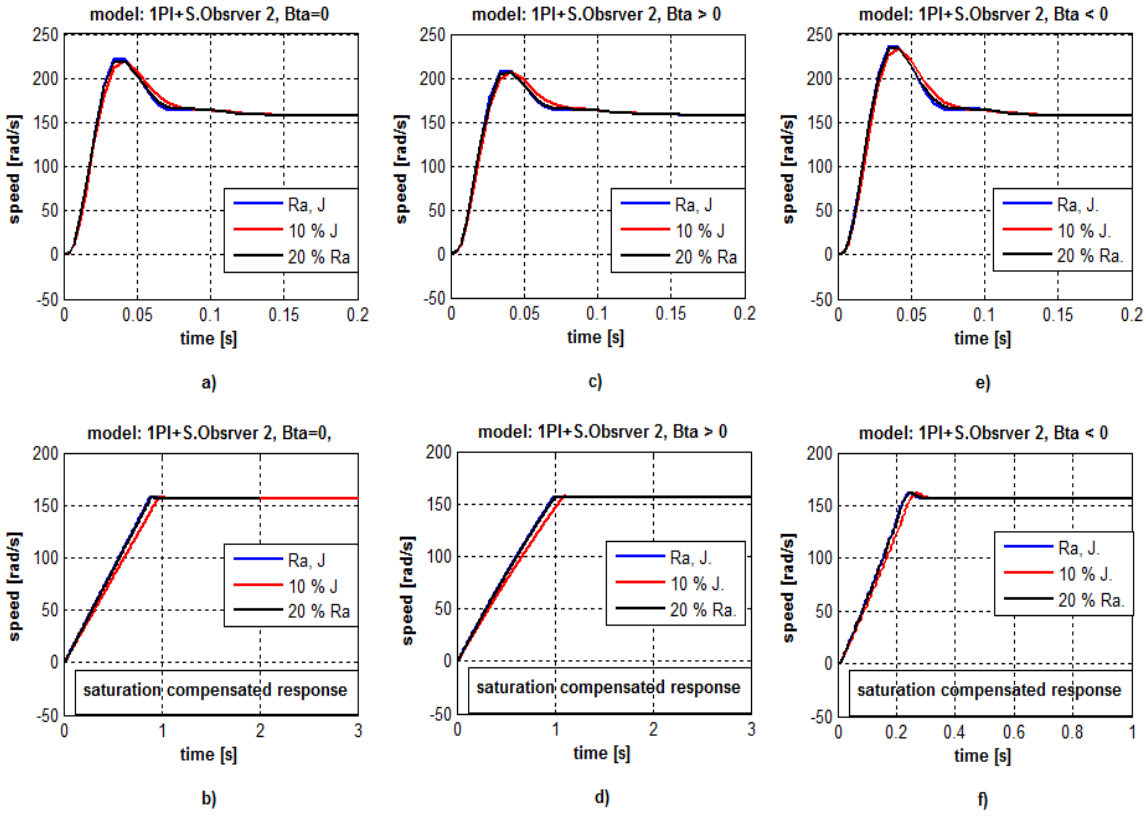

Figure 5.31 Effect of Drive Parameters Variation on the Optimized Performance of System Model with 1PI Speed Controller and State Observer of order 2: **a)**, **c)** and **e)** are Speed Responses under Mini-Max Optimization, **b)**, **d)** and **f)** are Responses under Mini-Max Optimization and Saturation Account.

5.5.1.2 System Model with 2PI Speed Controller and State Observer of order 2

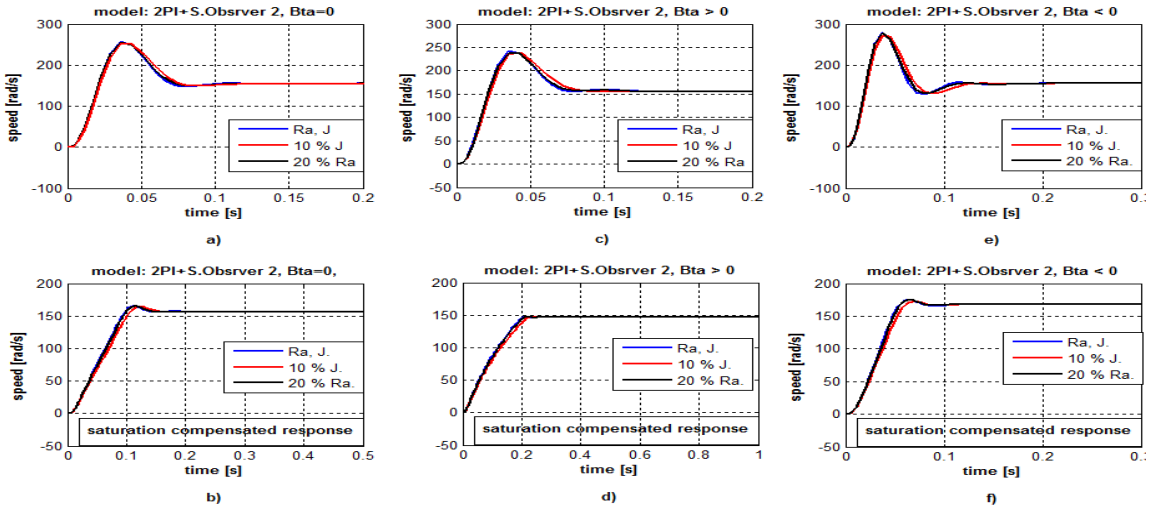

Figure 5.32 Effect of Drive Parameters Variation on the Optimized Performance of System Model with 2PI Speed Controller and State Observer of order 2: **a)**, **c)** and **e)** are Speed Responses under Mini-Max Optimization, **b)**, **d)** and **f)** are Responses under Mini-Max Optimization and Saturation Account.

5.5.1.3 System Model with 1PI Speed Controller and State Observer of order 5

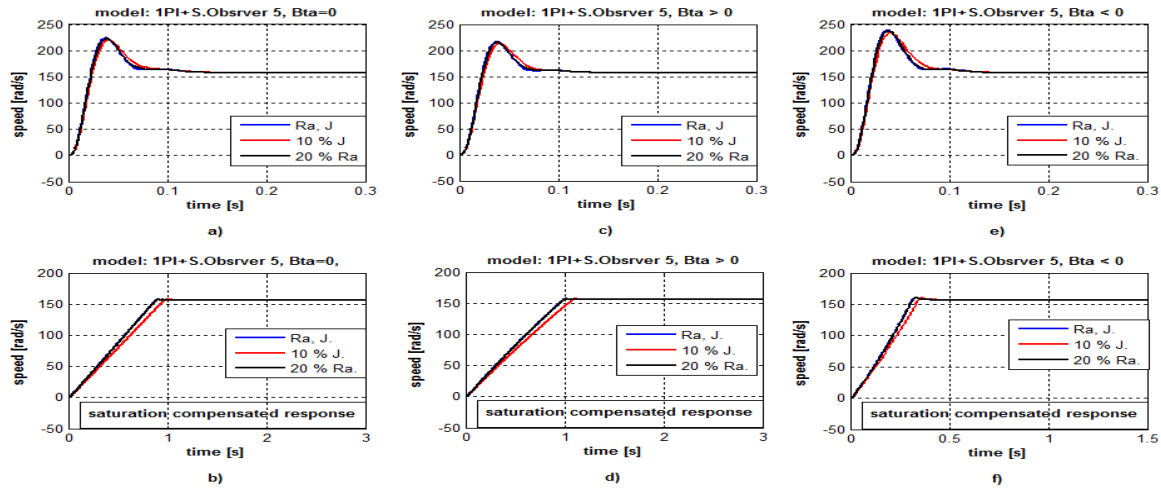

Figure 5.33 Effect of Drive Parameters Variation on the Optimized Performance of System Model with 1PI Speed Controller and State Observer of order 5: **a)**, **c)** and **e)** are Speed Responses under Mini-Max Optimization, **b)**, **d)** and **f)** are Responses under Mini-Max Optimization and Saturation Account.

5.5.1.4 System Model with 2PI Speed Controller and State Observer of order 6

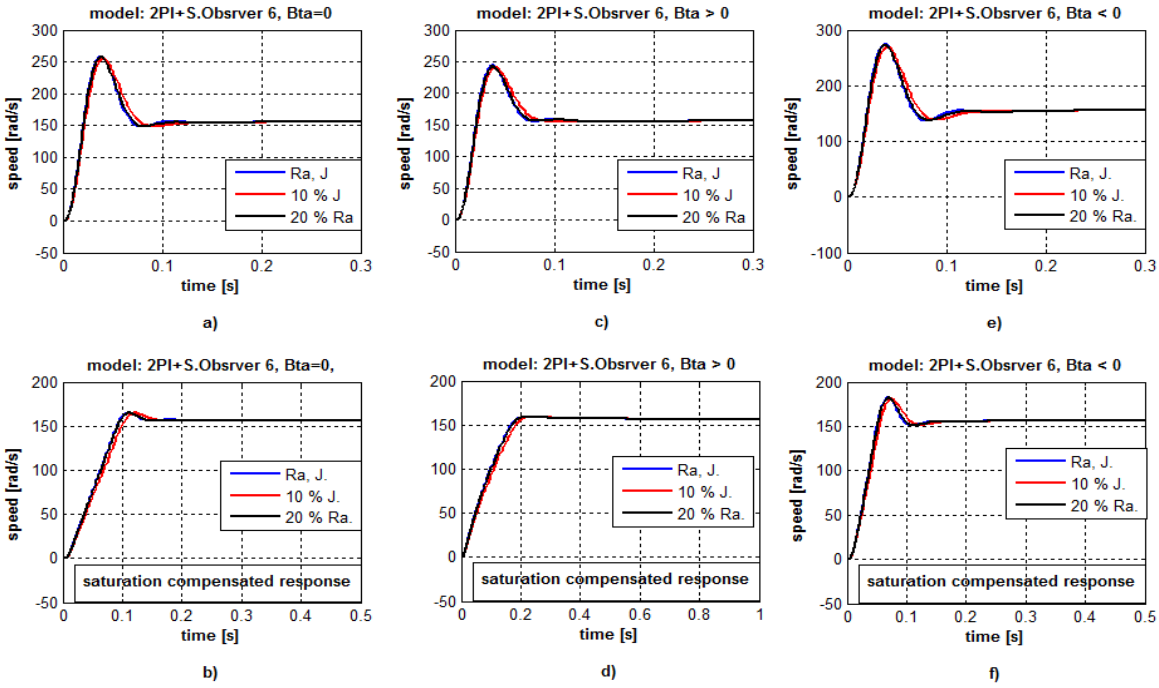

Figure 5.34 Effect of Drive Parameters Variation on the Optimized Performance of System Model with 2PI Speed Controller and State Observer of order 6: **a)**, **c)** and **e)** are Speed Responses under Mini-Max Optimization, **b)**, **d)** and **f)** are Responses under Mini-Max Optimization and Saturation Account.

5.5.2 Results Interpretation and Discussion

The plots clearly emphasize the effect of varying the armature resistance and moment of inertia on the dynamical behavior of each studied system model. To be consistent, the performances of the output speed response for each model and depending on the value of viscous friction coefficient are mentioned.

Obviously, the simulation results show that the response performance optimized using Mini-Max approach or optimized and compensated for saturation nonlinearity exhibits a negligible difference with and without parameters variation. This indicates the robustness of the achieved performances to the variation of these two most important parameters.

5.6 Conclusion

In this chapter the response of different models in presence of actuator saturation is investigated. It has been found that the actuator saturation limits lead to integrator windup phenomenon and affect seriously the drive performance by degrading the response quality, mainly appearing in large overshoot, large settling time and limit cycles that may provoke instability of the system.

In order to solve this problem, we have proposed a novel scheme of conditional integration anti-windup technique to compensate for the controller saturation and improve system's performance. The simulation results have shown the effectiveness of the used technique in enhancing the response quality and improving performance for all the studied models, where the response is significantly better than when the Conditional Integration compensator is not used. Obviously, we have had a response with highly improved overshoot and a much faster settling time, which is equivalent to a significant improvement in system's dynamic and steady state performance.

On the other hand, the sensitivity of the system performance to parameters variation is also studied, where 20 % of armature resistance and 10 % of moment of inertia variations are applied to verify its robustness property. Based on the obtained simulation results, the response performance optimized using Mini-Max approach or optimized and compensated for saturation nonlinearity exhibits a negligible difference with and without parameters variation. This proves the robustness of the achieved performances to the variation of these two most important parameters.

Throughout this study and according to the obtained simulation results, we can say that the viscous friction coefficient has no significant effect on the system's operational performance for all models.

General Conclusions and Perspectives

In light of the objectives stated at the beginning, we worked, throughout the realization of this thesis, to propose an optimization approach and compensation techniques in order to enhance, improve and perfecting the operational performance of the PI speed controlled and separately excited DC motor based drive system. The intention is to exploit rationally the material resources of the paper and steel rolling mill industries, where this drive finds its widespread employment.

First, a chosen system models, which are presented as candidates for best implementing the DC drive and responding the desired performance requirements, have been defined and explored.

The dynamic performance of these models is, therefore, assessed and evaluated in terms of the indices of rise time, settling time and percent overshoot. In this vein, the Mini-Max optimization approach is first applied to achieve improvement in dynamic and steady state performances by optimally selecting the parameters of PI speed controller or the first PI speed controller for those models where this controller is doubled. The simulation results have shown that an improvement in transient response characteristics (e.g., rise time, settling time and % overshoot), but with significant improvement is that obtained in percent overshoot. These results are compared to those obtained with IAE, ISE and ITAE integral-based minimization methods. This comparison has shown the superiority of the Mini-Max approach over the other methods in giving an important amelioration in system stability margin without losing the speed and accuracy performance of the control system's steady-state response.

In steel and paper rolling mill industries, the operation of DC drive is usually subjected to set point changes and load torque disturbances. In order to study its performance under these operational conditions, the models at hand have been stimulated using step, ramp, parabolic and higher order polynomial set point changes and load torque disturbance for accuracy assessment and evaluation. It is mentioned by simulation that, regardless of the viscous friction coefficient value, the employment of feed-forward technique enables, from one hand, a full compensation as it eliminates the finite value of steady state error produced due to set point changes and hence, increases model order of astatism by one. On the other hand, it is concluded, based on the obtained results, that the use of such technique did not, in general, satisfactorily neither compensate for steady state error nor improve the order of astatism due load torque disturbance for the studied models although a bit reduction of the finite value of steady state error of these models is achieved. This is understood because of the fact that this mechanical parameter variation is inherently accounted for by the use of state observer in each model.

These drives are also equipped with current limiter to protect against any damage of the drive components when abrupt set point change or load torque disturbance occur. Unfortunately, the presence of these devices may lead, under those conditions, to saturation of PI speed controller output and consequent serious degradation in system performance is evident. Therefore, the effect of inherent actuator saturation (non-linearity) on degrading the drive's transient and steady-state performances is also studied in this work. It is found that, with saturation account, the performance properties of the drive system response are dramatically deteriorated although the PI speed controller optimal parameters, already obtained with Mini-Max approach, are used. This can be appeared in large overshoot, large settling time and limit cycles indicating instability of the system. The simulation results have shown these facts with all studied models, where the current limit device is modeled by a saturation block added at the output of speed controller. Accordingly, the proposed novel conditional integration anti-windup compensation technique has shown its efficiency and effectiveness in overcoming these undesired effects and ensuring absolute stability of the system's response.

Finally, the robustness of the system models against parameters variation is studied. The sensitivity of system performances, which are achieved using Mini-Max optimization approach and those by compensation techniques are tested by taking, respectively, 20 % and 10 % variation of armature resistance and moment of inertia. The results were excellent in such a way that no effect can be stated regarding the armature resistance parameter variation and minor differences are illustrated due to moment of inertia variation, which seems to be a little bit exaggerated.

Finally, it is noticeable, according to the results of this whole study, that the viscous friction coefficient has had a small effect on the achieved dynamic performance optimization for all the studied system models. This is particularly apparent in the small difference of peak overshoot that has been characterized the obtained speed response as it is optimized using Mini-Max approach, this effect is, however, not significant. But this is not the case concerning the performances of accuracy, order of astatism, saturation nonlinearity compensation and sensitivity to parameters variation, where this coefficient has no influence.

Overall, regardless the value of viscous friction coefficient, the dynamic and steady-state performance as well as the order of astatism of the studied models representing the DC drive control system have been improved with better. In contrast to the other models, the DC drive system model with 1PI speed controller and state observer of order 2 has, however, exhibited better improved performances, which we elect it to be implemented.

Perspectives:

These promising results have led us to recommend incorporating the conditional integration anti-wind-up technique as well as the feed-forward compensation when implementing the PI speed controller and state observer based electromechanical DC drive system and using the Mini-Max approach as a simple, practical and model identification free optimization method for speed controller parameters tuning.

We consider, also, that extending the application of the proposed Mini-Max approach as well as the compensating techniques to AC drive systems represents a good idea if a future work is going to be done in this subject.

Appendices

A. Types of DC Motors

The different types of brushed DC motors are distinguished by the construction of the stator or the way the electromagnetic windings are connected to the power source. Regarding the stator construction, hence the way the stationary magnetic field is produced in the stator, we distinguish the permanent magnet and electromagnet DC motors as two types of brushed DC motors.

A.1 Permanent Magnet DC Motor

This type of DC motors is the most common brushed DC motors. It uses permanent magnets to produce the stationary stator magnetic field. PMDC motors are generally used in applications involving fractional horsepower for their cost effectiveness utilization in these applications with the following properties:

- Linearity of voltage vs. speed performance curve,
- Linear variation of the drawn current with the developed torque, and
- Quick response to input voltage changes due to the constancy of the produced stator magnetic field.

However, PMDC motor has the drawback of losing the magnetic properties of the permanent magnets over time.

A.2 Electromagnet DC Motor

In medium and high power applications, the motor manufacturer has enhanced the permanent magnet brushed DC motor by replacing the magnets with electromagnets formed from copper windings wound around a stator cores. With this conceptual enhancement, the previous drawback of PMDC motor is overcome and it is benefitted at the same time with the advantageous properties in its control. Depending on the way

the stator (field) windings and armature windings are connected to each other and to the source, we distinguish the following types.

A.1.1 Separately Excited DC Motor

This is the case of DC motor for which the armature and field windings are electrically separated from each other and the field winding is excited by a separate DC source of that of armature source. The schematic circuit diagram of separately excited DC motor is illustrated in Fig.A.1.

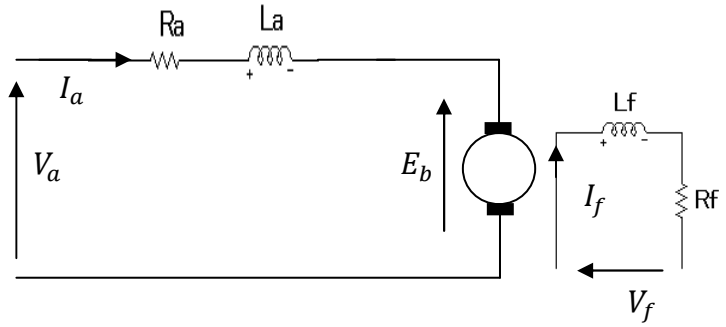

Figure A.1 Separately Excited DC Motor Equivalent Circuit.

A.1.2 Series DC motor

Series-wound Brushed DC (SWDC) motors have the field coil in series with the armature as it is depicted in Fig.A.2.

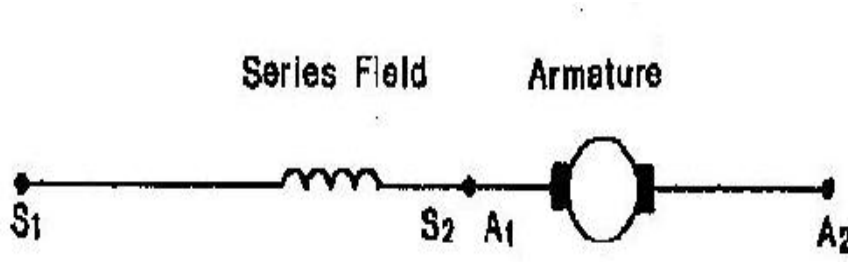

Figure A.2 Series DC Motor Schematic Representation

These motors are ideally suited for high-torque applications because the current in both the stator and armature increases under load. A drawback to SWDC motors is that

they do not have precise speed control like PMDC and shunt wound (SHWDC) motors have.

A.1.3 Shunt DC Motor

Shunt-wound Brushed DC (SHWDC) motors have the field coil in parallel (shunt) with the armature as it is shown in Fig.A.3.

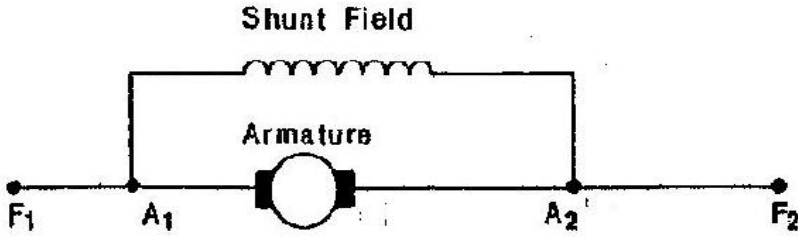

Figure A.3 Shunt DC motor.

The current in the field coil and the armature are independent. As a result, these motors have excellent speed control and are typically used in applications that require five or more horsepower.

A.1.4 Compound DC Motor

Compound Wound (CWDC) motors are combination of shunt-wound and series-wound motors as shown in Fig.A.4.

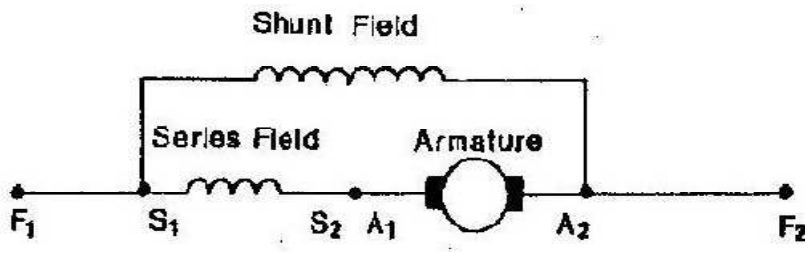

Figure A.4 Compound DC Motor

Consequently, this type of DC motor employs both series and a shunt fields. The performance of a CWDC motor is a combination of SWDC and SHWDC motors, they

have higher torque than a SHWDC motor while offering better speed control than SWDC motor.

B. Sate Observer Gain Matrix Parameters

The state observer is characterized by its gain matrix *L*, which is determined depending on the order of that observer. In the following table, we give these parameters corresponding to zero viscous friction coefficient for each state observer of the studied models.

Table B.1 Parameters of State Observers Gain Matrix Components

Gain Matrix Component	***State Observer of order 2***	***State Observer of order 5***	***State Observer of order 6***
L_1	12371.4	2584.4	103364
L_2	13846.8	-213798.0	1.7836*10^7
L_3	-	1511.42	8341377
L_4	-	47137.1	2930
L_5	-	27146.8	71427
L_6	-	-	33346.8

Bibliography

[1] S. Sivaranjani, R. Rajeswari, "*Simulation of MPC based Speed Control of Permanent Magnet Synchronous Motor Drive*", Journal of Theoretical and Applied Information Technology, Vol. 58, No.2, pp. 237-242, December 2013.

[2] R. Kumar, V. Girdhar, "*High Performance Fuzzy Adaptive Control for D.C. Motor*", International Archive of Applied Sciences and Technology **(**IAAST), Vol. 3, No. 3, pp. 01- 10, September 2012.

[3] L. Mohan, "*Comparison of PI and Adaptive Fuzzy PID Controllers for Speed Control of BLDC Motor*", International Journal of Innovative Research in Electrical, Electronics, Instrumentation and Control Engineering, Vol. 2, No. 2, pp. 1050-1054, February 2014.

[4] A. M. Bagheri, N. Zaeri, M. Yaghoobi, "*Comparison Performance between PID and LQR Controllers for 4- leg Voltage-Source Inverters*", International Conference on Circuits, System and Simulation, Vol.7, pp. 230-234, Singapore, 2011.

[5] W. S. Oh, K. M. Cho, S.Kim and H.J.Kim, "*Optimized Neural Network Speed Control of Induction Motor using Genetic Algorithm*", International Symposium on Power Electronics, Electrical Drives, Automation and Motion (SPEEDAM), pp. 13- 15, 2006.

[6] A. K. Singh, A.K. Pandey, "*Intelligent PI Controller for Speed Control of SEDM using MATLAB*", International Journal of Engineering Science and Innovative Technology (IJESIT) Vol. 2, No. 1, pp. 180-189, January 2013.

[7] R. K. Karsh, G. K. Choudhary, Ch. Kumar, "*Speed Control of Separately Excited DC Motor using Fuzzy Technique*", ACEEE International Journal on Electrical and Power Engineering, Vol. 2, No. 3, pp. 31-35, Nov. 2011.

[8] Ch.Chengaiah, K.Venkateswarlu, "*Comparative Study on DC Motor Speed Control using Various Controllers*", International Journal of Advanced Research in

Electrical, Electronics and Instrumentation Engineering, (IJAREEIE), Vol. 3, No.1 , pp. 6918-6925, January 2014.

[9] A. Tiwari, S. P. Dubey, "*Performance Analysis of Fuzzy based DC Motor Drive*", International Journal of Engineering Science and Innovative Technology (IJESIT) Vol. 2, No. 2, pp. 619-626, March 2013.

[10] G. V. Deshpande, S. S. Sankeshwari, "Speed *Control of Induction Motors using Hybrid PI Plus Fuzzy Controller*", International Journal of Advances in Engineering and Technology, Vol. 6, No. 5, pp. 2253-2261, Nov. 2013.

[11] J. Tavoosi, M. Alaei, B. Jahani, "*Neuro-Fuzzy Controller for Position Control of Robot Arm*", 5th Symposium on Advances in Sciences and Technology, Mashhad, Iran, May 12-14, 2011.

[12] B. Hu, G. K. I. Mann, R. G. Gosine, "*New Methodology for Analytical and Optimal Design of Fuzzy PID Controllers*", IEEE Transactions on Fuzzy Systems, Vol. 7, No. 5, pp. 521-539, October 1999.

[13] P. Kumar, K. P. Singh, "*Analysis on Separately Excited DC Motor using Proportional Integral Derivative Controller*", IJBSTR Research Paper, Vol. 1, No. 7, pp. 39-43, July 2013.

[14] J. Paulusová, L. Körösi, "*Design of PID Controller for PLC"*, Institute of Control and Industrial Informatics, Slovak University of Technology, Faculty of Electrical Engineering and Information Technology, May 2009.

[15] M. Boulouh, "*Optimization of High Order DC Electric Control Systems using Mathematical Algorithms*", Ph.D Thesis, Kharkov Polytechnic Institute, National Technical University, Kharkov, Ukraine, February 2001.

[16] F. A. Salem, "*Dynamic Modeling, Simulation and Control of Electric Machines for Mechatronics Applications*", International Journal of Control, Automation and Systems Vol. 1 No. 2, pp. 30-42, April 2013.

[17] J. Chiasson, "*Modeling and High-Performance Control of Electric Machines*", John Wiley & Sons, Inc., Publication, New York, 2005.

[18] S. Singh, A. K. Pandey, Dipraj, "*Design of PI Controller to Minimize the Speed Error of D.C. Servo Motor*", International Journal of Scientific and Technology Research, Vol. 1, No. 10, pp. 95-98, Nov. 2012.

[19] G. K. Mishra, A.K Pandey, A. Maurya, "*Combined Armature and Field Speed Control of DC Motor For Efficiency Enhancement*", International Journal of Electrical and Electronics Engineering (IJEEE), Vol. 1, No. 6, pp. 34-39, August 2014.

[20] M.A. Valenzuela, J.M. Bentley, and R.D. Lorenz, "*Evaluation of Torsional Oscillations in Paper Machine Sections*", IEEE Trans. on Ind. Applic., Vol. 41, No. 2, pp. 493-501, 2005.

[21] H. Liang, W. Ning, and Z. Jin-Hui, "*Multiobjective Optimization for Oontroller Design: Brief Paper*", Acta Automatica Sinica, Vol. 34, No. 4, April 2008.

[22] K. J. Astrom, and T. Hagglund, "*PID Controllers: Theory, Design and Tuning*", 2nd ed., Research Triangle Park, NC: Instrument Soc. Amer., USA, 1995.

[23] S. S. Raghuwanshi, K. Gupta, S. Manjrekar, D. Choudhary, Y. Mokhariwale, "*Analysis and Design of a Closed-Loop Converter- Controlled DC Drive*", International Journal of Engineering Trends and Technology, Vol. 3, No. 3, pp. 390-396, 2012.

[24] N. K. Shukla and S. K. Sinha, *"Fuzzy and PI Controller Based Performance Evaluation of Separately Excited DC Motor"*, International Journal of Emerging Trends in Electrical and Electronics (IJETEE*)*, Vol. 2, No. 1, pp. 12-18, April 2013.

[25] K. Ayyar, G. Gurusamy, K. Thanushkodi, "*Design of Speed Controller for Speed Control of Converter Fed DC Motor Drive using Model Order Reduction Technique*", European Journal of Scientific Research, Vol.76, No. 2, pp.288-299, 2012.

[26] D. B. Ender, "*Process control performance, not as good as you think*", Control Engineering, September 1993.

[27] N. Perić, I. Branica, I. Petrović, "*Modification and Application of Auto-Tuning PID Controller*", Proceedings of the 8th IEEE Mediterranean Conference on Control and Automation (MED 2000), Rio Patras, Greece, 17-19 July 2000.

[28] K.J. Astrom, and T. Hagglund, "*The Future of PID Control*", Control Engineering Practice (Elsevier), Pergamon, Vol. 9, pp. 1163–1175, 2001.

[29] K. H. Ang, G. C. Y. Chong, and Y. Li, "*PID Control System, Analysis, Design,*

and Technology", IEEE Trans. on Control Systems Technology, vol. 13, No. 4, pp. 559-576, July 2005.

[30] H. L. Wade, "*Basic and Advanced Regulatory Control: System Design and Application*", 2nd ed., the Instrumentation, Systems, and Automation (ISA) Society, USA, 2004.

[31] J. A. Shaw, "*The PID Control Algorithm How it Works, How to Tune it, and How to use it*", 2-nd Edition, Process Control Solutions, pp. 22/68, December 2003.

[32] L. A. Khan, A. Ahmed, U. A. Ahad, S. Z. Hussain, "*Design and Development of a Robust Control Adjustable Electrical DC Drive System using PI Controller*", Asian Research Publishing Network (ARPN), Journal of Engineering and Applied Sciences, Vol. 3, No. 3, pp. 55-60, June 2008.

[33] T. O. Kowalska, K. Szabat, "*Optimization of Fuzzy Logic Speed Controller for DC Drive System with Elastic Joints*", IEEE Trans. on Industry Applications, Vol. 40, No. 4, pp. 1138–1144, 2004.

[34] S. N. Vukosovic and M.R. Stojic, "*Suppression of Torsional Oscillations in a High Performance Speed Servo Drive*", IEEE Trans. on Ind. Electronics, Vol. 45, No. 1, pp. 108–117, 1998.

[35] T. M. O'Sullivan, C. M. Bingham, N. Schofield, "*Enhanced Servo Control Performance of Dual-Mass Systems*", IEEE Trans. on Ind. Electronic, Vol. 54, No. 3, pp. 1387-1399, 2007.

[36] M. Vasak, N. Peric, "*Robust Invariant Set-Based Protection of Multi-Mass Electrical Drives*", the International Journal for Computation and Mathematics in Electrical and Electronic Engineering, Vol. 29, No. 1, pp. 205-220, 2010.

[37] G. Zhang, J. Furusho, "*Speed Control of Two-Inertia System by PI/PID Control*", IEEE Trans. on Industrial Electronics, Vol. 47, No. 3, pp. 603–609, 2000.

[38] K. Szabat, T. O. Kowalska, "*Vibration Suppression in Two-Mass Drive System using PI Speed Controller and Additional Feedbacks – Comparative Study*", IEEE Trans. on Indus- trial Electronics, Vol. 54, No. 2, pp. 1193–1206, 2007.

[39] H. P. Beck, D. Turschner, "Commissioning of a State Controlled High-Powered Electrical Drive using Evolutionary Algorithms", IEEE Trans. on Mechatronics,

Vol. 6, No. 2, pp. 149–154, 2001.

[40] R. S. Burns, "*Advanced Control Engineering*", Butterworth-Heinemann, Linacre House, Jordan hill, oxford, 2001.

[41] J. J. D'Azzo, C. H. Houpis, S. N. Sheldon, "*Linear Control System Analysis and Design with MATLAB*", Fifth Edition, Revised and Expanded, Marcel Dekker, Inc., New York, 2003.

[42] L.V. Akimov, V.T. Dolbnia, and V.I. Kolotilo, "*Electric DC Drive Control Systems with State Observers*", Kharkov State Polytechnic University, Ukraine, 1998.

[43] A. Leva, C. Cox, A. Ruano, "*Hands-On PID Autotuning: a Guide to better Utilization"*, IFAC Professional Brief.

[44] S. Boyd, C. Barratt, "*Linear Controller Design: Limits of Performance*", Prentice-Hall, 1991.

[45] K. J. Aström, R. M. Murray, "*Feedback Systems: An Introduction for Scientists and Engineers*", Princeton University Press, Princeton, New Jersey, 2008.

[46] D. R. Coughanowr, "*Process Systems Analysis and Control*", Second Edition, McGraw-Hill International Editions, Chemical Engineering Series, New York , 1991.

[47] J. J. Distefano, A. R. Stubberud, W. J. Williams, "*Schaum's Outline of Theory and Problems: Feedback and Control Systems*"**,** Second Edition, McGraw-Hill Companies, Inc., New York, 1990.

[48] R. Ch. Chourasia, M. Kumar**,** "*Speed Control of S.E.D.C. Motor by using PI and Fuzzy Logic Controller*', International Journal of Soft Computing and Engineering (IJSCE), Vol. 3, No. 2, pp.135-139, May 2013.

[49] H. Chin, "*Feedback Control System Design*", MIT Open Course Ware, full 2009, http://ocw.mit.edu.

[50] K. P. Mohandas, "*Modern Control Engineering*", Sanguine Technical Publishers, Bangalore, India, 2006.

[51] M. Rasoulzadeh, M. B. Ghaznavi-Ghoushchi, "*Design and Implementation of CMOS Posicast Pre-Shaper for Vibration Reduction of Op-Amps*", Proceedings of the Word Congress on Engineering and Computer Science,WCECS 2009, San Francisco, USA,

October 20-22, 2009.

[52] X. Min, S. Yuan, C. Wen-Jian, "*Receding Horizon Optimization Approach to PID Controller Parameters Auto-Tuning*", ACTA Automatica Sinica, May 2005, Vol. 31, No. 3, p.459-63.

[53] A. O'Dwyer, "*PI and PID Controller Tuning Rules for Time Delay Processes: a Summary"*, Technical Report, Ed. 1, Dublin Institute of Technology, Kevin St., Dublin 8, Ireland, 15 May 2000.

[54] J. G. Ziegler, N. B. Nichols, "*Optimum Settings for Automatic Controllers*", Transactions of the ASME, Vol. 64, pp.759–768, 1942.

[55] D. Xue, Y. Q. Chen, and D. P. Atherton, "*PID Controller Design in: Linear Feedback Control: Chapter 6*", Society for Industrial and Applied Mathematics, 2007.

[56] Robert A. Paz, "*The Design of the PID Controller*", Klipsch School of Electrical and Computer Engineering, June 12, 2001.

[57] J. A. Miller, A. M. Lopez, C.L. Smith, P. W. Murrill, *"A Comparison of Controller Tuning Techniques"*, Control Engineering, pp. 72-75, Dec. 1967.

[58] Y. Q. Chen, Ch. H. Hu and K. L. Moore, "*Relay Feedback Tuning of Robust PID Controllers with Iso-Damping Property*", Proceedings of the 42nd. IEEE Conference on Decision and Control, pp. 2180-2185, Maui, Hawaii, USA, December 2003.

[59] K. J Astrom and T. Hagglund, "*Revising the Ziegler–Nichols Step Response Method for PID Control"*, Journal of Process Control, No. 14, pp. 635–650, 2004.

[60] R. C. Chang, S. H. Shen, and C. C. Yu, "*Derivation of Transfer Function from Relay Feedback Systems*", Industrial and Engineering Chemistry Research, Vol. 31, No. 3, pp. 855–860, 1992.

[61] A. Kh. Liaquat, A. Abrar, A. A. Umar and Z. H. Syed, "*Design and Development of a Robust Control Adjustable Electrical DC Drive System using PI Controller*", ARPN Journal of Engineering and Applied Sciences, Vol. 3, No. 3, pp. 55-60, June 2008.

[62] J. Ch. Shen, "*New Tuning Method for PID Control of a Plant with under-damped Response*", Asian Journal of Control, Vol. 2, No. 1, pp. 31-41, March 2000.

[63] A. Abdennour, F. A. Alturki, "*A Comparative Study of PI/PID Classical*

Intelligent Tuning Methods", Journal Engineering and Computer Sciences, Quassim University, Vol. 1, No. 1, pp. 29-42, 2008.

[64] D. E. Revera, M. Morari, and S. Skogestad, "*Internal Model Control for PID Controller Design*", Int. Eng. Chem. Process Des. Dev., California, No. 25, pp. 252-265, 1986.

[65] M. Shamsuzzoha and M. Lee, "*A Simple Analytical Controller Design for Integrating and First Order Unstable Time Delay Process*", School of Chemical Engineering and Technology, Yeungnam University, Korea, 2006.

[66] R. Vilanova, "*IMC based PID Design: Tuning Guide Lines and Automatic Tuning*", Journal of Process Control, No. 8, pp. 61–70, 2008.

[67] Z. Vukic, O. Kuljaca, "*Lectures on PID Controllers* », April 2002.

[68] S. Skogestad, "*Simple Analytical Rules for Model Reduction and PID Controller Tuning*", Journal of Process Control, Vol. 13, pp. 291-309, 2003.

[69] G. M. Vanderzalm, "*Tuning of PID-Type Controllers: Literature Overview*", Technische Universiteit Einhoven, 2004.

[70] H. Hjalmarsson , S. Gunnarsson, M. Gevers, "*A Convergent Iterative Restricted Complexity Control Design Scheme*", In: Proc. 33rd IEEE Conference on Decision and Control, Orlando, Florida, pp. 1735-1740, 1994.

[71] H. Hjalmarsson, S. Gunnarsson, M. Gevers, "*Model-Free Tuning of a Robust Regulator for a Flexible Transmission System*", European Journal of Control, Vol. 1, No. 2, pp.148-156, 1995.

[72] O. Lequin, M. Gevers, M. Mossberg, E. Bosmans, L. Triest, "*Iterative Feedback Tuning of PID Parameters: Comparison with Classical Tuning Rules*", Control Engineering Practice, Elsevier Science Ltd, Pergamon, No. 11, pp. 1023–1033, 2003.

[73] B. Wahlberg, "*On Iterative Feedback Tuning and Disturbance Rejection Using Simple Noise Models*", IFAC, Automatic Control, KTH, SE 100 44 Stockholm, 2005.

[74] H. Hjalmarsson, M. Gevers, S. Gunnarsson and O. Lequin, "*Iterative Feedback Tuning: Theory and Applications*", IEEE Control Systems Magazine, No. 18, pp. 26-41, 1998.

[75] E. Natsheh, K. A. Buragga, "*Comparison between Conventional and Fuzzy Logic PID Controllers for Controlling DC Motors*", International Journal of Computer Science Issues, Vol. 7, No. 5, pp. 128-134, September 2010.

[76] D. Xue, Y. Q. Chen, and D. P. Atherton, "*PID Controller Design, in: Linear Feedback Control*", Society for Industrial and Applied Mathematics, pp. 183-235, 2007.

[77] K. J. Astrom, H. Panagopoulos and T. Hagglund, "*Design of PI Controllers based on Non-Convex Optimization*", Automatica, Vol. 34, No. 5, pp. 585-601, 1998.

[78] H. Panagopoulos, K. J. Astrom, and T. Hagglund, "*Design of PID Controllers based on Constrained Optimization*", Proceedings of the American Control Conference San Diego, Califomia, June 1999.

[79] R. Argelaguet, "*A New Tuning of PID Controllers based on LQR Optimization*", In Preprints of the IFAC Workshop on Digital Control: Past, Present and Future of PID Control, pp. 303-308. 1996.

[80] N. J. Killingsworth, M. Krstic, "*PID tuning using Extremum Seeking; Online Model-Free Performance Optimization*", IEEE Control Systems Magazine, pp. 70-79, February 2006.

[81] B. Hu, G. K. I. Mann, R. G. Gosine, "*New Methodology for Analytical and Optimal Design of Fuzzy PID Controllers*", IEEE Transactions on Fuzzy Systems, Vol. 7, No. 5, pp.521-539, October 1999.

[82] V. Kumar, B. C. Nakra and A. P. Mittal, "*A Review on Classical and Fuzzy PID Controllers*", International Journal of Intelligent Control And Systems Vol.16, No.3, pp. 170-181, December 2011.

[83] E. B. M. Tayeb, A. T. Ali, "*Comparison of some Classical PID and Fuzzy Logic Controllers*", International Journal of Scientific & Engineering Research, Vol. 3, No.9, pp. 1-5, September 2012.

[84] J. Jantzen, "*Tuning of Fuzzy PID Controllers*", Technical University of Denmark, Department of Automation, Bldg 326, DK-2800 Lyngby, Denmark. Tech. Report No. 98-H 871 (fpid), April 16, 1999.

[85] N. Mutasim, O. Bouketir, Ch. E. Yong, "*Self-Tuning of PI Speed Controller*

Gains using Fuzzy Logic Controller", Modern Applied Science, Vol. 2, No. 6, pp. 55-65, November 2008.

[86] A. K. Dewangan, D. Sharma, Sh. Mishra, "*PID Controller Based Chopper-Fed DC Motor Drive Using Fuzzy Logic*", International Journal of Engineering Research and Applications (IJERA), Vol. 2, No. 3, pp.1073-1081, 2012.

[87] C. H. Lee and C. C. Teng, "*Tuning of PID Controllers for Stable and Unstable Processes based on Gain and Phase Margin Specifications"*, International Journal of Fuzzy Systems, Vol. 3, No. 1, pp. 346-355, 2001.

[88] CH. H. Lee, "*A Survey of PID Controller Design based on Gain and Phase Margins*", Invited Paper in International Journal of Computational Cognition, Vol. 2, No. 3, Pages 63-100, September 2004.

[89] D. Y. Lee, M. Lee, Y. Lee and S. Park, "*Mp Criterion Based Multiloop PID Controllers Tuning for Desired Closed Loop Responses*", Korean J. Chem. Eng., Vol. 20, No. 1, pp. 8-13, 2003.

[90] M. T. Ho, H. S. Wang, "*PID Controller Design with Guaranteed Gain and Phase Margins*", Asian Journal of Control, Vol. 5, No. 3, pp. 374-381, September 2003.

[91] K. G. Arvanitis, G. D. Pasgianos, G. Kalogeropoulos, "*Tuning PID Controllers for a Class of Unstable Dead Time Processes based on Stability Margins Specifications*", proceedings of the 15th Mediterranean Conference on Control and Automation, Athens, Greece, July 27-29, 2007.

[92] M. Nagurka, O. Yaniv, "*Robust PI Controller Design Satisfying Gain and Phase Margin Constraints*", Proceedings of the American Control Conference Denver, Colorado, pp. 3931-3936, June 4-6, 2003.

[93] M. A. R. Berger, P. R. Barros, "*Gain and Phase Margins Iterative Controller Tuning*", 8th International IFAC Symposium on Dynamics and Control of Process Systems, preprints Vol. 2, pp. 403-408, Cancun, Mexico, June 6-8, 2007.

[94] Y. K. Abbas, "*Genetic Algorithm Based PID Controller Design for a Precise Tracking of Two-Axis Piezoelectric Micropositioning Stage*", Al-Khawarizmi Engineering Journal, Vol.8, No.4, pp. 40-52, 2012.

[95] M. A. Awadallah, E. H. E. Bayoumi, H. M. Soliman, "*Adaptive Deadbeat Controllers for Brushless DC Drives using PSO and ANFIS Techniques*",

Journal of Electrical Engineering, Vol. 60, No. 1, pp. 3–11, 2009.

[96] M. Venmathi, K. Sujatha, S. Percis, A.Nalinithri, "*Fuzzy and ANN Tuning of PI Controller for Level Process Station*", ACS-International Journal on Computational Intelligence, Vol. 1, No. 2, pp. 3-21, Dec 2010.

[97] J. C. Shen, "*Fuzzy Neural Networks for Tuning PID Controller for Plants with Under-Damped Responses*", In IEEE Trans. On Fuzzy Systems, Vol. 9, No. 2, pp. 333-342, 2001.

[98] A. O'Dwyer, "*Handbook of PI and PID Controller Tuning Rules*", Imperial College Press London, U.K., 2003.

[99] J. Quevedo, T. Escobet, "*Digital Control: Past, Present and Future of PID Control*" in Proceedings, IFAC Workshop, Terrassa, Spain, Apr. 5–7, 2000.

[100] M. Lelic, "*PID Controllers in Nineties*", Corning Incorporated Science and Technology Division, New York, 1999.

[101] M. T. Jensen, "*A new Look at Solving Mini-Max Problems*", 4-Th Metaheuristics International Conference, MIC'2001, Porto, Portugal, July 16-20, 2001.

[102] J. V. Neumann, "*On the Theory of Games*", Mathematische Annalen, No. 100, pp. 295-320, 1928.

[103] A. I. Gull, "*Minimax Optimization of PI Regulator Parameters to Maximize the Stability Margin of Electromechanical Systems with Increased Q Factor*", Russian Electrical Engineering, Vol. 70, No. 5, pp. 39-44, 1999.

[104] A.I. Gull, M. Boulouh, "*Complex Criterion of Control Quality for Conditionally Stable Electromechanical Systems*", Journal of Russian Academy of Science (Elektrichestvo), No. 12, pp. 36-39, Moscow, Russia, 2006.

[105] A.I. Gull, M. Boulouh, "*Choice of Criteria and Optimization Principle of PI Regulator of Electromechanical System*", Transaction Vestnik of Polytechnic State University of Kharkov, No. 21, pp. 104-108, Kharkov, Ukraine, 1998.

[106] "*MATLAB Optimization Toolbox*", V 4.2 (R2009a), the MathWorks, Inc., 2009.

[107] M. schleicher, F. Blasinger, "*Control Engineering, a Guide for Beginners*", 3rd ed., Jumo GmbH and Co, Fulda, Germany, January 2003.

[108] L. Maret, "*Régulation Automatique : Complément au Traité D'électricité*", Presses Polytechniques Romandes, Suisse, 1992.

[109] E. Nikolov, S. Enev, "*Asservissement et Régulation Continue*", Université Technique de Sofia, 2009.

[110] Q. Chen, "*Reset Control Systems: Stability, Performance and Application*", A Ph.D. Dissertation, University of Massachusetts Amherst, September 2000.

[111] A. J. Koshkouei and K. J. Burnham, "*Control of DC Motors using Proportional Integral Sliding Mode*", Control Theory and Applications Centre, Coventry University, Coventry CV1 5FB, UK, 2008.

[112] C. Milosavljevic, "*Variable Structure Systems of Quasi Relay Type with Proportional-Integral Action*", the Scientific Journal Facta Universitatis, Series: Mechanics, Automatic, Control and Robotics Vol. 2, No. 7, pp. 301-314, 1997.

[113] T. H. Chiew, Z. Jamaludin, A. Y. Bani Hashim, K. J. Leo, L. Abdullah and N. A. Rafan, "*Analysis of Tracking Performance in Machine Tools for Disturbance Forces Compensation using Sliding Mode Control and PID Controller*", International Journal of Mechanical & Mechatronics Engineering IJMME-IJENS Vol.12, No. 6, pp. 34-40, December 2012.

[114] C. Schmid, "*Adaptive Sliding-Mode Control of Nonlinear Systems using Neural Network Approach*", In Proceedings of the 17th International Conference on Process Control, pp. 346-352, Strbske Pleso, Slovakia, June 9–12, 2009.

[115] Y. Stepanenko, Y. Caos, CH. Y. Su, "*Variable Structure Control of Robotic Manipulator with PID Sliding Surfaces*", International Journal of Robust and Nonlinear Control, Vol. 8, pp. 79-90, 1998.

[116] M. Zerikat, S. Chekroun, " *Adaptation Learning Speed Control for High-Performance Induction Motor using Neural Neworks*", Internation Journal of Signal, System Control and Engineering Application, Vol. 2, No. 1, pp. 15-21, 2009.

[117] K. B. M. Krishna, B. V. S. Goud, "*Speed Control of DC Motor through Position and Speed Tracking System Using Neural Networks*", International Journal of Electronic Engineering Research, Vol. 5, No. 1, pp. 87-103, 2013.

[118] M. Zerikat, S. Chekroun, "*High Performance Speed Tracking of Induction Motor using an Adaptive Fuzzy-Neural Network Control*", International Journal of Sciences and Techniques of Automatic Control and Computer Engineering,

Special Issue, CEM, pp. 516−531, December 2008.

[119] M. Gökbulut, B. Dandil, and C. Bal, "*A Hybrid Neuro-Fuzzy Controller for Brushless DC Motors*", Springer, pp. 125 – 132, 2006.

[120] Ch. K. Song, G. Khim, "*Improvement of Tracking Accuracy of Positioning Systems with Iron Core Linear DC Motors*", International Journal of Precision Engineering and Manufacturing Vol. 6, No.1, pp. 31-35, January 2005.

[121] M. Mihajlov, V. Nikolić, D. Antić, "*Position Control of an Electro-Hydraulic Servo System using Sliding Mode Control Enhanced by Fuzzy PI Controller*", the Scientific Journal, Facta Universitatis, series: Mechanical Engineering, Vol.1, No. 9, pp. 1217-1230, 2002.

[122] M. Malek, P. Makys, M. Stulrajter, "*Feedforward Control of Electrical Drives – Rules and Limits*", Advances In Electrical and Electronic Engineering, Vol. 9, No. 1, pp. 35-42, March 2011.

[123] B. J. Chalmers, "*Influence of Saturation in Brushless Permanent Magnet Drives*", IEE proc. B, Electr. Power Appl., Vol.139, No.1, 1992.

[124] C.T. Johnson and R.D. Lorenz, "*Experimental Identification of Friction and its Compensation in Precise, Position Controlled Mechanism*" IEEE Trans. Ind. Applicat., Vol. 28, No. 6, 1992.

[125] I. Karaskakovski, G. Shutinoski, "*Comparison of Sliding Mode and Proportional Integral Control for Brushless DC Motor*", Electronics, Sozopol, Bulgaria, 21-23 September, 2005.

[126] Martin Bak, "*Control of Systems with Constraints*", *Ph.D. Thesis*, Department of Automation, Technical University of Denmark, Building 326, DK-2800 Kongens Lyngby, Denmark, November 2000.

[127] X. L. Li, J. G. Park, and H. B. Shin, "*Comparison and Evaluation of Anti-Windup PI Controllers*", Journal of Power Electronics, Vol. 11, No. 1, pp. 45-50, January 2011.

[128] D. Vrancic, "*Design of Anti-Windup and Bumpless Transfer Protection*", Ph.D Thesis. University of Ljubljana. Ljubljana, SLO, 1997.

[129] F. Cupertino, D. Naso, L. Salvatore and B. Turchiano, "*Design of Cascaded Controllers for DC Drives using Evolutionary Algorithms*", *IEEE*, 2002.

[130] Y. LI, K. H. Ang, and G. C. Y. Chong, "*PID Control System Analysis and Design*", IEEE Control Systems Magazine, Vol. 26, No. 1, pp. 32-41, February 2006.

[131] N. J. Krikelis and S. K. Barkas, "*Design of Tracking Systems Subject to Actuator Saturation and Integral Wind-Up*", International Journal of Control, Vol. 39, No.4, pp. 667–682, Jul. 1984.

[132] A. Visioli, "*Advances in Industrial Control - Practical PID Control, Chapter 2, pp.37*", Springer-Verlag London Limited, 2006.

[133] M. V. Kothare, P. J. Campo, M. Morari and C. N. Nett, "*A Unified Framework for the Study of Anti-Windup Design*", Automatica, Vol. 30, No. 12, pp. 1869–1883, 1994.

[134] N. J. Krikelis, "*State Feedback Integral Control with Intelligent Integrator*", International Journal of Control, Vol. 32, No. 3, pp. 465–473, May 1980.

[135] C. Bohn and D. P. Atherton, "*An Analysis Package Comparing PID Anti-Windup Strategies*", IEEE Control Systems, Vol.4, pp.34-40, 1995.

[136] C. Bohn and D. P Atherton, "*A Simulink Package for Comparative Studies of PID Anti-windup Strategies*", IEEE/IFAC Joint Symposium, 7 March 1994.

[137] H.A. Fertik and C.W. Ross, "*Direct Digital Control Algorithms with Anti-Windup Feature*," *Z.S.A. Trans.*, 22nd Annual Conf. and. Exhibit., Vol. 6, No. 4, pp. 317-328, Chicago, 1967.

[138] H. B. Shin, "*New Anti Windup PI Controller for Variable-Speed Motor Drives*", IEEE Trans. Ind. Electron., Vol. 45, No. 3, pp. 445-450, Jun. 1998.

[139] J. G. Park, J. H. Chung, and H. B. Shin, "*Anti-Windup Integral-Proportional Controller for Variable-Speed Motor Drives*," Journal of Power Electronics, Vol. 2, No. 2, pp. 130–138, Apr. 2002.

[140] K. Ohishi, E. Hayasaka, T. Nagano, M. Harakawa, and T. Kanmachi, "*High-Performance Speed Servo System Considering Voltage Saturation of a Vector Controlled Induction Motor*," IEEE Trans. Ind. Electron., Vol. 53, No. 3, pp. 795–802, Jun. 2006.

[141] J. W. Choi and S. C. Lee, "*Anti-windup Strategy for PI-type speed controller*", IEEE Trans. Ind. Electron., Vol. 56, No. 6, pp. 2039-2046, Jun. 2009.

[142] J. Espina, T. Arias, J. Balcells and C. Ortega, "*Speed Anti-Windup PI Strategies Review for Field Oriented Control of Permanent Magnet Synchronous Machines*", TIEG, Dep. d'Enginyeria Electrònica. Universitat Politècnica de Catalunya. C. Colom 1. 08222 Terrassa.

[143] H. Markaroglu, M. Guzelkaya, I. Eksin, E. Yesil, "*Tracking Time Adjustment in Back Calculation Anti-Windup Scheme*", Proceedings 20th European Conference on Modelling and Simulation Wolfgang Borutzky, Alessandra Orsoni, Richard Zobel, ECMS, 2006.

[144] R. Hanus, M. Kinnaert, and J. L. Henrotte, "*Conditioning Technique, a General Anti-Windup and Bumpless Transfer Method*", Automatica, Vol. 23, No. 6, pp. 729-739, Nov. 1987.

[145] J. K. Seok, K. T. Kim, and D. C. Lee, "*Automatic Mode Switching of P/PI speed Control for Industry Servo Drives using Online Spectrum Analysis of Torque Command*," IEEE Trans. Ind. Electron., Vol. 54, No. 5, pp. 2642–2647, Oct. 2007.

[146] K. S. Walgama, S. Ronnback, and J. Sternby, "*Generalization of Conditioning Technique for Anti-Windup Compensators*", Proc. Inst. Elect.Eng., Vol. 139, No. 2, pp. 109-118, Mar. 1992.

[147] Y. Peng, D. Vrancic, and R. Hanus, "*Anti-Windup, Bumpless and Conditioned Transfer Techniques for PID Controllers*", IEEE Control Systems, Vol.5, pp.48-57, 1996.

[148] K.J. Astrom and L. Rundqwist, "*Integrator Windup and How to Avoid It*", Proceeding of the American Control Conference, Pittsburgh, pp. 1693-1698, 1989.

[149] H. Ayad, S. Doubabi, A. Hamzaoui, "*A Windup Compensator for Systems with Saturation Actuators using Adaptive Fuzzy Logic*", IFAC, 2002

[150] M. Tharayil, A. Alleyne, "*A Generalized PID Error Governing Scheme for SMART/SBLI Control*", Proceedings of the American Control Conference Anchorage, AK, pp. 346-351, May 8-10, 2002.

[151] J. S. Freudenberg, C. V. Hollot, D. P. Looze, "*A First Graduate Course in Feedback Control*", Revised January 7, 2003.